

Development of Techniques for Recycling the Waste Phosphors and Rare Earth Elements from End-of-Life Fluorescent Lamps

A Dissertation

Presented in Partial Fulfillment of the Requirements for the

Degree of Doctor of Philosophy

with a

Major in Chemistry

in the

College of Graduate Studies

University of Idaho

by

Wen-Lung Chang

Major Professor: Chien M. Wai, Ph.D.

Committee Members: Thomas E. Bitterwolf, Ph.D.; I. Francis Cheng, Ph.D.;

Leslie Baker, Ph.D.

Department Administrator: Ray von Wandruszka, Ph.D.

May 2018

Authorization to Submit Dissertation

This dissertation of Wen-Lung Chang, submitted for the degree of Doctor of Philosophy with a major in Chemistry and titled "Development of Techniques for Recycling the Waste Phosphors and Rare Earth Elements from End-of-Life Fluorescent Lamps," has been reviewed in final form. Permission, as indicated by the signatures and dates given below, is now granted to submit final copies to the College of Graduate Studies for approval.

Major Professor: _____ Date: _____

Chien M. Wai, Ph.D.

Committee Members: _____ Date: _____

Thomas E. Bitterwolf, Ph.D.

_____ Date: _____

I. Francis Cheng, Ph.D.

_____ Date: _____

Leslie Baker, Ph.D.

Department

Administrator: _____ Date: _____

Ray von Wandruszka, Ph.D.

Abstract

Rare earth elements (REEs), the vitamins for modern societies, have been considered some of the most critical elements. They are essential in various industrial applications. With rapid growth in the consumption of rare earths due to the development of new clean energy and defense-related technologies, the demand for these elements have become higher and higher. However, opening a new mine is an expensive, time-intensive process. As a result, reclaiming the rare earth metals from REE-containing end-of-life electronics has become one approach of reducing US dependence on import of these critical materials.

The phosphor material used in fluorescent lighting, containing rare earth elements such as cerium, europium, lanthanum, terbium and yttrium, is one of the most accessible sources of REEs in our daily life. Annually, over 680 million fluorescent lamps are reportedly disposed of in the United States. It not only increases the environmental burden but is also a waste of valuable rare earth elements. Therefore, developing innovative technologies of recycling REEs from end-of-life fluorescent lamps has become critical.

In fluorescent lamps, mercury is used to generate UV light with a wavelength of 254 nm, which in turn excites the phosphors to produce visible light. Mercury is highly toxic and listed as a hazardous substance by the USEPA. To reuse or reclaim spent rare earth phosphors, the first step is to remove mercury from them. The traditional ways for removing mercury from phosphors are either time-consuming or energy-intensive. By using a NaCl/NaOCl solution with the assistance of ultrasound, the mercury level in the spent phosphors can be reduced rapidly in a few minutes and meet the USEPA standards for universal non-hazardous wastes.

The rare earth elements in the fluorescent phosphors exist in various chemical forms. Typically, europium and yttrium are in oxide forms; cerium, lanthanum and terbium are doped in phosphate or aluminate matrices. Rare earth oxides are soluble in acids, and therefore, the europium and yttrium in spent fluorescent phosphors can be easily extracted by acids. However, phosphate and aluminate matrices are more chemically stable. As a result, extracting cerium, lanthanum and terbium from the phosphors requires a pretreatment procedure. By pretreating the phosphors with sodium peroxide at 650 °C, cerium, lanthanum and terbium in the treated phosphors become extractable by supercritical fluid carbon dioxide (sc-CO₂). The extraction efficiencies for cerium, lanthanum and terbium are over 96% using a tri-n-butylphosphate-HNO₃ extractant in sc-CO₂.

With the assistance of ultrasound, direct extraction of the REEs from the phosphors by nitric acid at elevated temperature is also possible. For example, with nitric acid of 11M at 80°C under sonication for 1 hour over 99% of cerium, europium, lanthanum and yttrium as well as 93% of terbium could be extracted from the fluorescent phosphors.

Acknowledgments

I would like to express the deepest appreciation to my major Professor, Dr. Chien M Wai, who has the attitude and the substance of a great scientist: he continually generates innovative ideas about development and applications of new techniques. Working with him has made me realize what standing on the shoulder of giants is like. Without his guidance and persistent help, this dissertation would not have been possible.

I would like to thank my committee members, Dr. Thomas Bitterwolf and Dr. Leslie Baker. Dr. Bitterwolf not only gave me advise but also generously offered me the access to his lab and instruments. Dr. Baker took the time out of her busy schedule to analyze my samples and teach me how to use ICP-OES. I also appreciate the guidance and help from Dr. Robert V Fox, Donna Baek, and Mary Case of Idaho National Laboratory (INL). The trainings I received from them gave me a clear idea about how to design supercritical extraction system and experiments.

Special thanks go to Arron Steiner of WSU GeoAnalytical Lab, who went out of his way to analyze my samples on the weekend before the deadline for submitting my first draft of dissertation. Without the data, I would not have been able to finish my first draft and do my dissertation defense as scheduled. In addition, a thank you to David Gover and Aaron Babino of the Glass Shop, Charles Cornwall of the Metal Shop, Erin Linskey of Anatek Labs, and all the friends who have given me assistance and support.

Finally, I would also like to thank to Critical Material Institute for their financial support for part of my research.

Dedication

This dissertation is gratefully dedicated to my parents. They have always hoped their son to become a doctor. Pursuing a Ph.D. in Chemistry is challenging. Without their love and support, this accomplishment would not have been achieved

Table of Contents

Authorization to Submit Dissertation	ii
Abstract	iii
Acknowledgements	v
Dedication	vi
Table of Contents	vii
List of Figures	x
List of Tables	xiv
Chapter 1: Introduction	1
1.1. Background	1
1.2. Research Objectives	4
1.3. Strategies	5
1.3.1. Reuse of the phosphors from waste fluorescent lamps- mercury removal	5
1.3.2. Recovery of rare earth elements from waste phosphors	8
1.3.2.1. Recovery of rare earth elements from waste phosphors through supercritical fluid extraction.....	10
1.3.2.2. Recovery of rare earth elements from waste phosphors with ultrasonic assistance	14
1.4. Experimental approaches.....	18
1.5. Achievement.....	21
References.....	22
Chapter 2: Ultrasound-Assisted Mercury Removal of Rare Earth Phosphors from End-of-Life Fluorescent Lamps and Its Potential of Reusability	28
2.1. Introduction.....	29
2.2 Experimental section.....	34
2.2.1 Waste Samples collection, chemicals, instruments and analysis methods.....	34
2.2.2. Mercury removal by thermal desorption.....	35
2.2.3. Mercury removal by NaCl/NaOCl solution with and without sonication.....	35
2.2.4. Mercury removal by DI water with sonication	36
2.3. Results and Discussion.....	36
2.3.1. Collection of phosphors from used fluorescent lamps using sonication in a liquid system.....	36
2.3.2. Mercury removal by thermal desorption.....	37

2.3.3. Mercury removal with 0.2M/0.5M NaCl/NaOCl solution in oil bath.....	38
2.3.4. Ultrasound-assisted removal of mercury with 0.2M/0.5M NaCl/NaOCl solution in a sonication bath.....	40
2.3.5. Ultrasound-assisted removal of mercury with 0.2M/0.5M NaCl/NaOCl solution using an ultrasonic liquid processor	41
2.3.6. Assessment of mercury removal through mass balance	43
2.3.7. Concentration effect	44
2.3.8. Time effect	46
2.3.9. Toxicity characteristic leaching procedure (TCLP)	47
2.3.10. Ultrasound-assisted mercury removal with deionized water using an ultrasonic liquid processor	51
2.3.11. Potential of Reusability	52
2.4. Conclusions	57
Acknowledgements	57
References	58

Chapter 3: Selective Extraction of Rare Earth Elements from Spent Commercial Fluorescent Phosphors Using Supercritical Fluid Carbon Dioxide62

3.1. Introduction	63
3.2. Experimental Section	66
3.2.1. Chemicals and materials.....	65
3.2.2. Experimental apparatus	65
3.2.3. Characterization of the phosphors.....	68
3.2.4. Sodium peroxide pretreatment of phosphors materials	69
3.2.5. Extraction using TBP-HNO ₃ adduct	70
3.3 Results and Discussion.....	71
3.3.1. Characterization and pretreatment of the phosphors	71
3.3.2. TBP-HNO ₃ complex preparation.....	79
3.3.3. Extraction of rare earth elements from fluorescent phosphor materials under atmospheric conditions and selectivity	79
3.3.4. Extraction of rare earth elements from fluorescent phosphor materials vis supercritical CO ₂	85
3.3.5. Mass balance of rare earth elements	87
3.4 Conclusion	88
Acknowledgments.....	89

References	90
------------------	----

**Chapter 4: The Influence of Ultrasound on the Extraction of Rare Earth Elements
from Phosphors of End-of-Life Fluorescent Lamps92**

4.1 Introduction	93
4.2 Experimental Section	96
4.2.1. Waste phosphor materials, chemicals	96
4.2.2. Experimental set-up, instruments and experiment methods	97
4.3. Results and Discussion.....	100
4.3.1. Characterization of the phosphor	101
4.3.2. Comparison of extraction with ultrasonic and without ultrasonic influence	102
4.3.3. Sonication time effect.....	104
4.3.4. Temperature effect	105
4.3.5. Solvent concentration effect	109
4.3.6. Kinetics Study	111
4.3.7. Ultrasonically-assisted pretreatment of fluorescent phosphors using H ₂ O and NaOH solutions	119
4.4 Conclusion	128
Acknowledgments.....	128
References	129

List of Figures

Figure 1-1. Strategies for recycling waste phosphors from end-of-life fluorescent lamps.....	5
Figure 1-2. The basic principle of supercritical CO ₂ extraction	11
Figure 1-3. Sound wave	14
Figure 1-4. Frequency ranges corresponding to ultrasound, with rough guide of some applications	15
Figure 1-5. Schematic presentation of transient acoustic cavitation yielding energy release	16
Figure 1-6. The physical effects of cavitational bubbles near a solid surface	16
Figure 1-7. Thermal desorption method	18
Figure 1-8. Flow chart for sonication mercury removal method	19
Figure 1-9. Flow chart for recovery of rare earth elements from waste phosphors with supercritical CO ₂	20
Figure 2-1. Ultrasound-assisted collection of rare earth phosphors from used compact fluorescent lamps. (a) Sonication bath (42kHz 100 watt) with a compact fluorescent lamp, (b) the lamp after 30 seconds of sonication and rinsing	37
Figure 2-2. Roasting waste phosphors in a tube furnace: Removal mercury from the phosphors by heating at elevated temperatures for 1 hour. The phosphors were collected from used Sylvania fluorescent lamps	38
Figure 2-3. Mercury removal with NaCl/NaOCl (0.2M/0.5M) solution in 50°C oil bath.....	39
Figure 2-4. Mercury removal with NaCl/NaOCl (0.2M/0.5M) solution: 1) Rate of mercury removal from the phosphors oil bath at 50°C; 2) removal of mercury from the phosphors in sonication bath at 50°C; 3) mercury removal from the phosphor using an ultrasonic liquid processor.	42
Figure 2-5. Mass balance of mercury content before and after the reaction for each time span	44
Figure 2-6. 5-minute sonication of phosphors in NaCl/NaOCl solutions of various concentrations. B prefixes to the solutions made with bleach; P to the solutions made with pure sodium hypochlorite. 0.2M/0.5M NaCl/NaOCl is the default concentration. The concentrations of the other solutions were made to be the fractions or multiples of the 0.2M/0.5M NaCl/NaOCl. For example: 0.5 x Default = 0.1M/0.25M NaCl/NaOCl.....	45
Figure 2-7. Comparison between 5-minute and 15-minute sonication of phosphors in solutions of various concentrations. B prefixes to the solutions made with bleach; P to the solutions made with pure sodium hypochlorite. 0.2M/0.5M NaCl/NaOCl is the default concentration. The concentrations of the other solutions were made to be the fractions or multiples of the 0.2M/0.5M NaCl/NaOCl	46

Figure 2-8. Leached mercury level after TCLP was performed on the original phosphor and the phosphor samples treated under the default concentration in oil bath. B prefixes to the solutions made with bleach; 0.2M/0.5M NaCl/NaOCl is the default concentration	48
Figure 2-9. Leached mercury level in the solution after TCLP was performed on the samples treated under the default concentration. B prefixes to the solutions made with bleach; 0.2M/0.5M NaCl/NaOCl is the default concentration	49
Figure 2-10. TCLP results for phosphors sonicated in NaCl/NaOCl solutions of various concentrations for 5 minutes. B prefixes to the solutions made with bleach; P to the solutions made with pure sodium hypochlorite. 0.2M/0.5M NaCl/NaOCl is the default concentration. The concentrations of the other solutions were made to be the fractions or multiples of the 0.2M/0.5M NaCl/NaOCl	50
Figure 2-11. TCLP results for 15-minute sonication of phosphors in NaCl/NaOCl solutions of various concentrations. B prefixes to the solutions made with bleach; P to the solutions made with pure sodium hypochlorite. 0.2M/0.5M NaCl/NaOCl is the default concentration. The concentrations of the other solutions were made to be the fractions or multiples of the 0.2M/0.5M NaCl/NaOCl	50
Figure 2-12. Sonication with water (no temperature control): Mercury removal by sonication of the phosphor in water with an ultrasound probe at room temperature.	52
Figure 2-13. Emission spectra for (a) Original Sylvania phosphor; (b) phosphor heated at 600°C for 1 hour; (c) phosphor sonicated in 0.1M/0.25M NaCl/NaOCl solution for 5 minutes; (d) phosphor sonicated in 0.15M/0.375M NaCl/NaOCl solution for 5 minutes; (e) phosphor sonicated in 0.2M/0.5M NaCl/NaOCl solution for 5 minutes; (f) phosphor sonicated in 0.2M/0.5M NaCl/NaOCl solution for 15 minutes.....	53
Figure 2-14. SEM images for (a) Original Sylvania phosphor; (b) phosphor heated at 600°C for 1 hour; (c) phosphor sonicated in 0.1M/0.25M NaCl/NaOCl solution for 5 minutes; (d) phosphor sonicated in 0.15M/0.375M NaCl/NaOCl solution for 5 minutes; (e) phosphor sonicated in 0.2M/0.5M NaCl/NaOCl solution for 5 minutes; (f) phosphor sonicated in 0.2M/0.5M NaCl/NaOCl solution for 15 minutes	56
Figure 3-1. Schematic diagram of the SFE system	67
Figure 3-2. Flowchart for sodium peroxide pretreatment	69
Figure 3-3. (a) The weight increase rate for each metal in treated-washed-annealed trichromatic phosphor. (b) The weight increase rate for each metal in treated-washed Sylvania phosphor	74
Figure 3-4. The fluorescence spectra for the Trichromatic phosphor, green phosphor and blue phosphor.....	75
Figure 3-5. Fluorescent spectra before and after pretreatment for (a) Trichromatic phosphor (b) Sylvania phosphor.....	76
Figure 3-6. The SEM micrograph of original Trichromatic phosphor.	77

Figure 3-7. The SEM micrograph of pretreated Trichromatic phosphor.....	77
Figure 3-8. The SEM micrograph of original Sylvania phosphor	78
Figure 3-9. The SEM micrograph of pretreated Sylvania phosphor.....	78
Figure 3-10. TBP-HNO ₃ extraction under atmospheric conditions for original Trichromatic phosphor (TRI), treated-non-washed Trichromatic phosphor (tnw-TRI), and treated-washed-annealed Trichromatic phosphor (twa-TRI).	83
Figure 3-11. TBP-HNO ₃ extraction under atmospheric conditions for original Sylvania phosphor (SYL), treated-non-washed Sylvania phosphor (tnw-SYL), and treated-washed-annealed Sylvania phosphor (twa-SYL)	83
Figure 3-12. Acid leaching on Sylvania phosphor with 7M HNO ₃ at 60°C for 2 hours	84
Figure 3-13. Solubility of rare earth oxides and non-rare earth oxides in TBP-HNO ₃ adduct (mg·mL ⁻¹) at 60°C.....	84
Figure 3-14. Supercritical extraction efficiencies for (a) treated-washed-annealed Trichromatic phosphor (b) treated-washed-annealed Sylvania phosphor	86
Figure 3-15. (a) The weight percent of the remaining rare earth elements in the Trichromatic phosphor residue after Sc-CO ₂ extraction. (b) The weight percent of the remaining rare earth elements in the Sylvania phosphor residue after Sc-CO ₂ extraction.	88
Figure 4-1. Experimental set-up for sonication experiments.....	98
Figure 4-2. Extraction efficiencies of rare earth elements from fluorescent phosphors with and without sonication.....	103
Figure 4-3. Extraction efficiencies of rare earth elements from phosphors with 9M HNO ₃ , sonication at 30°C for 10, 20, 30, 40 min.....	105
Figure 4-4. The temperature changes of a 20-mL aqueous solution vs sonication time	106
Figure 4-5. Extraction efficiencies for sonication of Sylvania phosphor with 9M HNO ₃ for 10, 20, 30, 40 min without temperature control	107
Figure 4-6. Extraction efficiencies for sonication of Sylvania phosphor with 9M HNO ₃ for 10, 20, 30, 40 min without temperature control.	108
Figure 4-7. Extraction efficiencies for sonication of Sylvania phosphor at 80°C for 40 min at with 1M, 3M, 5M, 7M, 9M HNO ₃ solutions	110
Figure 4-8. Extraction efficiency of rare earth metals from fluorescent phosphors with 11M HNO ₃ at 80°C for 1 hour	110
Figure 4-9. Influence of ultrasound on the yield and kinetics of the extraction of cerium, lanthanum and terbium from fluorescent phosphors with 9M HNO ₃ solution at 60°C.	

(Results obtained from sonication experiments are prefixed with Soni-; results obtained from oil bath experiments are prefixed with Oil-.).....	111
Figure 4-10. R^2 for extraction of cerium, lanthanum, and terbium at various temperatures	112
Figure 4-11. Rate constant of extraction of cerium, lanthanum and terbium with 9M HNO_3 under sonication without temperature control and at 303, 313, 333, 343 and 353K (30°C, 40°C, 60°C, 70°C and 80°C)	114
Figure 4-12. Extraction of rare earth elements in luminescent materials at (a) 313, (b) 333 (c) 343 and (d) 353 K. (e) No temperature control. Time—0 indicates the start of the ultrasonic extraction.....	118
Figure 4-13. Arrhenius plots for the dissolution reactions of Ce, La and Tb with 9M HNO_3 under sonication at 313, 333, 343 and 353 K	118
Figure 4-14. Acid leaching of non-treated, H_2O and NaOH treated phosphors with 1M HNO_3 in an oil bath at 60°C for 40 minutes, where H_2O -soni-1hr-60°C represents the phosphor material was pretreated by sonication at 60°C with H_2O for one hour; NaOH-soin-1hr-60°C represents the phosphor material was pretreated by sonication at 60°C with NaOH for one hour and so on	121
Figure 4-15. Acid leaching of non-treated, H_2O and NaOH treated phosphors with 9M HNO_3 under sonication at 80°C for 40 minutes	121
Figure 4-16. Acid leaching of non-treated, H_2O and H_2O_2 treated phosphors with 1M HNO_3 under sonication at 60°C for 40 minutes.....	122
Figure 4-17. (a) non-treated phosphor (b) phosphor sonicated with H_2O at 80°C for 1 hour (c) phosphor sonicated with NaOH at 80°C for 1 hour	124
Figure 4-18. SEM micrograph of non-treated Sylvania phosphor	124
Figure 4-19. SEM micrograph of the phosphor sonicated with H_2O at 80°C for 1 hour	125
Figure 4-20. SEM micrograph of the phosphor sonicated with NaOH at 80°C for 1 hour	125
Figure 4-21. SEM micrograph of the phosphor ultrasonically extracted with 11M HNO_3 80°C for 1 hour	126
Figure 4-22. Fluoresce spectra of 1) non-treated phosphor; 2) phosphor sonicated with H_2O at 80°C for 1 hour; 3) phosphor sonicated with 12M NaOH at 80°C for 1 hour; 4) phosphor that has been ultrasonically extracted with 11M HNO_3 80°C for 1 hour	127

List of Tables

Table 1-1. Maximum concentration of contaminants for the toxicity characteristic (Source: electronic code of federal regulations)	8
Table 1-2. Chemical formula for fluorescent phosphor materials	9
Table 2-1. Land Disposal Restrictions (Source: Treatment Technologies for Mercury in Soil, Waste, and Water, EPA)	31
Table 2-2. The percentage of residual mercury in the phosphors versus sonication time for each treatment method.....	42
Table 3-1. Chemical formula for fluorescent phosphor materials	64
Table 3-2. Extraction under atmospheric pressure.....	70
Table 3-3. Extraction under supercritical conditions	71
Table 3-4. Metal content of Sylvania and Trichromatic phosphor (mg g ⁻¹ dry non-treated material).....	72
Table 3-5. Metal content (mg g ⁻¹ dry material) for Sylvania phosphor and Trichromatic phosphor before and after sodium peroxide treatment. Δ stands for the weight difference before and after the treatment, and Δ % stands for increase rate of weight.	73
Table 4-1. Rare-earth-containing phosphors	94
Table 4-2. Extraction under ultrasonic conditions	98
Table 4-3. Extraction under traditional agitation conditions	99
Table 4-4. Pretreatment under ultrasonic conditions	99
Table 4-5. Rare earth metal content of Sylvania phosphor (mg. g ⁻¹ dry phosphor material)	101
Table 4-6. Coefficient of determination (R^2) for extraction of cerium, lanthanum, and terbium from fluorescent phosphor with 9M HNO ₃ solution under sonication without temperature control and at 30°C, 40°C, 60°C, 70°C, 80°C (303, 313, 333, 343 and 353K).	112
Table 4-7. Rate constant k of extraction of cerium, lanthanum and terbium with 9M HNO ₃ under sonication without temperature control and at 303, 313, 333, 343 and 353K (30°C, 40°C, 60°C, 70°C and 80°C).	113
Table 4-8. Slopes of Arrhenius plots and activation energies for Ce, La and Tb.....	115

Chapter 1: Introduction

1.1. Background

Rare earth elements (REEs) consist of 17 elements including 15 lanthanides plus scandium and yttrium. Due to their unique optical, electrical, magnetic and catalyst properties¹⁻², REEs are usually called the vitamins of a modern society. They are widely used in many electronics and communication devices including fluorescent light bulbs, lasers, phosphors for TV screen and computer display, magnets, wind turbines, telecommunications, defense technologies, etc³. The United States entered the market in the mid-1960s when the demand of color television soared. Up to the early 1990s, the U.S.A. still dominated most of the world's supply of rare earth oxide market. China entered the rare earth market and started selling rare earths at very low prices in between the late 1980s and the early 90's. By the late 90's, China's low-cost products had flooded the market. As a result, the US mining companies cut production and then went inactive. Eventually they were driven out of the rare earth mining business. According to estimates by the U.S. Geological Survey, there are approximately 120 million metric tons of worldwide rare earth reserves. China owns the highest proportion of these reserves, which are estimated at some 44 million metric tons.⁴ With rapid growths in the consumption of rare earths due to the development of new clean energy and defense-related technologies, these elements have received more and more attention. Currently, only a handful of mines supply REEs to the entire world, and most of them are located in China. Bayan Obo, the largest REE mine in the world, provides 40-50% of all REEs. By 2010, Bayan Obo and other REE mines in China provided approximately 97%

of the world's basic rare earth oxide production⁵. Despite only having a third of the world's deposits, China dominates global rare earth supply. With the attempt to develop its own industry for the 17 minerals and raise the price of REEs, China imposed restrictions on exports of REEs in 2009, which resulted in escalated concerns about the future accessibility of rare earths. Consequently, industrial countries such as Japan, the United States, and countries of the European Union face tighter supplies and higher prices for rare earths. Therefore, the United States requested consultations with China in World Trade Organization (WTO) regarding China's restrictions on the export of various forms of rare earths, tungsten and molybdenum on the 13th of March in 2012. China has dropped its quota system restricting exports of rare earth minerals after losing the WTO case in 2015⁶. In spite of China's ending of its export restrictions, in order to alleviate the dependence on rare earth supplies from China, developing methods to recycle rare earth elements from electronic wastes has become a research area of considerable interest in recent years, and reopening or developing new rare earth mines are some of the strategies actively pursued by the U.S.A.

Seeking and mining new rare earth ores can be costly and time-consuming. In general, mining operations take 4 stages: exploration, development, operation and closure. The lead time of each stage ranges from 2 to 20 years⁷, not to mention the social and environmental impacts that mining activities may cause. Thus, developing methods to recycle rare earth elements from end-of-life products, including fluorescent light bulbs, magnets, batteries, electronics, etc., is one of the U.S. Department of Energy's strategies described in the "Critical Materials Strategy" report^{8, 9}. We generally call it urban mining. The advantages of urban mining include shorter operation time, relatively low cost, reduced amount of waste, and environmental friendliness. It provides a sustainable way of obtaining rare earth minerals. One

of the most accessible sources containing rare earth elements in our daily life is the phosphors coated on the inner wall of fluorescent lamps. According to the Australian consultant Kingsnorth from IMCOA, from 2006 to 2008, approximately 7% of global consumption of rare earth metals was used in phosphors. In the U.S. alone, more than 680 million fluorescent lamps are disposed annually, but most of them are not recycled¹⁰.

Fluorescent lamps, which rely on mercury for their operation, have become the most important electrical lighting devices over the past few decades due to their high lighting efficiencies. When electricity passes through a fluorescent lamp, the mercury vapor in the lamp will generate ultraviolet radiation (254 nm), which in turn excites the white coating on the inner wall of the lamp tube to emit visible light. The light-emitting coating is typically a mixture of phosphors that contain rare earth elements in the forms of oxides, phosphates, or aluminates. Although only about 7% of global consumption of rare earth metals was used in phosphors, the cost accounted for 32% of the global rare earth market value in 2008.¹¹ It's because the REEs used in phosphors must be 99.999% pure, and even only a tiny amount of impurities can change the color characteristics of a given phosphor. To produce phosphors with these high purities, many more steps are required for the purification process, which inevitably causes significant raise of the prices for the REEs used in phosphors. The extensive use of fluorescent lamps over the years has caused not only growing concerns over their proper disposal, but also a great deal of resource waste. Thus, recycling or reusing rare earth phosphors has become one of the strategies described in the U.S. Department of Energy Critical Materials reports. This strategy will reduce America's demand for rare earth raw materials and minimize environmental impacts. It also increases America's supply diversities and securities of critical materials.^{8,9}

1.2. Research objectives

In this research, the central idea revolves around using most cost-efficient, simple and environment-friendly methods to recycle the waste phosphors of end-of-life fluorescent lamps. The goal of our study focuses on the development of novel technologies to give the waste phosphors from end-of-life fluorescent lamps a new life so that we can reduce the amount of waste and utilize natural resources in a sustainable way. Our strategies for recycling fluorescent phosphors are as follows:

- (1) To reuse the waste phosphors
- (2) To recover the rare earth elements from waste phosphors.

To achieve our goals, we have looked up a number of references. Eventually, we generated some ideas and formed our research plans (Figure 1-1.):

- (a) Removing mercury in a way that does not significantly damage the physical and chemical properties of the phosphors from end-of-life fluorescent lamps and reuse them.
- (b) Recovering rare earth elements from waste phosphors through supercritical fluid extraction using a TBP-HNO₃ adduct system.
- (c) Leaching or treating waste phosphors using various reagents such as nitric acid and sodium hydroxide with ultrasonic assistance.

Each plan will be discussed in the following sections.

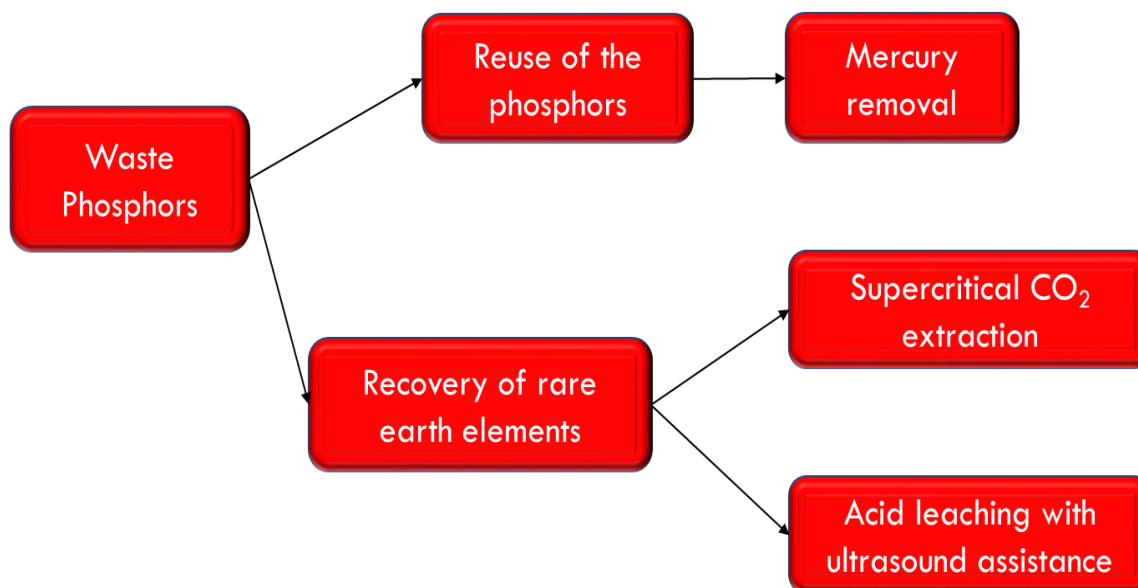


Figure 1-1. Strategies for recycling waste phosphors from end-of-life fluorescent lamps

1.3. Strategies

1.3.1. Reuse of the phosphors from waste fluorescent lamps- mercury removal

Mercury, a heavy silvery d-block element with an atomic number of 80, is the only liquid metallic element at standard conditions for temperature and pressure. It is well-known for its toxicity, which is not only extremely poisonous to cause acute and chronic harm to human health, but also contaminative to the environment^{12, 13, 14}. When elemental mercury is released into the environment, it will be eventually deposited into soils and water and transformed to methyl-mercury, which can enter the food chain through food uptake by fish. Consumption of contaminated fish is responsible for most human mercury exposure, potentially leading to adverse health effects, such as impaired neurological development of

fetuses, infants, and children. Elemental mercury can also be inhaled as a vapor and absorbed through lungs. In spite of its toxicity, it has various applications in devices and industry, including thermometers, barometers, manometers, sphygmomanometers and fluorescent lamps. Mercury is especially essential to achieve the generation of ultraviolet radiation in fluorescent lamps. In a fluorescent lamp, when an electric current passes through the tube containing argon and a small amount of mercury vapor, invisible ultraviolet light is generated, which will in turn excite the fluorescent coating (called phosphor) on the inner wall of the tube and emit visible light. The study done by National Electrical Manufacturers Association (NEMA) has determined the minimal mercury required for fluorescent lamps. An individual F40T12 (the most commonly used fluorescent lamp, tubular type 40 W/T12, length of 122 cm and 3,8 cm of diameter) lamps rated for 20,000 h of life requires 10 mg of mercury (0.7 μl), and therefore an insufficiency of mercury level in fluorescent lamps will lead to premature failure¹⁵. This is called “mercury starvation” within the industry.

Due to the reactive properties of metallic mercury, it interacts with all the components of a lamp and form stronger bonds, and becomes dispersed throughout the lamp during operations¹⁶. During the operation of a lamp, the metallic mercury will be oxidized and adsorbed onto the phosphor powder and other lamp components, which causes the reduction of the mercury to be volatilized^{17, 18, 19, 20}. In order to avoid premature failure, the average amount of mercury inserted into fluorescent lamps by manufacturers are generally set to no less than 15 mg so that the minimum amount in an individual lamp will not drop down to less than 10 mg, and lead to a foreshortened life due to insufficient mercury¹⁵.

The mercury content of fluorescent lamps differs depending on the manufacturer, the wattage, the type of lamps (linear or compact), the year of manufacturing, and their age.

Because of the presence of mercury, all end-of-life fluorescent lamps are considered hazardous by the U.S. Environmental Protection Agency (USEPA). According to federal regulations (40 CFR §273.5, applicability: lamps), a lamp is a hazardous waste if it exhibits one or more of the characteristics identified in part 261, subpart C of this chapter (Chapter I). Based on the standards on the Table 1 in 40 CFR §261.24, a solid waste that exhibits the characteristic of toxicity has the EPA Hazardous Waste Number specified in Table 1 which corresponds to the toxic contaminant causing it to be hazardous. Most end-of-life fluorescent lamps with mercury concentration greater than 0.2 parts per million, by the Toxicity Characteristic Leaching Procedure (TCLP), should be managed as hazardous waste²¹. As a result, the first step to reuse the waste phosphors from end-of-life fluorescent lamps is either to completely remove the mercury content from them or lower the mercury content level down to less than 0.2 parts per million by the TCLP test.

Our goal is to develop a novel method that is strong enough to remove the mercury from waste phosphors but weak enough not to damage the crystalline structure so that the phosphor powders can be reused in the fluorescent lamp production. If they are reusable, but the lighting efficiency of old phosphors is not as good as brand new ones, they could be used to mix with a certain ratio of new phosphors to manufacture lighting devices with new applications.

Table 1-1. Maximum concentration of contaminants for the toxicity characteristic
(Source: electronic code of federal regulations)

EPA HW No. ¹	Contaminant	CAS No. ²	Regulatory Level (mg/L)
D004	Arsenic	7440-38-2	5.0
D005	Barium	7440-39-3	100.0
D018	Benzene	71-43-2	0.5
D006	Cadmium	7440-43-9	1.0
D019	Carbon tetrachloride	56-23-5	0.5
D020	Chlordane	57-74-9	0.03
D021	Chlorobenzene	108-90-7	100.0
D022	Chloroform	67-66-3	6.0
D007	Chromium	7440-47-3	5.0
D023	o-Cresol	95-48-7	⁴ 200.0
D024	m-Cresol	108-39-4	⁴ 200.0
D025	p-Cresol	106-44-5	⁴ 200.0
D026	Cresol		⁴ 200.0
D016	2,4-D	94-75-7	10.0
D027	1,4-Dichlorobenzene	106-46-7	7.5
D028	1,2-Dichloroethane	107-06-2	0.5
D029	1,1-Dichloroethylene	75-35-4	0.7
D030	2,4-Dinitrotoluene	121-14-2	³ 0.13
D012	Endrin	72-20-8	0.02
D031	Heptachlor (and its epoxide)	76-44-8	0.008
D032	Hexachlorobenzene	118-74-1	³ 0.13
D033	Hexachlorobutadiene	87-68-3	0.5
D034	Hexachloroethane	67-72-1	3.0
D008	Lead	7439-92-1	5.0
D013	Lindane	58-89-9	0.4
D009	Mercury	7439-97-6	0.2
D014	Methoxychlor	72-43-5	10.0
D035	Methyl ethyl ketone	78-93-3	200.0
D036	Nitrobenzene	98-95-3	2.0
D037	Pentachlorophenol	87-86-5	100.0
D038	Pyridine	110-86-1	³ 5.0
D010	Selenium	7782-49-2	1.0
D011	Silver	7440-22-4	5.0
D039	Tetrachloroethylene	127-18-4	0.7
D015	Toxaphene	8001-35-2	0.5
D040	Trichloroethylene	79-01-6	0.5
D041	2,4,5-Trichlorophenol	95-95-4	400.0
D042	2,4,6-Trichlorophenol	88-06-2	2.0
D017	2,4,5-TP (Silvex)	93-72-1	1.0
D043	Vinyl chloride	75-01-4	0.2

1.3.2. Recovery of rare earth elements from waste phosphors

Fluorescent lamps, linear or compact type, typically employ phosphors containing rare earth elements yttrium (Y), lanthanum (La), cerium (Ce), europium (Eu), and terbium (Tb). The rare earth phosphors are applied as a coating to the inside surface of the lamps. When a voltage is applied, an electric current will pass through the mercury vapor in a lamp and excites

short-wave ultraviolet light, which causes the rare earth elements-doped phosphor coating to emit lights of different wavelengths in the visible region. The end-of-life fluorescent lamps contain reusable rare earth materials of significant importance to industry and defense needs of the U.S.A. Rare earth phosphors used in fluorescent lamps come in different chemical forms which can be divided into four categories: phosphate, aluminate, borate and silicate matrices^{22, 23}, which are shown in Table 2²⁴. Borate and silicate systems are not fully developed and therefore, the phosphors in the market are either the application of phosphate, aluminate alone or mixed. In general, Red phosphors contain rare earth oxides and can dissolve in acids with or without heating. When rare earths, however, are doped in phosphate or aluminate matrices, they are difficult to be extracted by conventional acid leaching processes. Converting them to oxides under appropriate conditions, such as elevated temperature and oxidizing reagents, is one method to make them become extractable with acids.

Table 1-2. Chemical formula for fluorescent phosphor materials²⁴

Phosphor	Red	Green	Blue
Phosphate matrix	$\text{Y}_2\text{O}_3:\text{Eu}^{3+}$	$\text{LaPO}_4:\text{Ce}^{3+}, \text{Tb}^{3+}$	$(\text{Ba}, \text{Sr}, \text{Ca})_5 (\text{PO}_4)_3 \text{Cl}:\text{Eu}^{2+}$
Aluminate matrix	$\text{Y}_2\text{O}_3:\text{Eu}^{3+}$	$\text{CeMgAl}_{11}\text{O}_{19}:\text{Tb}^{3+}$	$\text{BaMgAl}_{10}\text{O}_{17}:\text{Eu}^{2+}$
Borate matrix	$\text{Y}_2\text{O}_3:\text{Eu}^{3+}$	$\text{GdMgB}_5\text{O}_{10}:\text{Ce}^{3+}, \text{Tb}^{3+}$	$\text{Ca}_2\text{B}_5\text{O}_8\text{Cl}:\text{Eu}^{2+}$
Silicate matrix	$\text{Y}_2\text{O}_3:\text{Eu}^{3+}$	$\text{Y}_2\text{SiO}_3:\text{Ce}^{3+}, \text{Tb}^{3+}$	$\text{BaZrSi}_3\text{O}_9:\text{Eu}^{2+}$

1.3.2.1. Recovery of rare earth elements from waste phosphors through supercritical fluid extraction

Generally, in analytical chemistry there are 2 steps before instrumental analysis: 1. sampling; 2. sample preparation. Traditional procedures for wet chemistry sample preparation require a considerable amount of solvents to achieve extraction, separation and purification of samples. Acid leaching and solvent extraction are the typical approaches to dissolve and separate lanthanides from solid materials. As a result, a great amount of liquid waste has been produced. Using those solvents not only is costly but also does great harm to our fragile environment. Unlike traditional solvent extraction, supercritical fluid extraction (SFE) is a technique that employs supercritical fluid as the solvent to perform extraction. A supercritical fluid is formed when a substance is above its critical pressure (P_c) and temperature (T_c). Above critical point, this substance will become a phase between gas and liquid, which makes it flow like a liquid and diffuse like a gas. It exhibits liquid-like solvation capability and yet processes gas-like mass transfer properties. Its density changes as its pressure and temperature change. At a given temperature above the T_c , increasing pressure will increase the density of the fluid, and therefore the solvating power is then increased. Consequently, we say that the solvating power of a supercritical fluid is “tunable”. Carbon dioxide is the most commonly used fluid in SFE due to its moderate critical parameters, inexpensiveness, easy accessibility, nonexplosive nature, and non-toxicity. The relatively low critical point of CO_2 ($P_c = 72.9 \text{ atm}$, $T_c = 31.3 \text{ }^\circ\text{C}$) makes it an attractive extraction medium. These properties makes supercritical carbon dioxide an ideal alternative for extracting lanthanides from porous solid materials^{25,26}. The principle of how supercritical carbon dioxide (Sc-CO_2) extraction works is illustrated in Figure 1-2²⁷.

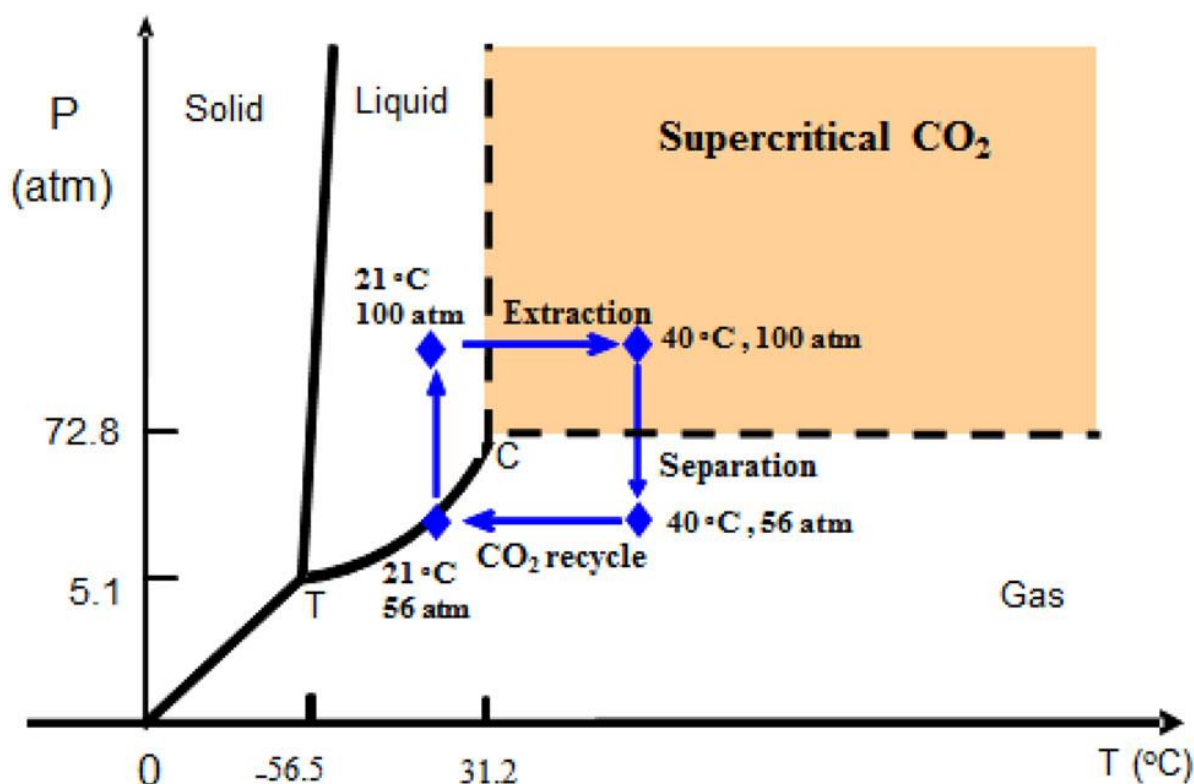


Figure 1-2. The basic principle of supercritical CO₂ extraction

When the pressure and temperature are at a point above the critical point, extraction starts. After extraction, sc-CO₂ is depressurized and therefore gasified, which allows separation of CO₂ and facilitates the collection of extracts. CO₂ may be collected and recycled for the future extraction.

CO₂ molecules are known to have a linear structure without polarity. Polar molecules and metal ions are not soluble in sc-CO₂. As a result, this technique had been mainly applied to extract non-polar compounds. However, due to the change of environmental regulations and the increasing costs of disposal of liquid solvent wastes, studies of metal extraction using sc-CO₂ as a solvent started in the early 1990s. Through binding to chelating agents, the charges

of metal ions can be neutralized and may become soluble in sc-CO₂. In 1991, Laintz et al. first reported quantitative measurements of solubility of metal chelates in sc-CO₂²⁸. In 1998, Carrott et al. discovered highly sc-CO₂ soluble uranium organophosphorus complexes²⁹. By using CO₂-soluble ligand acid complexes, tri-n-butylphosphate-nitric acid (TBP-HNO₃), direct dissolution of uranium oxides (UO₂, U₃O₈, and UO₃) and lanthanide oxides (Ln₂O₃) in sc-CO₂ was demonstrated^{30,31}. These complexes have a general formula TBP(HNO₃)_x(H₂O)_y. These ligand acid complexes are typically prepared by mixing TBP with HNO₃. When one aliquot of TBP mixes with another equal volume aliquot of concentrated HNO₃, the nitric acid will be extracted into the TBP phase forming a Lewis acid–base complex of the formula TBP(HNO₃)_{1.8}(H₂O)_{0.6}³². Therefore, despite the fact that supercritical CO₂ is non-polar, the polarity of supercritical CO₂ can be altered to stretch its applications by adding a miscible polar ligand or modifier to achieve extraction of metal ions or polar molecules.

Researchers have widely studied extraction of rare earth elements or lanthanides using sc-CO₂ as a substitute for traditional organic extraction solvents. By using TBP-nitric acid adduct system, we are able to extract rare earth elements from phosphors and carry them out with supercritical CO₂. In 2005 R Shimizu et al. reported their supercritical fluid extraction efficiencies of rare earth elements from luminescent material in waste fluorescent lamps, in which the yields for Yttrium and Europium reached 99.7 and 99.8%, respectively. However, the efficiencies of Ce, La and Tb were less than 7%³³. As shown in Table 2, in lighting phosphors, europium and yttrium in red phosphors are generally in oxide forms, but in green and blue phosphors, Ce, La, Tb and Eu are doped in chemically stable phosphate or aluminate matrices. The structures are so stable, especially the aluminate-based phosphors, so that it is not possible to be destroyed by mineral acids. In order to improve supercritical extraction of

rare earth elements from waste phosphors, we adopted alkali fusion method to convert those elements to their oxide forms.

Alkali fusion method is to thermally decompose insoluble substances by heating the mixture of alkali and insoluble substance, such as ores and sodium hydroxide, at an elevated temperature to cause destruction of the structure of substances and achieve the conversion from insoluble to soluble substances. It has been widely used to extract aluminum and various rare and precious metals^{34, 35, 36}. Porob et al. converted phosphors into a mixture of oxides by heating them with sodium carbonate at 1000 °C³⁷. Zhang et al. performed 2-step acid leaching. Their results show that hydrochloric acid is better than sulfuric acid in the first acid leaching step, and sodium hydroxide is better than sodium carbonate in the alkali fusion process. The leaching rates for all rare earth metals reached over 97%.³⁸ Wu et al.³⁹ reported an optimal condition for phosphor calcination treatment, in which the mixture with the Na₂O₂-to-phosphor mass ratio of 1.5 : 1 was calcinated at 650°C for 50 minutes. The aluminate matrix was successfully decomposed, under which more than 99.9% REEs are recovered.

In summary, alkali fusion method will be used to pretreat waste phosphors to break down the phosphate or aluminate matrices and convert the rare earth metals into their oxide forms. TBP-HNO₃ ligand acid complexes will then be combined with supercritical carbon dioxide to achieve extraction of rare earth metals from waste phosphors.

1.3.2.2. Recovery of rare earth elements from waste phosphors with ultrasonic assistance

When an object vibrates, sound will be produced. Sound is a form of energy traveling through medium (air, water, etc.) as longitudinal waves. Sound waves consist of areas of high and low pressure called compressions and rarefactions, respectively as shown in Figure 1-3.

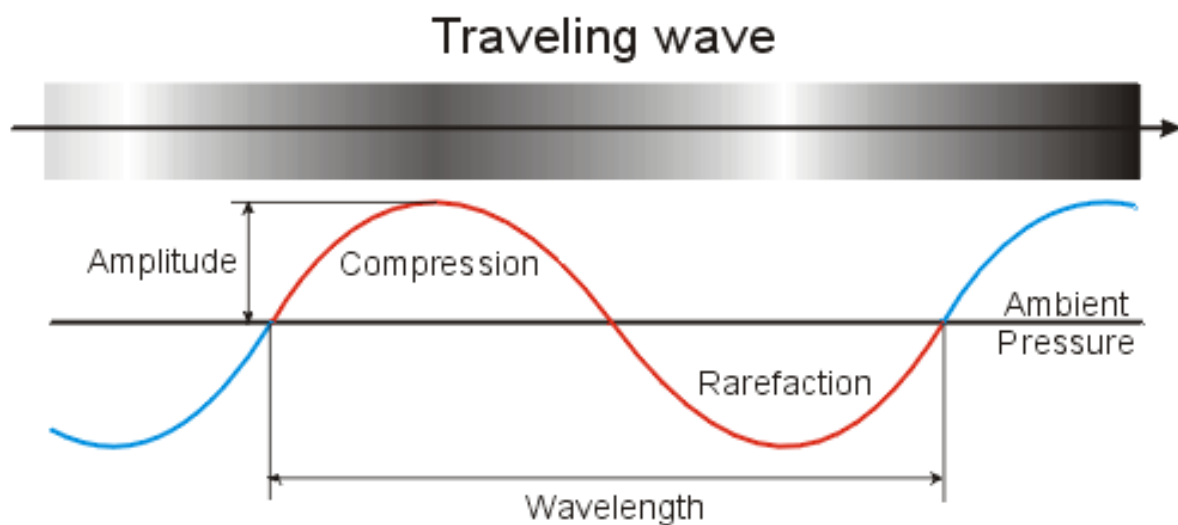


Figure 1-3. Sound wave (<https://method-behind-the-music.com/mechanics/physics/>).

In general, sound can be classified to 3 big categories based on its frequency: infrasound, acoustic and ultrasound. Human hearing is in the range of 20 Hz to 20 kHz. Sound above 20 kHz is ultrasound and below 20 Hz is infrasound. Other animals have different hearing ranges (Figure 1-4.). Many applications of ultrasound have developed over the years, including teeth cleaning in dental hygiene, underwater detection (SONAR), sonography, acoustic targeted drug delivery, ultrasonic testing, etc.

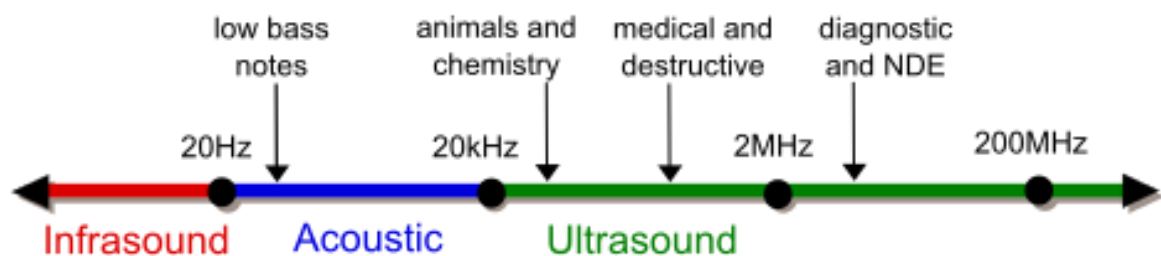


Figure 1-4. Frequency ranges corresponding to ultrasound, with rough guide of some applications (Source: Wikipedia).

The application of ultrasound in chemistry field is called sonochemistry. When ultrasound passes through a solution, regions of high and low pressure will be created corresponding to the periodic compression and rarefaction phases. As shown in Figure 1-5⁴⁰, air molecules dissolved in the solution form small air bubbles and grow during the low-pressure cycles. At the compression phases, these small bubbles and the matters inside will be squeezed by the high external pressure aggressively and shrink. These bubbles oscillate, growing a little more during the rarefaction phase of the sound wave than they shrink during the compression phase. This process continues until the external pressure is greater than the internal pressure and the bubbles collapse. The phenomenon of formation, growth and collapse of acoustic bubbles is called cavitation. This phenomenon gives rise to not only chemical but also physical effects. The collapse of cavitation bubbles creates local hotspots. Under proper conditions, the temperature and pressure inside the bubbles can reach as high as 5000 K, and 1000 atm^{41, 42}. Therefore, particles collide and interact inside these micro “chemical facilities” and generate energy as high as 13 eV⁴³. Furthermore, when bubbles are near a solid surface as shown in Figure 1-6, they will collapse in an asymmetrical fashion and form high-speed microjets. These microjets are responsible for surface deformation and rapid mass transfer. Therefore, acoustic cavitation provides unique environments for chemical

reactions. Various applications have been developed using ultrasound in the field of chemical engineering: waste-water treatment, organic synthesis, sonochemistry and solid-liquid extraction^{44, 45}.

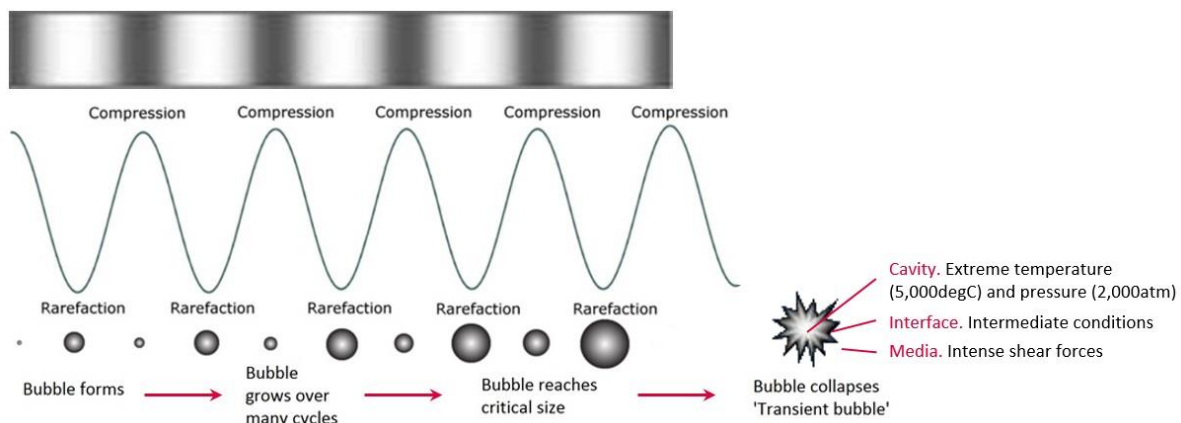


Figure 1-5. Schematic presentation of transient acoustic cavitation yielding energy release

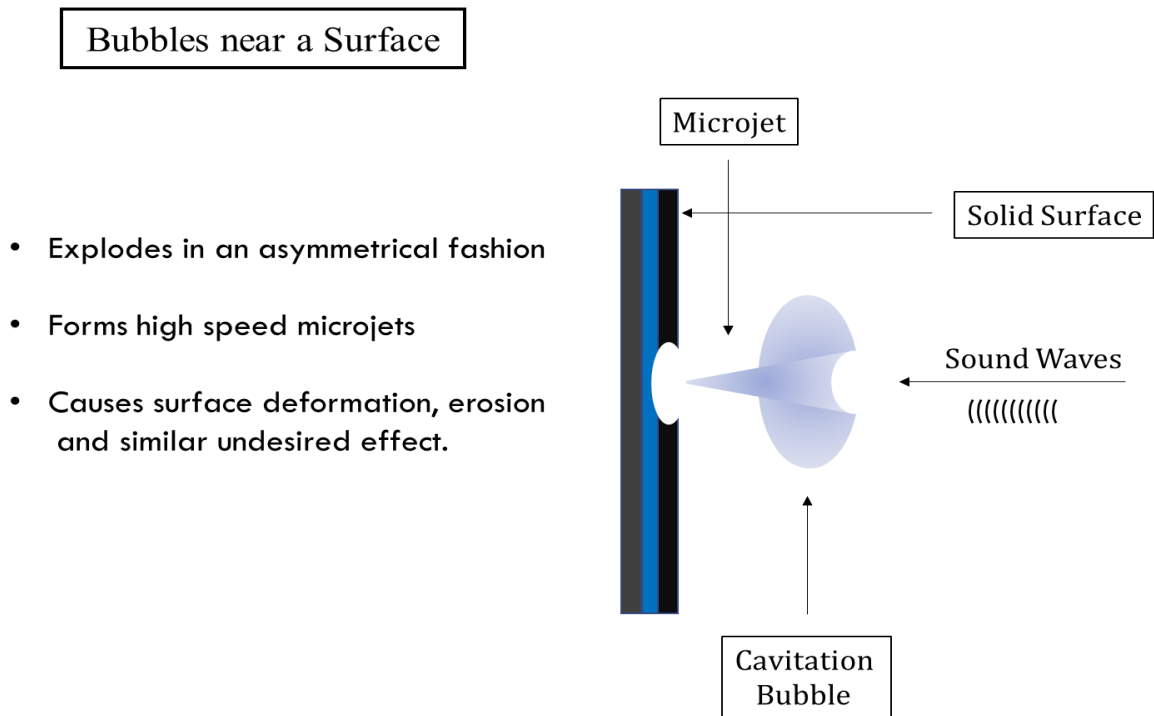


Figure 1-6. The physical effects of a cavitation bubble near a solid surface

Medicinal and aromatic plants are the biggest resource of active ingredients for the pharmaceutical, cosmetics, food industries as well as pest control in agriculture⁴⁶. Solid-liquid extraction with proper solvents is one of the traditional methods to obtain the active ingredients or natural products from plants. Ultrasonically enhanced solvent extraction has been used to release the bioactive constituents from herbs. The technique for ultrasonic enhancement of the extraction yield started in the 1950s with laboratory scale experiments⁴⁷. Since then, a number of studies related to ultrasonically assistant extraction of natural products or herbal bioactive principles have been reported⁴⁸. Extraction of saponin from ginseng was studied by Li et al.⁴⁹ With ultrasonic assistance, the yields of both total extract and saponin increased by approximately 15 wt%, and 30 wt% at an acoustic pressure 67 kPa, respectively. In addition, the yield increases with the acoustic pressure. Romdhane and coworker investigated the extraction of pyrethrines from pyrethrum flowers and oil from woad seeds, and an acceleration of the kinetics and of the yield of the extraction was obtained⁵⁰.

The fact that extraction of natural active ingredients from plants and herbs can be enhanced by ultrasound has been proved and many related applications have been developed. However, the applications of ultrasonic enhancement of extraction of metals are not as common. In this part of research, we will take advantage of the chemical and physical effects that ultrasound generates to achieve extraction of rare earth elements from the waste phosphors of end-of-life fluorescent lamps. Many factors govern the influence of ultrasound: ultrasound frequency, temperature, sonication time, etc. In this work, the influence of different parameters was investigated.

1.4. Experimental approaches

- (a) *Removing mercury from waste phosphor and using thermal desorption or sonication method while maintaining reusable.*

Thermal desorption- According to literature, thermal desorption is the most commonly used method to remove mercury. As shown in Figure 1-7, a certain amount of waste phosphor was placed in a crucible and put into a furnace for an hour. The temperature started from 100°C with an increment of 100°C.

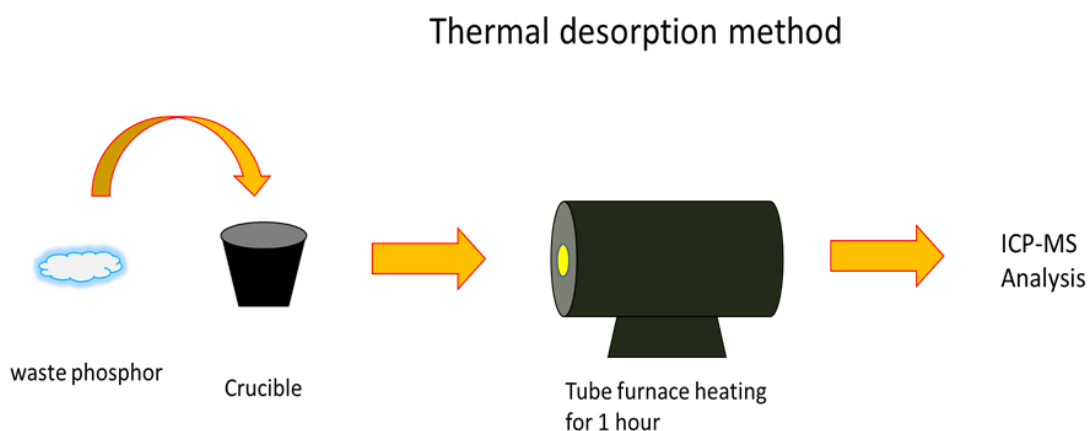
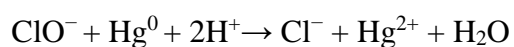


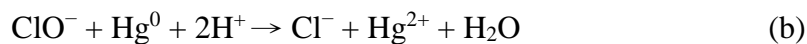
Figure 1-7. Thermal desorption method

Sonication- Mercury interacts with hypochlorite over a wide pH range. A maximum of oxidation was observed at pH = 6.5–6.9, which is consistent with the maximum decomposition rate of hypochlorite. The proposed reactions are as follows⁵¹:

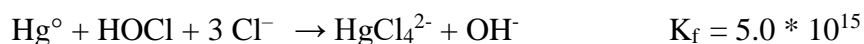
i) in acidic solution:



ii) in neutral solution:



Twidwell and Thompson proposed the following reaction⁵²:



Coskun et al. reported 96% mercury leaching efficiency from waste phosphors was reached by using 0.2M NaCl/0.5M NaOCl solution at 50°C and stirring for 2 hours⁵³. Therefore, our plan is to use water, and NaCl/NaOCl solutions which are made from both commercial bleach and sodium hypochlorite as the hypochlorite sources to treat waste phosphors under the influence of ultrasound on various time spans and see whether we can achieve a better efficiency.

After both treatments, the phosphors were analyzed with ICP-MS for mercury content and their reusability will be examined by scanning electron microscope (SEM) and fluorescence spectroscopy to check their particle images and spectra. The flow chart for sonication mercury removal is shown in Figure 1-8.

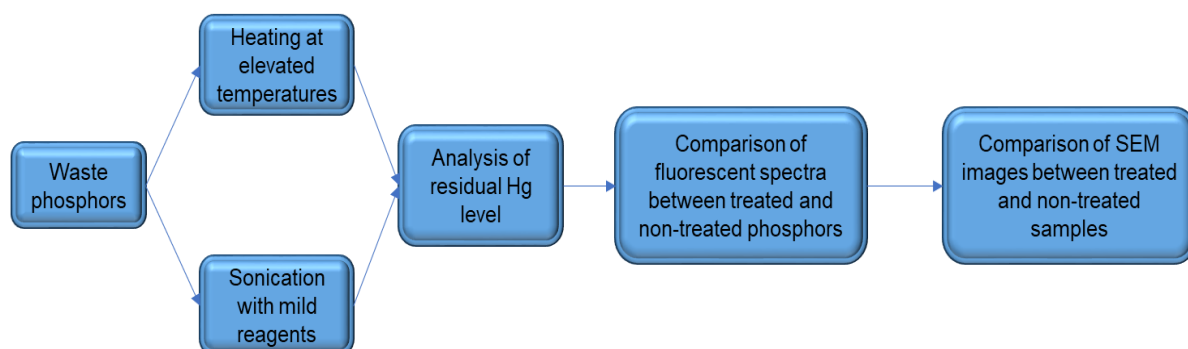


Figure 1-8. Flow chart for sonication mercury removal method

- (b) *Recovering rare earth elements from pretreated waste phosphor through supercritical fluid extraction using a TBP-HNO₃ system.*

Due to the stable nature of blue and green phosphors, a pretreatment method appears to be necessary before supercritical extraction. Wu et al. investigated the calcination of green phosphor ($\text{Ce}_{0.67}\text{Tb}_{0.33}\text{MgAl}_{11}\text{O}_{19}$) using sodium peroxide system, and the phosphor was converted to the mixtures of Na_2CeO_3 , Na_2TbO_3 , MgO_2 , NaAlO_2 and Na_4SiO_4 . The optimal molten salt calcining conditions were found to be 650 °C, 50 min, and 1.5 : 1 of Na_2O_2 -to-waste mass ratio³⁹. Therefore, we employed Wu's method with modification to treat waste phosphors and decompose the metrics before carrying out supercritical extraction. In order to evaluate the rare earth extraction efficiencies with the TBP-HNO₃ complex, we conducted experiments under atmospheric pressure prior to performing supercritical extractions. After the extraction experiments, we compared the results for supercritical extraction of non-treated and treated waste phosphors.

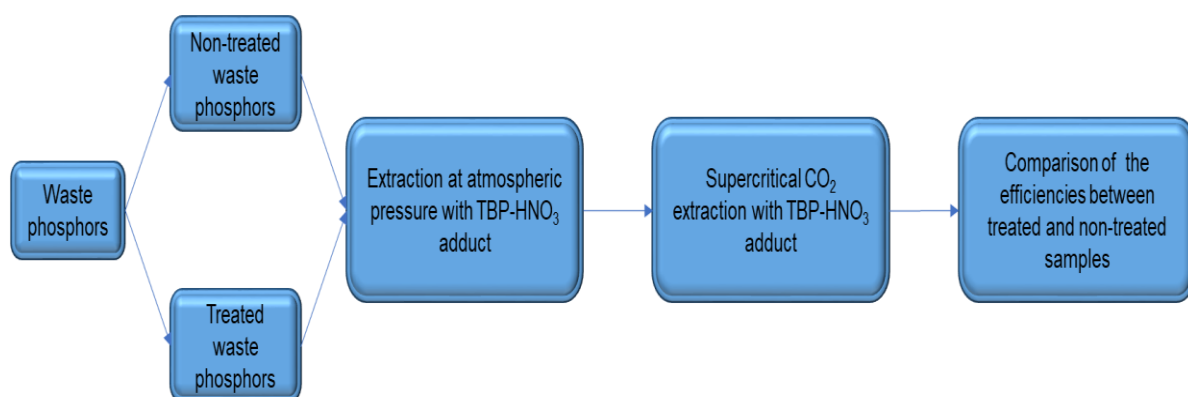


Figure 1-9. Flow chart for recovery of rare earth elements from waste phosphors with supercritical CO₂

- (c) *Leaching rare earth elements from waste phosphor using reagents with ultrasonic assistance*

Phosphor powders were sonicated with various reagents such as nitric acid, sodium hydroxide, hydrogen peroxide, and DI water. The leachates of the experiments are analyzed to calculate the percentage of leached rare earth elements remained in the residue. Fluorescence spectroscopy and SEM will be used to check the difference between before and after the process.

1.5. Achievement

- (A) By using NaCl/NaOCl solutions made from commercial bleach with the assistance of ultrasound, the mercury level of spent phosphors from end-of-life fluorescent lamps was successfully reduced to 3.5% of the original level in 5 minutes. In addition, it was below the maximum concentration of contaminants for the toxicity characteristic. That is- the USEPA standard of mercury for non-hazardous wastes was met.
- (B) By pretreating spent phosphors with sodium peroxide at 650°C, cerium, lanthanum and terbium in the treated phosphors become extractable by supercritical fluid carbon dioxide (sc-CO₂). The extraction efficiencies for cerium, lanthanum and terbium are over 96% using a tri-n-butylphosphate-HNO₃ extractant in sc-CO₂.
- (C) With nitric acid of 11M at 80°C under sonication for 1 hour, yields over 99% of cerium, europium, lanthanum and yttrium as well as 93% of terbium were extracted from the fluorescent phosphors.

References

1. Saini, S. M.; Singh, N.; Nautiyal, T.; S., A., Optical properties of heavy rare earth metals (Gd–Lu). *Solid State Communication* **2006**, *140*, 125-129.
2. Croat, J. J.; Herbst, J. F.; Lee, R. W.; Pinkerton, F. E., High-energy product Nd–Fe–B permanent-magnets *Applied Physics Letters* **1984**, *44*, 148-149.
3. Binnemans, K.; Jones, P. T.; Blanpain, B.; Van Gerven, T.; Yang, Y.; Walton, A.; Buchert, M., Recycling of rare earths: a critical review. *Journal of Cleaner Production* **2013**, *51*, 1-22.
4. Mineral Commodity Summaries 2017. U.S. Geological Survey: 2017; pp 128-129.
5. Humphries, M., Rare Earth Elements: The Global Supply Chain 2013; pp 1-27.
6. https://www.wto.org/english/tratop_e/dispu_e/cases_e/ds431_e.htm. (accessed 10/2/2017).
7. Hartman, H. L.; Mutmanský, J. M., *Introductory mining engineering*. 2002.
8. Critical Materials Strategy (2010). U.S. Department of Energy: 2010; pp 1-170.
9. Critical Materials Strategy (2011). U.S. Department of Energy: 2011; pp 1-190.
10. *Environmental Impact Analysis: Spent Mercury-Containing Lamps (4th edition)* National Electrical Manufacturers Association: 2000; pp 1-9.
11. Schüler, D.; Buchert, M.; Liu, R.; Dittrich, S.; Merz, C. *Study on Rare Earths and Their Recycling* The Greens/EFA Group in the European Parliament 2011; pp 1-140.
12. USEPA <http://www.epa.gov/mercury>. (accessed 10/2/2017).
13. Engelhaupt, E., Do compact fluorescent bulbs reduce mercury pollution? *Environ. Sci. Technol.* **2008**, *42* (22), 8176-8176.

14. Eckelman, M. J.; Anastas, P. T.; Zimmerman, J. B., Spatial Assessment of Net Mercury Emissions from the Use of Fluorescent Bulbs. *Environ. Sci. Technol.* **2008**, *42* (22), 8564–8570.
15. USEPA, Comments Related to Industry Source Reduction Efforts. Response to comments document. Final rule on hazardous waste lamps. USEPA, Ed. 1998; pp 1-22.
16. Dang, T.; Frisk, T.; Grossman, M., Applications of surface analytical techniques for study of the interactions between mercury and fluorescent lamp materials. *Analytical and Bioanalytical Chemistry* **2002**, *373* (7), 560-570.
17. Aucott, M.; McLinden, M.; Winka, M., Release of Mercury from Broken Fluorescent Bulbs. *Journal of the Air & Waste Management Association* **2003**, *53* (2), 143-151.
18. Jang, M.; Hong, S. M.; Park, J. K., Characterization and recovery of mercury from spent fluorescent lamps. *Waste Management* **2005**, *25* (1), 5-14.
19. Raposo, C.; Windmüller, C. C.; Durão Júnior, W. A., Mercury speciation in fluorescent lamps by thermal release analysis. *Waste Management* **2003**, *23* (10), 879-886.
20. Toolkit for identification and quantification of mercury releases UNEP Chemicals: 2005; pp 1-275.
21. USEPA, Introduction to Hazardous Waste Identification (40 CFR Parts 261). 2005; pp 1-26.
22. Ronda, C. R., Phosphors for lamps and displays: an applicational view. *Journal of Alloys and Compounds* **1995**, *225* (1), 534-538.
23. Jüstel, T.; Nikol, H.; Ronda, C., New Developments in the Field of Luminescent Materials for Lighting and Displays. *Angewandte Chemie International Edition* **1998**, *37*, 3085-3103.

24. Tian, Z. C. L., The status Quo of rare-earth three primary colors phosphor for lamps. *Chin Light Light* **2012**, *5*, 21-23.
25. Loyland, S.; Yeh, M.; Phelps, C.; Clark, S., Effects of supercritical fluid extractions on metal ion partitioning as indicated by sequential extractions. *J of Radioanal Nucl Chem* **2001**, *248*, 493-499.
26. Mincher, B.; Fox, R.; Holmes, R.; Robbins, R.; Boardman, C., Supercritical fluid extraction of plutonium and americium from soil using thenoyltrifluoroacetone and tributylphosphate complexation. *Radiochim Acta* **2001**, *89*, 613-617.
27. Mincher, B. J.; Wai, C. M. W.; Fox, R. V.; Baek, D. L.; Yen, C.; Case, M. E., The separation of lanthanides and actinides in supercritical fluid carbon dioxide. *J Radioanal Nucl Chem* **2016**, 2543-2547.
28. Laintz, K. E.; Wai, C.; Yonker, C.; Smith, R., Solubility of fluorinated metal diethyldithiocarbamates in Supercritical carbon dioxide. *The Journal of Supercritical Fluids* **1991**, *4* (3), 194-198.
29. J. Carrott, M.; E. Waller, B.; M. Wai, C.; J. Carrott, M.; G. Smart, N., High solubility of $\text{UO}_2(\text{NO}_3)_2 \cdot 2\text{TBP}$ complex in supercritical CO_2 . *Chemical Communications* **1998**, (3), 373-374.
30. Samsonov, M. D.; Wai, C. M.; Lee, S.-C.; Kulyako, Y.; Smart, N. G., Dissolution of uranium dioxide in supercritical fluid carbon dioxide. *Chemical Communications* **2001**, *18*, 1868-1869.
31. Enokida, Y.; Yamamoto, I.; Wai, C. M.; Gopalan, A. S.; Jacobs, H. K., Extraction of uranium and lanthanides from their oxides with a high-pressure mixture of TBP- HNO_3 - H_2O - CO_2 . In *ACS Symposium Series*, 2003; Vol. 860(Supercritical Carbon Dioxide), pp 10-22.

32. Enokida, Y.; Tomioka, O.; Lee, S.-C.; Rustenholz, A.; Wai, C., Characterization of a tri-n-butyl phosphate-nitric acid complex: a CO₂-soluble extractant for dissolution of uranium dioxide. *Ind Eng Chem* **2003**, *42* (21), 5037-5041.
33. Shimizu, R.; Sawada, K.; Enokida, Y.; Yamamoto, I., Supercritical fluid extraction of rare earth elements from luminescent material in waste fluorescent lamps. *The Journal of Supercritical Fluids* **2005**, *33* (3), 235-241.
34. Paulino, J. F.; Afonso, J. C.; Mantovano, J. L.; Vianna, C. A.; Silva Dias da Cunha, J. W., Recovery of tungsten by liquid-liquid extraction from a wolframite concentrate after fusion with sodium hydroxide. *Hydrometallurgy* **2012**, *127* (Supplement C), 121-124.
35. Manhique, A. J.; Focke, W. W.; Madivate, C., Titania recovery from low-grade titaniferous minerals. *Hydrometallurgy* **2011**, *109* (3), 230-236.
36. Wang, X.; Zheng, S.; Xu, H.; Zhang, Y., Leaching of niobium and tantalum from a low-grade ore using a KOH roast-water leach system. *Hydrometallurgy* **2009**, *98* (3), 219-223.
37. Porob, D. G.; Srivastava, A. M.; Nammalwar, P. K.; Ramachandran, G. C.; Comanzo, H. A. Rare earth recovery from fluorescent material and associated method. US8137645 B2, 2012.
38. Zhang, S.-G.; Yang, M.; Liu, H.; Pan, D.-A.; Tian, J.-J., Recovery of waste rare earth fluorescent powders by two steps acid leaching. *Rare Metals* **2013**, *32* (6), 609-615.
39. Wu, Y.; Wang, B.; Zhang, Q.; Li, R.; Yu, J., A novel process for high efficiency recovery of rare earth metals from waste phosphors using a sodium peroxide system. *RSC Advances* **2014**, *4* (16), 7927-7932.
40. <http://sonicat-systems.com/technology/>. (accessed 10/7/2017).

41. Bang, J. H.; Suslick, K. S., Applications of Ultrasound to the Synthesis of Nanostructured Materials. *Advanced Materials* **2010**, *22* (10), 1039-1059.
42. Xu, H.; Zeiger, B. W.; Suslick, K. S., Sonochemical synthesis of nanomaterials. *Chemical Society Reviews* **2013**, *42* (7), 2555-2567.
43. Flannigan, D. J.; Suslick, K. S., Plasma formation and temperature measurement during single-bubble cavitation. *Nature* **2005**, *434* (7029), 52-55.
44. Hiraide, M.; Mikuni, Y.; Kawaguchi, H., Solid-liquid extraction with an ammoniacal EDTA solution for the separation of traces of copper from aluminium. *Anal. Sci.* **1995**, *11* (4), 689-691.
45. Pokhrel, N.; Vabbina, P. K.; Pala, N., Sonochemistry: Science and Engineering. *Ultrasonics Sonochemistry* **2016**, *29* (Supplement C), 104-128.
46. Rice, E. L., *Biological control of weeds and plant diseases, Advances in Applied Allelopathy*. University of Oklahoma Press: 1995.
47. Schmall, A.; Brau.-Rundschau, S., *Chem. Abstr.* **1954**, *47*, 2932.
48. Vinatoru, M., An overview of the ultrasonically assisted extraction of bioactive principles from herbs. *Ultrasonics Sonochemistry* **2001**, *8* (3), 303-313.
49. Li, H.; Ohdaira, E.; Ide, M., Effects of Ultrasound on Extraction of Saponin from Ginseng. *Japanese Journal of Applied Physics* **1994**, *33* (5B), 3085-3087.
50. Romdhane, M.; Gourdon, C., Investigation in solid-liquid extraction: influence of ultrasound. *Chemical Engineering Journal* **2002**, *87*, 11-19.
51. Liu, S.-Y.; Nengzi, L.-C.; Qu, B.; Liu, P.; Ye, Z.-X., Simultaneous Removal of Elemental Mercury in Aqueous Potassium Hypochlorite by Oxidation. *Environmental Engineering Science*. **2010**, *27* (4), 323-327.

52. Twidwell, L. G.; Thompson, R. J., Recovering and recycling Hg from chlor-alkali plant wastewater sludge. *Journal of The Minerals Metals & Materials Society* **2001**, 53, 15-17.
53. Coskun, S.; Civelekoglu, G., Recovery of Mercury from Spent Fluorescent Lamps via Oxidative Leaching and Cementation. *Water, Air, & Soil Pollution* **2015**, 226 (6).

Chapter 2: Ultrasound-Assisted Mercury Removal of Rare Earth Phosphors from End-of-Life Fluorescent Lamps

Abstract

Due to the current trends of development in renewable energy, rare earth elements (REEs) are receiving more and more attention. Reclaiming the rare earth metals from REE-containing end-of-life electronics has become an active research area. The phosphors of end-of-life fluorescent lamps are rich in REEs such as cerium, europium, lanthanum, terbium and yttrium. Two strategies for recycling are either to reuse the phosphors or to recover the REEs. However, toxic mercury is employed in fluorescent lamps to generate UV light to excite the phosphors which produce visible light. As a result, removing mercury becomes important. NaCl/NaOCl solutions were reported to be able to remove mercury from Chlor-Alkali plant wastewater sludge and fluorescent phosphors. However, traditional agitation methods usually require extended time to process. In this investigation, an ultrasound-assisted mercury removal method is reported. Under sonication, the mercury level in the spent phosphors can be reduced rapidly in a few minutes and meet the USEPA standards for universal non-hazardous wastes. The potential of reusing waste phosphors is discussed.

2.1. Introduction

Fluorescent lamps, which rely on mercury for their operation, have become the most important electrical lighting devices over the past few decades due to their high lighting efficiencies. When electricity passes through a fluorescent lamp, the mercury vapor in the lamp will generate ultraviolet radiation (254 nm), which in turn excites the white coating on the inner wall of the lamp tube to emit visible light. The light-emitting coating is typically a mixture of phosphors that contain rare earth elements (REEs) in the forms of oxides, phosphates, or aluminates. Because of REEs' unique optical, electrical, magnetic and catalyst properties, they are listed as the critical materials by the U.S. Department of Energy¹⁻². Approximately 7% of global consumption of rare earth metals was used in phosphors, but the cost accounted for 32% of the global rare earth market value in 2008³. It's because the REEs used in phosphors must be 99.999% pure, and even only a few ppm of impurities can change the color characteristics of a given phosphor. To produce phosphors with these high purities, many more steps are required for the purification process, which inevitably causes significant raise of the prices for the REEs used in phosphors. Annually, more than 680 million fluorescent lamps are estimated to be disposed of in the U.S.⁴. The extensive use over the years has caused not only growing concerns over their proper disposal, but also a great deal of resource waste. Thus, recycling or reusing rare earth phosphors has become one of the strategies described in the U.S. Department of Energy Critical Materials reports. This strategy can reduce America's demand for rare earth raw materials and minimize environmental impacts. It also increases America's supply diversities and securities of critical materials¹⁻².

Because of the presence of mercury, all end-of-life fluorescent lamps are considered hazardous by the U.S. Environmental Protection Agency (USEPA). According to National

Electrical Manufacturers Association (NEMA), a typical F40T12 (the most commonly used fluorescent lamp, tubular type 40 W/T12, length of 122 cm and 3.8 cm of diameter) lamp rated for 20,000 h of life requires a minimum of 10 mg of mercury ($0.7 \mu\text{l}$)⁵. An insufficient amount of mercury in a fluorescent lamp will lead to premature failure, so-called “mercury starvation” within the industry. Due to the reactive nature of mercury, it interacts with all the components of a lamp and becomes dispersed throughout the lamp. The mercury will also be oxidized and adsorbed onto the phosphor matrix and all other lamp components during operation⁶⁻¹¹. To avoid premature failure, the average amount of mercury inserted into fluorescent lamps by manufacturers is generally set to no less than 15 mg for an F40T12⁵, and for a typical compact fluorescent lamp (CFL), the amount of mercury is approximately 5 mg¹². The mercury content of fluorescent lamps differs depending on the manufacturer, the wattage, the type of lamp (linear or compact), the year of manufacture, and age.

According to federal regulations for land disposal restrictions (LDRs) (40 CFR §268.40), mercury wastes are categorized as low mercury, high mercury, or elemental mercury wastes. Table 2-1¹³ describes the applicability of treatment standards for each of these wastes¹³⁻¹⁴. That is, if we are looking to dispose of waste phosphors, for example, by landfill, 0.025 mg/L TCLP (Toxicity Characteristic Leaching Procedure)¹⁵ has to be met. However, if we are looking to reclaim end-of-life fluorescent lamps instead of discarding them, the secondary materials are subject to the standards under 40 CFR §273 (standards for universal waste management) and §261.24 (identification and listing of hazardous waste). That is, the concentration of mercury in the phosphors from end-of-life fluorescent lamps cannot exceed the maximum concentration listed in the table 1 of 40 CFR § 261.24, which is 0.2 mg/L TCLP.

Table 2-1. Land Disposal Restrictions (Source: Treatment Technologies for Mercury in Soil, Waste, and Water, EPA)

Type of Waste	Land Disposal Restrictions
Low mercury waste (contain less than 260 mg/kg of total mercury)	If retorted, 0.2 mg/L TCLP If other technologies are used – 0.025 mg/L TCLP (solidification/stabilization often used to meet this level)
High mercury waste (contain greater than 260 mg/kg total mercury)	Required to be roasted or retorted until waste becomes a low mercury waste. Residuals then required to meet 0.2 mg/L TCLP
Elemental mercury waste (with radioactive contamination)	Required be treated using amalgamation

There are various mercury treatment technologies such as solidification/stabilization, solid washing, vitrification and so on¹³, but the conventional methods generally employed for removal of mercury from used rare earth-containing phosphors are thermal desorption and chemical leaching¹⁶⁻¹⁸. Thermal desorption is the most widely used method, in which the spent rare earth-containing phosphors are heated under elevated temperatures above mercury boiling point (375°C) to vaporize the mercury content. The baking process is energy-intensive, and requires specially-designed equipment to condense and collect mercury. An operational system under negative pressure is usually employed to avoid escape of mercury vapor. Researchers have been developing methods to facilitate the thermal desorption process^{7, 16, 19-20}. Pogrebnaja et al. used an alkaline solution as a neutralizing reagent to obtain a complex compound of mercury from lamp powders before submitting it to a thermal treatment¹⁹. Jang et al. heated mercury-containing phosphors above the boiling point of mercury (375 °C) for 4–20 h in a retort. The mercury vapor was condensed in the scrubber and then collected in a decanter. Additional treatments such as bubbling through nitric acid were employed to remove impurities after the thermal process⁷. Fujiwara and Fujinami investigated substances that can

assist the reduction of mercury species and lower the temperature of thermal desorption process¹⁶. As for chemical leaching, in Cogar et al.'s report, ionic exchange method was employed to recover mercury from the resulting solution derived from the extraction of phosphor powder in a chemical process²⁰. Chemical leaching of mercury from phosphors with sodium chloride/sodium hypochlorite in aqueous solution was also reported²¹. Coskun et al. obtained the optimal results for mercury removal by heating NaCl/NaOCl (0.2M/0.5M) solution with waste phosphors at 2-h contact time, pH 7.5, 50°C, a 1:2 solid-to-liquid ratio (g/ml) and a 120-rpm agitation speed, in which 96% of mercury could be transferred into solution²¹. Although this process is quite effective, it is time-consuming, and pH control is required.

Ultrasound has been used in various applications in chemical engineering: waste-water treatment, organic synthesis, sonochemistry and solid-liquid extraction²²⁻²⁴. Application of ultrasonic radiation to liquid will cause a phenomenon called cavitation, i.e. formation, growth and collapse of acoustic bubbles. This phenomenon gives rise to both chemical and physical effects. The collapse of cavitation bubbles creates local hotspots, and inside these hotspots, the temperature and pressure can reach as high as 5000°C, and 1000 atm. Furthermore, when bubbles are near a solid surface, they will collapse in an asymmetrical fashion and form high-speed microjets. These microjets are responsible for surface deformation and rapid mass transfer²⁵⁻²⁶. Therefore, acoustic cavitation provides unique environments for chemical reactions.

As mentioned earlier, REEs used in phosphors are required to be highly pure (99.999%). Consequently, the prices of the REEs sold to phosphor manufacturers are much higher than those used by manufacturers of other REE applications¹. If an efficient method

could be developed to reduce mercury level in spent fluorescent phosphors down to an acceptable level, and at the same time, the light emitting properties still remain the same, reuse of rare earth phosphors may become practical and economically desirable. Some studies regarding reuse of used phosphors were reported. Takahashi et al. developed a 2-step liquid-liquid extraction method to separate red, blue and green phosphors from used fluorescent lamps. In this method, aqueous and organic solvents were mixed with different reagents, respectively. In each step, distinct types of phosphors were extracted to different phases. For example, in step 1, the blue phosphor was extracted to the organic phase while the red and green phosphors were extracted to the aqueous phase; In step 2, the green phosphor was extracted into the organic phase, and the red phosphor separated from the green powders remained in the aqueous phase²⁷. Liu et al. invented a procedure to regenerate trichromatic phosphors from used rare earth phosphors. The waste phosphors were first washed with an acetic acid solution and then ethanol. The washed phosphors were then mixed and ground with the same amount of glass balls. The obtained powders were heated in the mixture of H₂ (5%)/N₂ (95%) at 600°C for 1 hour. Finally, the resulting powders were calcined at 500°C for 30 min in air to get the product. Compared to new phosphors, the regenerated phosphors lost approximately 5–15% luminous efficiency²⁸.

In this paper, we report a simple process of collecting phosphors in a liquid system from fluorescent lamps incorporating sonication and an ultrasound-assisted leaching method to reduce mercury level of the fluorescent phosphors down to the USEPA standards at a relatively low temperature in a shorter reaction time with sodium chloride/sodium hypochlorite solutions, in which commercial laundry bleach used as the source of sodium hypochlorite was evaluated. The reusability of used fluorescent phosphors after the treatment

will also be discussed. The details of our procedures and the emission properties of the phosphors after mercury removal are given in the following sections.

2.2. Experimental Section

2.2.1. Waste samples collection, chemicals, instruments and analysis methods

Sylvania phosphor powders were collected in 2 separate ways for different purposes. For evaluation of the efficiency of ultrasound-assisted phosphor collection technique, phosphors were collected by immersing fluorescent lamp sections into the water of a sonication bath (Fisher Scientific FH60H, 100-Watt, 42 kHz). For mercury removal experiments, in order to reduce the chance of losing mercury content of the phosphors into the water in sonication bath before experiments, the phosphor material was scratched manually from end-of-life Sylvania fluorescent lamps and collected in a 250-mL plastic bottle. This bottle was well capped and placed in a desiccator. Sodium hypochlorite solution (10%-15%) was purchased from Sigma Aldrich. Commercial 1-gallon Clorox bleach solution with 8.25% sodium hypochlorite (NaOCl) was obtained from a local store. Sodium chloride was purchased from EMD Chemicals Inc. A sonication bath and an ultrasonic liquid processor (Sonics, VCX130) were both used to conduct mercury removal experiments. After the experiments, all the treated phosphor samples were digested following USEPA SW846 Method 3050B, and the mercury content was analyzed using ICP-MS (Agilent 7700x) with a Cetac 520 Autosampler following SW846 Method 6020A. Toxicity Characteristic Leaching

Procedure (TCLP) was performed following USEPA SW-846 Test Method 1311. Fluorescence spectra were obtained using a fluorescence spectrometer (FluoroMax-3, Horiba).

2.2.2. Mercury removal by thermal desorption

In this study, samples of approximately 250 mg waste phosphors were transferred into nickel crucibles and heated in a tube furnace at elevated temperatures for one hour in increments of 100°C until all mercury was removed from the waste phosphors.

2.2.3. Mercury removal by NaCl/NaOCl solution with and without sonication

NaCl/NaOCl solutions of various concentrations were prepared by using both sodium hypochlorite solution purchased from Sigma Aldrich and commercial 1-gallon Clorox bleach as the sources of sodium hypochlorite. Samples of approximately 250 mg waste phosphors with 20 ml of the prepared solutions were transferred into 30 ml vials. These vials were well capped. In these experiments, the vials were divided into 3 sets. Each set of the vials was agitated in a unique way: (a) Magnetically stirred at 120 rpm in a 50°C oil bath; (b) Sonicated in a 50°C sonication bath. The ultrasonic frequency and power were the default settings (42 kHz, 100 Watt); (c) Sonicated by an ultrasonic liquid processor. The ultrasonic processor was inserted into the vials at room temperature. The sonication amplitude was set as 80%, and sonication time as 2 seconds of pause for every 8 seconds of sonication. After sonication, all the samples were centrifuged, and the supernatants were decanted and collected. The phosphor powder residues were then washed with 10 ml deionized water and centrifuged 3 times totally. All the supernatants from the same trial were collected individually, and 50 µl of concentrated nitric acid was added to each vial to stabilize the mercury. Solid samples were air dried before ICP-MS analysis.

2.2.4. Mercury removal by DI water with sonication

In order to compare the efficiency of mercury removal with NaCl/NaOCl solutions under ultrasound influence, samples of 250 mg waste phosphor were sonicated with 20 ml of deionized water using an ultrasonic liquid processor. After experiments, samples were processed through the same procedure as the previous section.

2.3. Results and Discussion

2.3.1. Collection of phosphors from used fluorescent lamps using sonication in a liquid system

A simple method of collecting rare earth phosphors from end-of-life fluorescent lamps is to use water bath under sonication as illustrated in Figure 2-1. A section of compact fluorescent lamp is placed into a beaker with water, and the beaker is immersed in a sonication bath (42 kHz, 100 watt). After 30-60 seconds of sonication, the white rare earth phosphor coating is totally removed from the inner wall of the lamp (Figure 1b) with gentle shaking. After rinsing, the phosphor powder in water can be filtered, dried, and stored in a desiccator for further experiments. Compared to other phosphor collection methods such as scratching phosphors from lamp tubes or pulverizing the phosphor along with the glass lamp tubes, ultrasound-assisted collection method is simple, safe, time-efficient and able to remove the phosphor coating completely from the tubes.



Figure 2-1. Ultrasound-assisted collection of rare earth phosphors from used compact fluorescent lamps. (a) Sonication bath (42kHz 100 watt) with a compact fluorescent lamp, (b) the lamp after 30 seconds of sonication and rinsing.

2.3.2. Mercury removal by thermal desorption

Approximately 250 mg of the collected phosphor was transferred to a nickel crucible and roasted at elevated temperatures for one hour. The mercury content in the treated samples were then analyzed by ICP-MS after digestion. The results in Figure 2 show that when the samples are roasted for 1 hour at 600°C and above, the mercury content in the phosphor is undetectable, which is consistent with those reported in the literature⁸. Mercury removed from waste phosphors through roasting becomes vapor and can be collected in a closed system by condensation. Nevertheless, the process requires high energy input and special-designed equipment. It is also time-consuming and may have complications of mercury contamination of the system.

Thermal Desorption

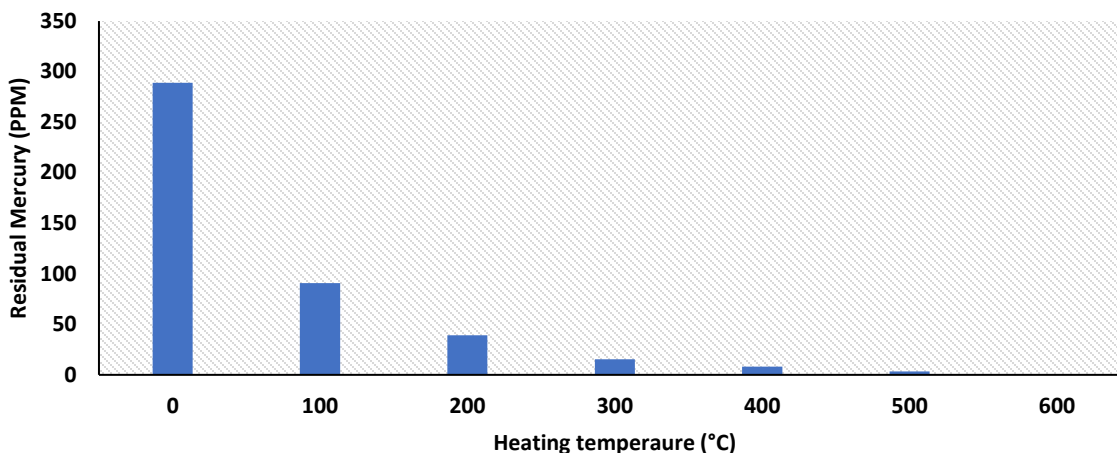
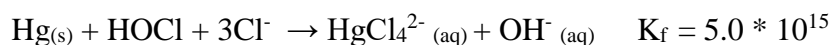


Figure 2-2. Roasting waste phosphors in a tube furnace: Removal mercury from the phosphors by heating at elevated temperatures for 1 hour. The phosphors were collected from used Sylvania fluorescent lamps.

2.3.3. Mercury removal with 0.2M/0.5M NaCl/NaOCl solution in oil bath

Mercury in rare earth-containing phosphors can also be removed by sodium hypochlorite/sodium chloride aqueous solutions as reported by Coskun and Civelekoglu²¹. According to this report, 96% of mercury could be leached by using NaCl/NaOCl (0.2M/0.5M) solution from used fluorescent lamp samples of the nonspecific source at 2-h contact time, pH 7.5, 50°C, a 1:2 solid-to-liquid ratio (g/ml) and a 120-rpm agitation speed. The source of the fluorescent lamps was not specified. The reaction for mercury removal involves the formation of water soluble HgCl_4^{2-} species²⁹.



In order to evaluate this idea, we conducted our experiments by applying Coskun et al.'s optimal concentration and temperature, 0.2M/0.5M NaCl/ NaOCl solutions at 50 °C, for mercury removal from waste phosphors. In this study, we did not control the pH of the

solutions. In addition, we used a different solid-to-liquid ratio (g/ml) from that of Coskun et al.'s because their samples contained pulverized glass, which makes the high solid-to-liquid ratios possible due to the higher density of glass. Also, commercial 1-gallon Clorox bleach solution (8.25% w/w) was used as the sources of sodium hypochlorite. Figure 2-3 shows the results of mercury reduction using 0.2M/0.5M NaCl/NaOCl solutions in oil bath. According to our results, mercury in the phosphors could be reduced to about 10% (~30 ppm) in 30 minutes of contact with NaCl/NaOCl solutions. It should be noted that the phosphors used in our investigation were obtained from used Sylvania fluorescent lamps. The result is roughly consistent with Coskun et al.'s report. Apparently, NaCl/NaOCl solutions work for mercury removal. However, a longer agitation time or different conditions may be required to increase the efficiencies or to further reduce the mercury level in the phosphors. Consequently, we conducted our subsequent experiments with ultrasonic assistance to improve mercury removal efficiencies.

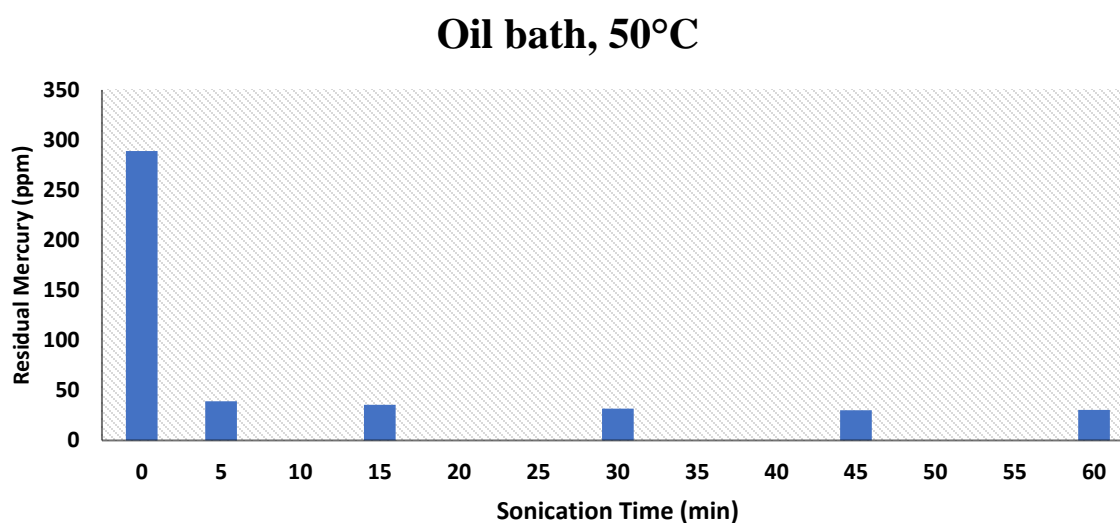


Figure 2-3. Mercury removal with NaCl/NaOCl (0.2M/0.5M) solution in 50°C oil bath

2.3.4. Ultrasound-assisted removal of mercury with 0.2M/0.5M NaCl/NaOCl solution in a sonication bath

Ultrasound is known to facilitate dissolution of certain solid materials in liquids³⁰. It can generate not only physical effects such as extremely high local temperature and pressure but also chemical effects induced by the high temperature and pressure, such as free radical reactions. Cavity formation, growth and collapse in liquids and the subsequent induced sonochemistry are often very complicated. However, sonication has been used and proven to be an effective agitation method for enhancing the rate of reaction, mass transfer, increasing the yield and altering the reaction pathways in various chemical processes due to its high-frequency vibration and/or sonochemical effects³¹⁻³³. The effect of ultrasound for removing mercury from the rare earth phosphors in NaOCl/NaCl (0.2M/0.5M) solutions was investigated using a sonication bath at 50 °C. As shown in Figure 2-4, under sonication, the efficiency of mercury removal was significantly increased. For example, after 45 minutes of sonication, the mercury level in the phosphor was reduced from 289 ppm to 16.6 ppm (~5.7%) of the original mercury content. Compared to the value obtained from the experiments without sonication, i.e. 10.5%, the efficiency improved approximately 45%. The enhanced mercury removal under the influence of ultrasound must be related to the cavitation and sonochemistry occurring in the system, which possibly makes the conversion of mercury trapped in the phosphors into water-soluble mercury species, presumably $(\text{HgCl}_4)^{2-}$, much more efficient. The ultrasound-assisted hypochlorite leaching process for removing mercury from the rare earth-containing phosphors could possibly be a more attractive alternative way than thermal desorption method due to the fact that: (1) it does not require a long leaching time and high energy input; (2) the mercury removed from the phosphors is trapped in an aqueous solution. This way, an expensive, special-designed close system used to collect the mercury vapor may

not be necessary. According to this study, recycling rare earth phosphors from spent fluorescent lamps including phosphor collection and mercury removal can be both processed simultaneously in an aqueous environment with the aid of ultrasound. Mercury leached in the aqueous solution can be finally collected using conventional methods known in the literature³⁴⁻³⁷.

2.3.5. Ultrasound-assisted removal of mercury with 0.2M/0.5M NaCl/NaOCl solution using an ultrasonic liquid processor

Sonication can also be done by inserting an ultrasonic liquid processor into NaCl/NaOCl solutions. In this case, samples of waste phosphor with a 0.2M/0.5M NaCl/NaOCl solution were sonicated at room temperature using an ultrasonic liquid processor (Sonics, VCX 130) at 20 kHz, 130 watts and 80% amplitude for various agitation times. When the sonication process was carried out with direct insertion of an ultrasonic processor, removal of mercury became even more rapid and efficient than in sonication bath. With only 5 minutes of sonication, the mercury level in the phosphor already dropped down to 2.9% of the original mercury content. The results and comparison are shown in Figure 2-4 and Table 2-1. The sonication process started at room temperature (22 °C). As time went by, the temperature of the solutions and glass vials kept increasing with application of ultrasound. Ultrasound is known to produce cavitation phenomenon in aqueous solutions. The subsequent collapse of the cavitation bubbles leads to high localized temperatures and pressures in the system. The temperature of the aqueous system was expected to rise as a result of the cavitation phenomenon and the absorption of acoustic energy. The temperature of the system increased as sonication time increased. In general, the temperature approximately reached up to the range of 70°C to 80°C after 15 minutes of sonication, depending on the conditions. Presumably,

the combination of temperature rises and sonochemical effects occurring inside the system promoted the conversion of the trapped mercury in the phosphors into water-soluble mercury species.

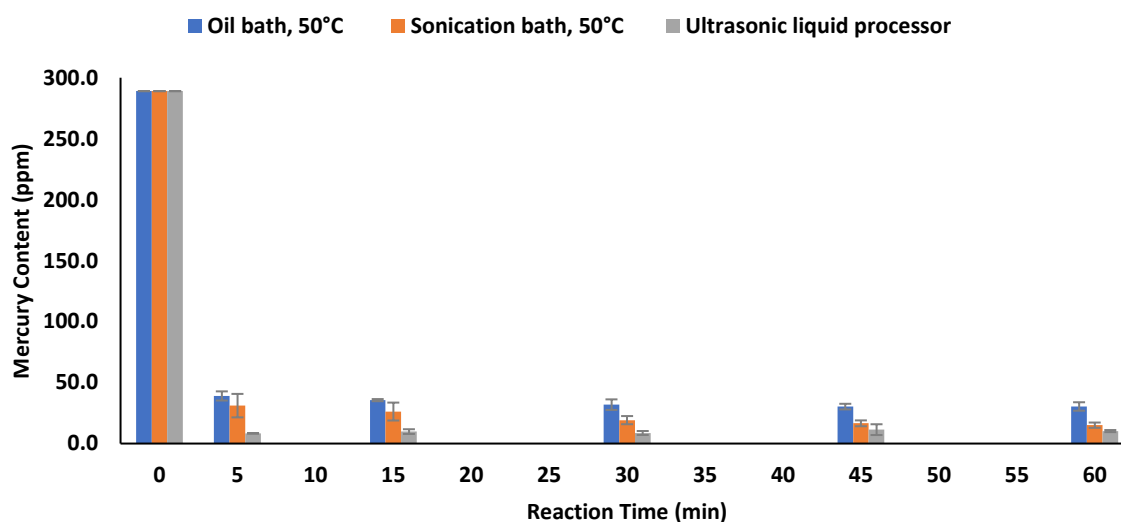


Figure 2-4. Mercury removal with NaCl/NaOCl (0.2M/0.5M) solution: 1) Rate of mercury removal from the phosphors oil bath at 50 °C; 2) removal of mercury from the phosphors in sonication bath at 50 °C; 3) mercury removal from the phosphor using an ultrasonic liquid processor.

Table 2-2. The percentage of residual mercury in the phosphors versus sonication time for each treatment method.

Time (min)	Oil Bath, 50°C	Sonication Bath, 50°C	ultrasonic liquid processor
0	100%	100%	100%
5	13.5%	10.8%	2.9%
15	12.3%	9.1%	3.4%
30	11.0%	6.6%	3.0%
45	10.5%	5.7%	3.9%
60	10.5%	5.2%	3.5%

2.3.6. Assessment of mercury removal through mass balance

After the experiments of ultrasound-assisted removal of mercury with 0.2M/0.5M NaCl/NaOCl solutions using an ultrasonic liquid processor, both the phosphor powder residues and supernatants were sent for ICP-MS mercury analysis. The results are shown in Figure 2-5. According to our results, there are variations in the recovery of each experiment. Except for the experiment of 5-min sonication, which is slightly under-recovered, the rest are all slightly over-recovered. We attribute the under-recovery and over-recovery to human errors in the process of sample preparation, handling and system errors of instrumental analysis. The latter trials tend to have over-recovery rates. The reason could be because the ultrasonic liquid processor was not cleaned properly and the residual mercury from the previous experiment was carried over to the next one. However, the average recovery rate is 109.1%. The relative standard deviation of the trials is 7.2%. It is safe to say that our mass balance is within an acceptable range. Based on our results, we can also see that the average residual mercury level in the phosphor residues is 3.6% and the standard deviation is 1.0%. Therefore, we can make the following assumptions: 1) In general, over 96% of the mercury in the phosphors can be extracted to 0.2M/0.5M NaCl/NaOCl solutions within the first 5 minutes with an ultrasonic liquid processor since longer sonication times did not further and significantly lower the mercury content in the phosphors to the extent of the first 5 minutes; 2) This condition could have reached its equilibrium since extended sonication times did not make any significant differences. As a result, different conditions will need to be applied to further reduce the mercury level.

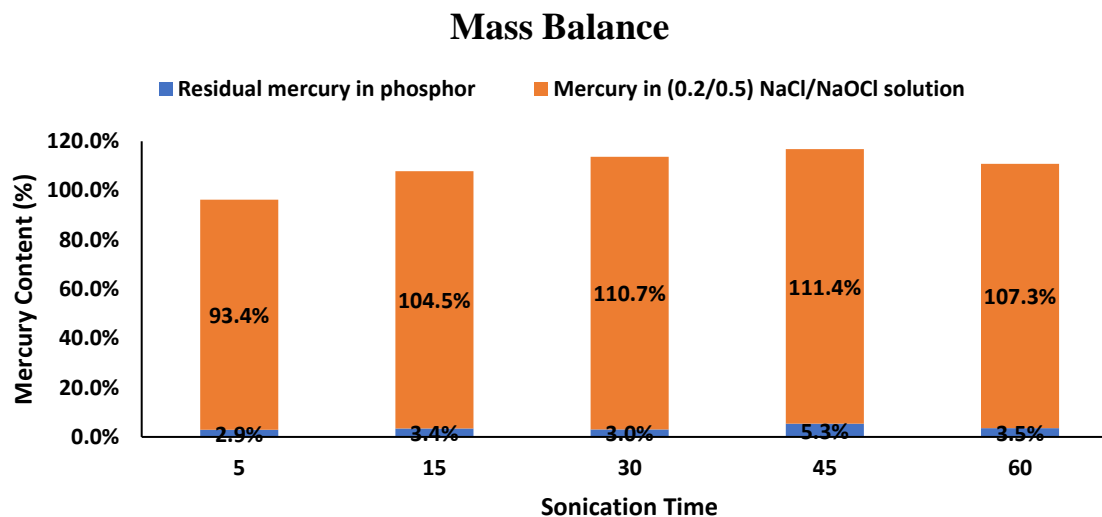


Figure 2-5. Mass balance of mercury content before and after the reaction for each time span

2.3.7. Concentration effect

In order to improve the efficiencies of mercury removal, we investigated the influence of various concentrations for NaCl/NaOCl solutions with sonication using an ultrasonic liquid processor since it provides the most efficient way to remove mercury. We set 0.2M/0.5M NaCl/NaOCl as the default concentration and made solutions that were either fractions or multiples of the default concentration. Due to the fact that the highest available concentration of sodium hypochlorite in the commercial bleach is 8.5%, and that we would like to compare the influences between the commercial bleach and pure sodium hypochlorite solutions, we prepared the solutions using both commercial bleach and pure sodium hypochlorite solutions. In the following Figures, B is prefixed to the solutions made from the commercial bleach and P to the ones made from pure sodium hypochlorite solutions. For example: B-2 x Default stands for 0.4M/1.0M NaCl/ NaOCl solution made with bleach. Figure 2-6 shows the results for phosphors sonicated in NaCl/NaOCl solutions of various concentrations for 5 minutes. In

general, the higher the concentration, the better the efficiency, except for the solution [B-2 x Default]. Compared to the result of phosphorus sonicated in solution [B-2 x Default], solution [P-2 x Default] had a much better efficiency. [B-2 x Default] and [P-2 x Default] have the same concentration of sodium hypochlorite, the only difference is that the commercial bleach contains other chemical components in it. The results seem to tell us that solutions made from pure sodium hypochlorite solutions give better efficiencies in mercury removal.

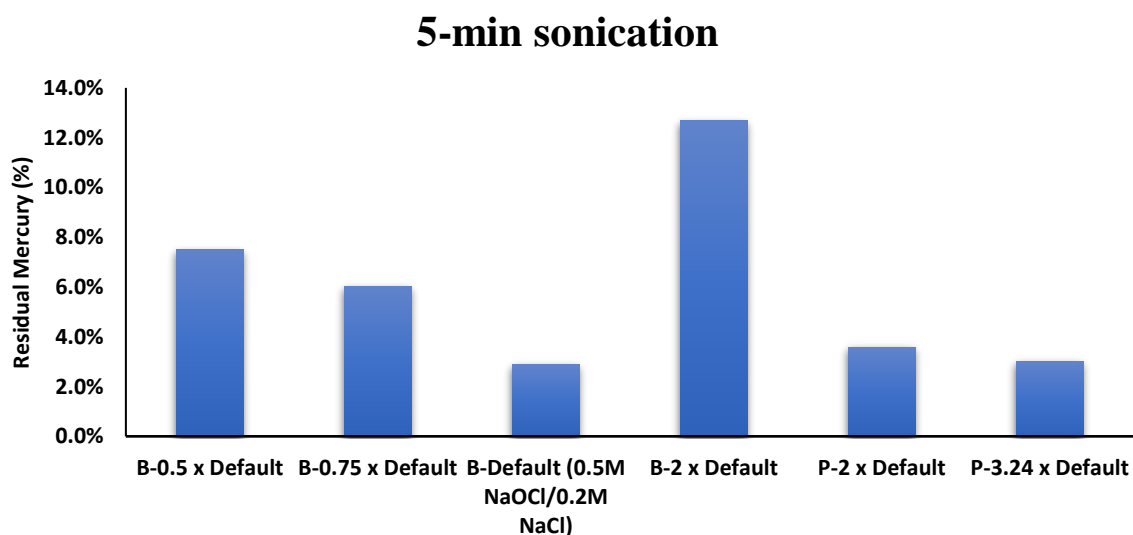


Figure 2-6. 5-minute sonication of phosphorus in NaCl/NaOCl solutions of various concentrations. B prefixes to the solutions made with bleach; P to the solutions made with pure sodium hypochlorite. 0.2M/0.5M NaCl/NaOCl is the default concentration. The concentrations of the other solutions were made to be the fractions or multiples of the 0.2M/0.5M NaCl/NaOCl. For example: 0.5 x Default = 0.1M/0.25M NaCl/NaOCl

2.3.8. Time effect

As we mentioned in the mass balance section, the default concentration seemed to reach its equilibrium. Consequently, the residual mercury only fluctuates around 3.3% and would not go down any more, even with an extended sonication time. For the solutions of higher concentrations, the residual mercury level further went down as we increased sonication time. As illustrated in Figure 2-7, when sonication time was increased from 5 minutes to 15 minutes, the efficiencies for the NaCl/NaOCl solutions with higher concentrations were further improved and remained the same trend as in Figure 2-6. [B-2 x Default] condition still had the least efficiency. The reason is unclear. Perhaps, when we increase the concentration of NaCl/NaOCl solutions, the other chemical components in the bleach can cause negative effects on mercury removal.

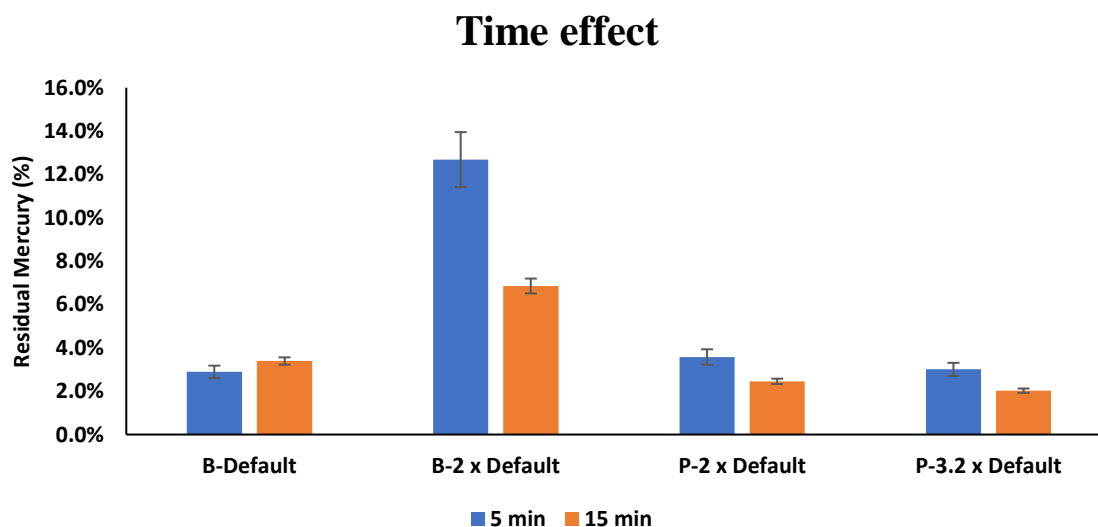


Figure 2-7. Comparison between 5-minute and 15-minute sonication of phosphors in solutions of various concentrations. B prefixes to the solutions made with bleach; P to the solutions made with pure sodium hypochlorite. 0.2M/0.5M NaCl/NaOCl is the default concentration. The concentrations of the other solutions were made to be the fractions or multiples of the 0.2M/0.5M NaCl/NaOCl.

2.3.9. Toxicity characteristic leaching procedure (TCLP)

Even though we have achieved 98% of mercury removal from waste phosphors in only 15 minutes, percentage is only a relative measurement. In addition, our ultimate goal is to meet the requirements and standards of the USEPA. Thus, the treated phosphors were evaluated to see whether the results meet the EPA's standards. Toxicity characteristic leaching procedure (TCLP) is a chemical extraction analysis method to simulate leaching through a landfill, which is employed by the USEPA to determine whether a waste is hazardous or not³⁸. Basically, TCLP is carried out by leaching a waste sample with an acetic acid /sodium hydroxide solution at a 1:20 sample-to-solvent ratio. This leachate mixture is then placed in an extraction vessel, which is rotated at 30 ± 2 rpm for 18 ± 2 hours to simulate an extended leaching time in the ground. The leachate solution is then sent for analysis. If TCLP analytical results are lower than the TCLP contamination standards, the waste is considered non-hazardous. USEPA has different standards and regulations for different purposes. For land disposal, the wastes are subject to the land disposal restrictions (LDRs) (40 CFR §268.40), in which the maximum concentration for mercury is 0.025 ppm TCLP. If they are above these standards, the waste must be taken to a hazardous waste disposal facility and the cost of disposal will increase significantly. For universal waste management purpose, the maximum concentration for mercury is 0.2 ppm TCLP. Therefore, we performed TCLP on the samples that had been treated with NaCl/NaOCl solutions of various concentrations under sonication.

As mentioned in the previous section, 0.2M/0.5M NaCl/NaOCl was set as the default concentration. TCLP was performed on the original phosphor and the phosphor treated in the oil bath. The results in Figure 2-8 indicate that the treatment in oil bath did lower the TCLP

mercury level, but they are still far from meeting the USEPA standards for universal waste management (0.2 ppm) and land disposal (0.025 ppm).

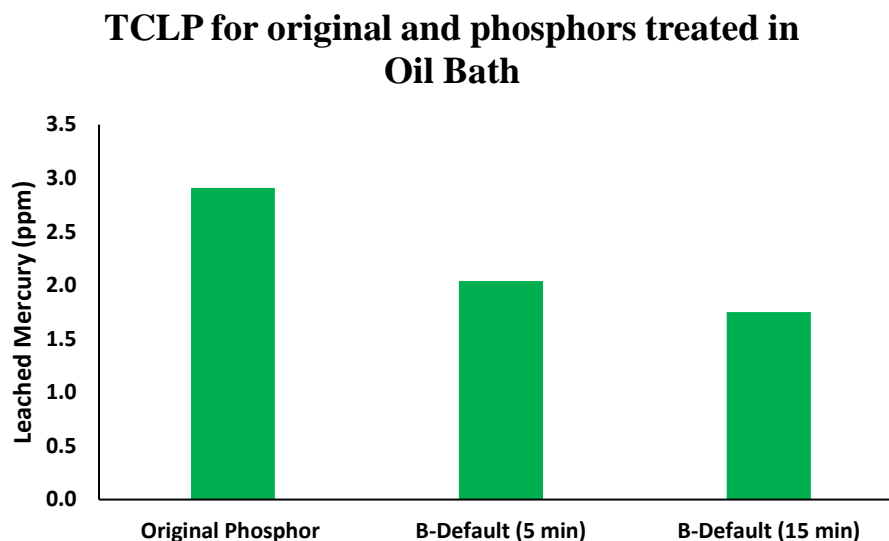


Figure 2-8. Leached mercury level after TCLP was performed on the original phosphor and the phosphor samples treated under the default concentration in oil bath. B prefixes to the solutions made with bleach; 0.2M/0.5M NaCl/NaOCl is the default concentration.

Figure 2-9 shows the TCLP results for phosphors sonicated using ultrasonic liquid processor in the solutions of default concentration at various sonication times. The TCLP results went down as sonication time increased. Also, within the first 5 minutes, the TCLP level already lowered down below the EPA mercury standard for universal waste management. However, it was not low enough to meet the mercury standard for land disposal under the default concentration, even though the samples were sonicated for 1 hour. As a result, changing conditions seems to be a better strategy. Thus, we performed TCLP on the phosphors that were sonicated in NaCl/NaOCl solutions of different concentrations for 5 minutes. The results in Figure 2-10 basically follow the same trend as previous sections. As the samples were

treated with solutions of higher concentrations, less mercury could be leached out via TCLP. Also, under the same condition, solutions made from pure sodium hypochlorite solutions have better efficiencies. Once again, all the results met the standard for universal waste management, but none of them met the standard for land disposal.

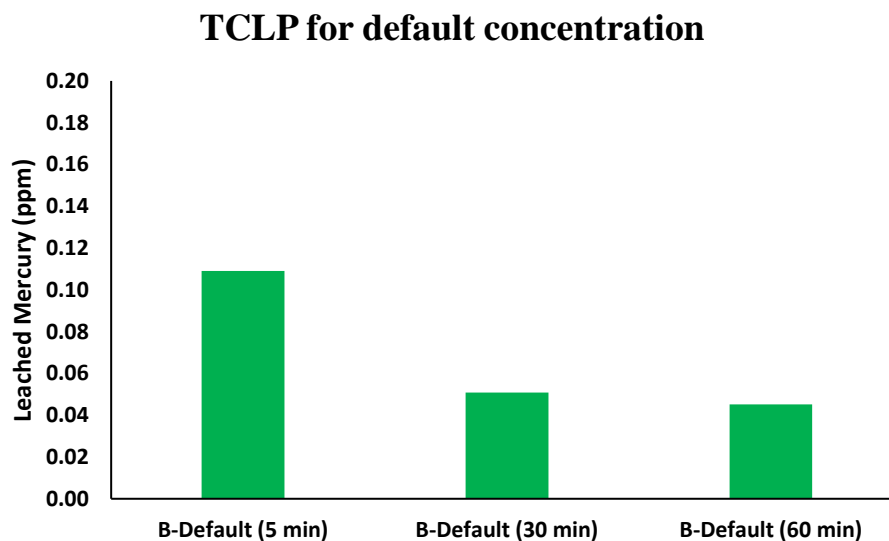


Figure 2-9. Leached mercury level after TCLP was performed on the samples treated under the default concentration under sonication. B prefixes to the solutions made with bleach; 0.2M/0.5M NaCl/NaOCl is the default concentration.

TCLP for 5-min Sonication with various concentrations

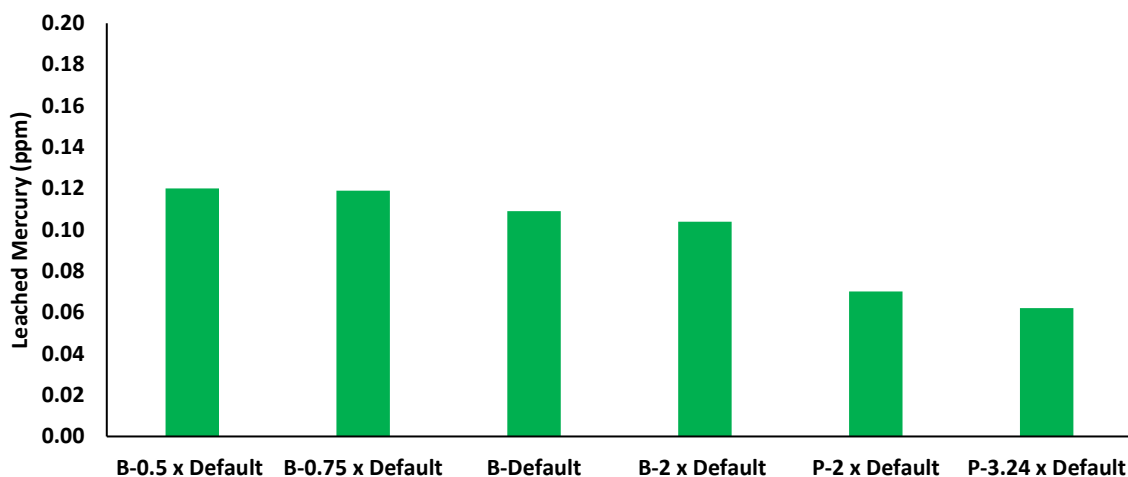


Figure 2-10. TCLP results for phosphors sonicated in NaCl/NaOCl solutions of various concentrations for 5 minutes. B prefixes to the solutions made with bleach; P to the solutions made with pure sodium hypochlorite. 0.2M/0.5M NaCl/NaOCl is the default concentration. The concentrations of the other solutions were made to be the fractions or multiples of the 0.2M/0.5M NaCl/NaOCl.

TCLP for 15-min sonication with various concentrations

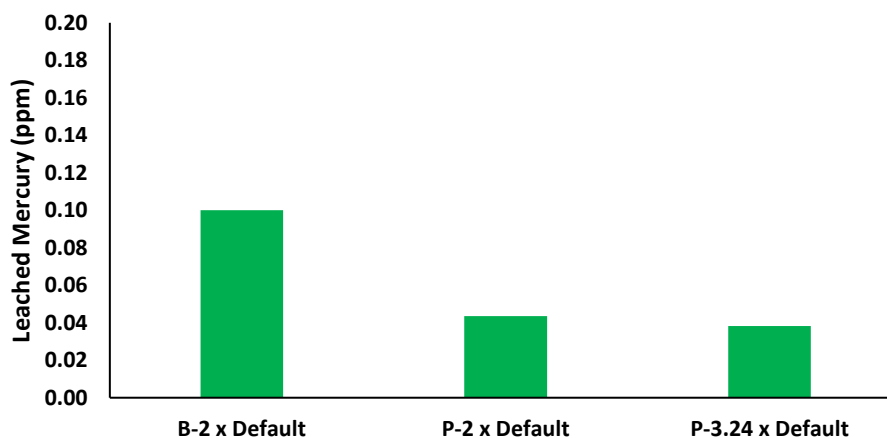


Figure 2-11. TCLP results for 15-minute sonication of phosphors in NaCl/NaOCl solutions of various concentrations. B prefixes to the solutions made with bleach; P to the solutions made with pure sodium hypochlorite. 0.2M/0.5M NaCl/NaOCl is the default concentration. The concentrations of the other solutions were made to be the fractions or multiples of the 0.2M/0.5M NaCl/NaOCl.

Since longer sonication times and higher concentrations can improve the reduction of mercury level in the TCLP leachate solutions, we took the best 3 conditions from the 5-min sonication experiments and carried out the experiments for 15 minutes. In Figure 2-11, the results show that with 15-min of sonication, the most concentrated solution could bring the mercury level down to 0.0382 ppm. Although it still does not meet the USEPA standard for land disposal (0.0250 ppm), but it is very close.

2.3.10. Ultrasound-assisted mercury removal with deionized water using an ultrasonic liquid processor

If ultrasound can facilitate mercury removal in a hypochlorite solution, would sonication of mercury-containing phosphors with deionized water help us achieve the same results? If water could be used as the reagent instead of hypochlorite solutions, the removal of mercury from waste phosphors would become further cost-efficient and environmentally friendly. To evaluate this idea, we used the same set of experiments, but replaced the hypochlorite solutions with deionized water. In Figure 2-12, we can see that the mercury content of the phosphor dropped to a certain level after 15 min of sonication in water. However, after 15 mins the mercury level did not drop significantly any more. Without hypochlorite, sonication with the ultrasonic processor can also remove some mercury from the phosphors, however, conversion of the trapped mercury into water-soluble mercury species is rather limited. Obviously, sonication alone is not sufficient to reduce mercury significantly.

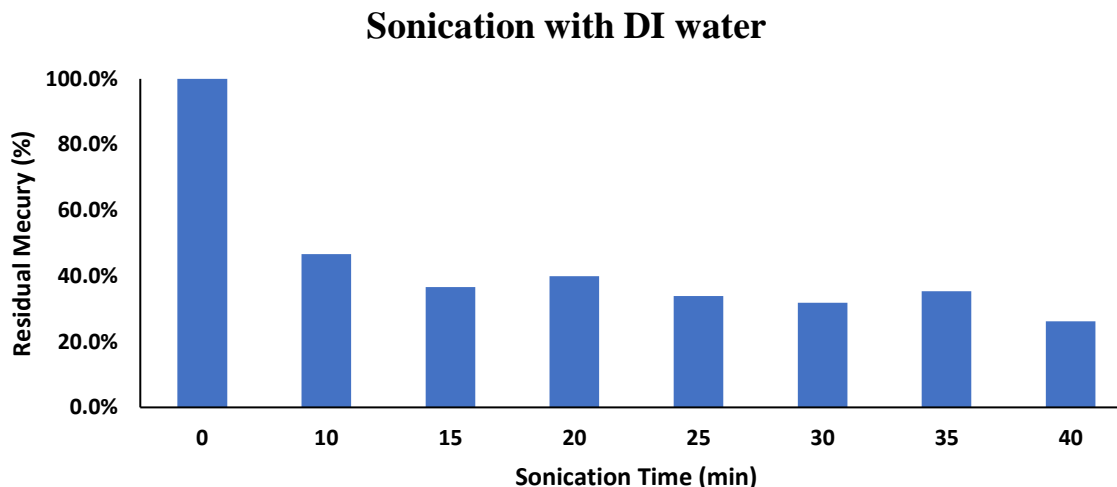


Figure 2-12. Sonication with DI water: Mercury removal by sonication of the phosphor in water with an ultrasound probe at room temperature.

2.3.11. Potential of Reusability

A typical fluorescent emission spectrum of the phosphor collected from a new Sylvania fluorescent lamp using an excitation wavelength of 254 nm is shown in Figure 2-13. The excitation wavelength of 254 nm was employed because the mercury vapor in fluorescent lamps generates UV light of 254 nm to excite the rare earth phosphors to produce visible light when electric current passes through. Consequently, by using this wavelength, we will be able to obtain the fluorescence emission of fluorescent lamps. In Figure 2-13, the peak around 508 nm is the peak of second order Ryleigh scattering. The peak around 625nm is for red phosphors; the peaks around 557nm, 598nm and 636 are green phosphors; the blue phosphor is around 460nm. The fluorescence emission spectra of several treated phosphor samples and the new Sylvania phosphor were compared. In Figure 2-13, those treated samples exhibited resemblance of emission spectra with the one from a new Sylvania lamp. The relative position

of each peak of all the samples are nearly identical. The height of each peak does not necessarily reflect the strength of the emission because the spectra were taken with solid samples that were held between 2 quartz slides, in which the powder is hard to be distributed evenly and conduct quantitative measurement. Figure 2-14 (a)-(e) are the SEM micrographs were for original and the treated phosphors. Compared to the original phosphor, the ones treated with 600°C heating and most dilute solution shows similar morphological features. These 2 conditions might have a potential of reusability.

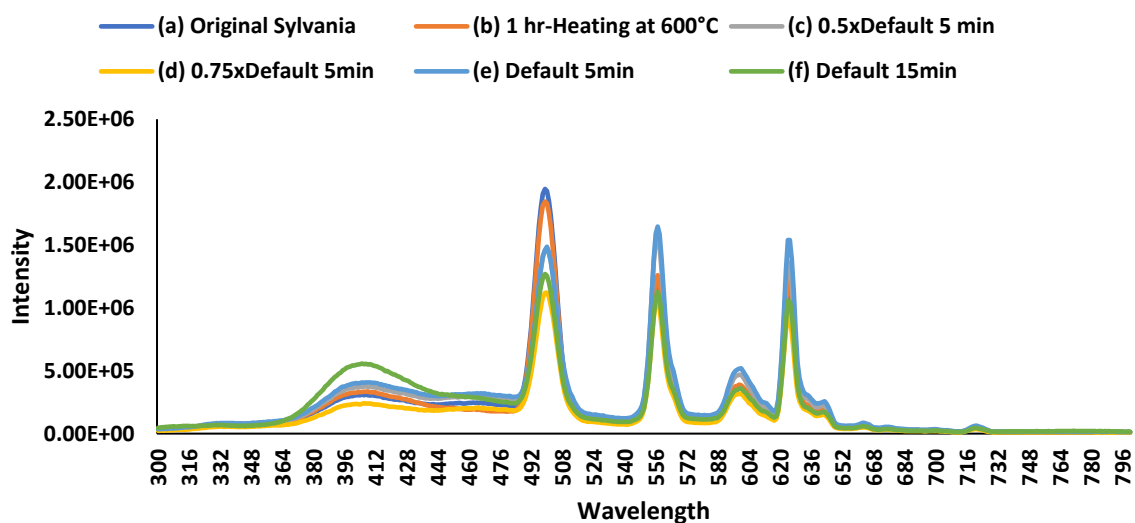
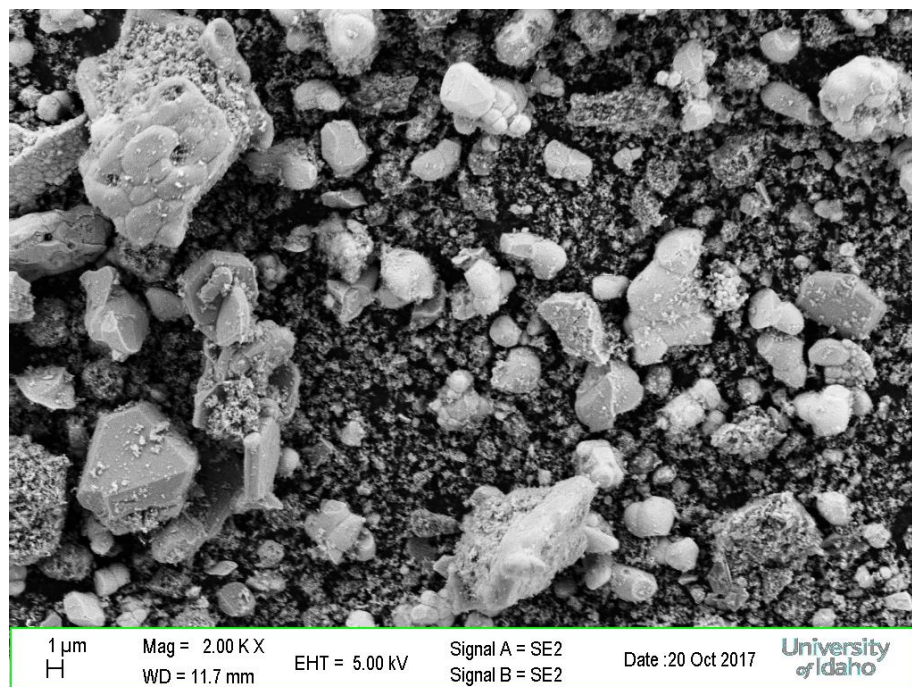
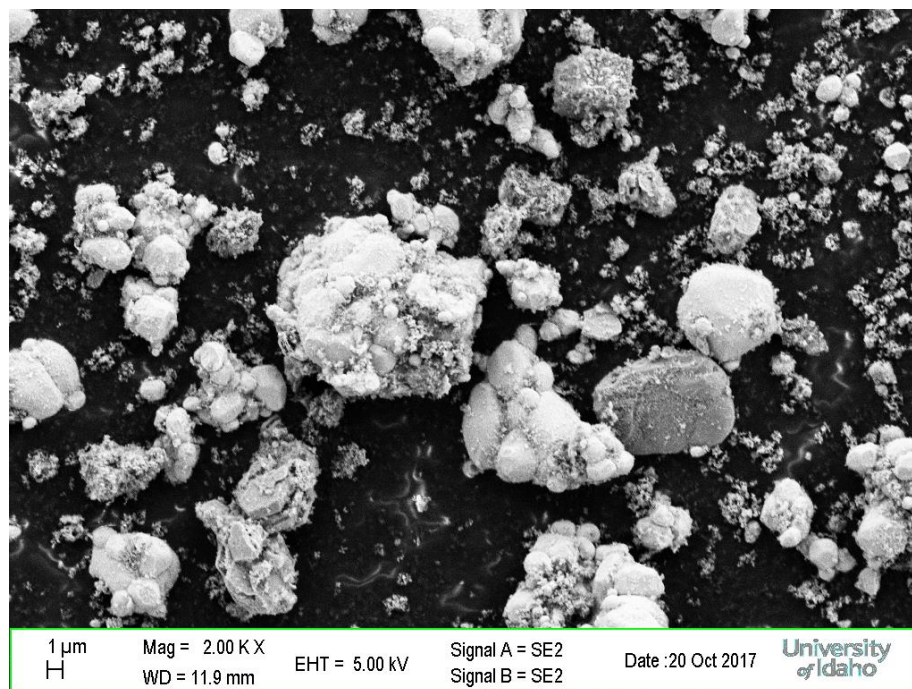


Figure 2-13. Emission spectra for (a) Original Sylvania phosphor; (b) phosphor heated at 600°C for 1 hour; (c) phosphor sonicated in 0.1M/0.25M NaCl/NaOCl solution for 5 minutes; (d) phosphor sonicated in 0.15M/0.375M NaCl/NaOCl solution for 5 minutes; (e) phosphor sonicated in 0.2M/0.5M NaCl/NaOCl solution for 5 minutes; (f) phosphor sonicated in 0.2M/0.5M NaCl/NaOCl solution for 15 minutes

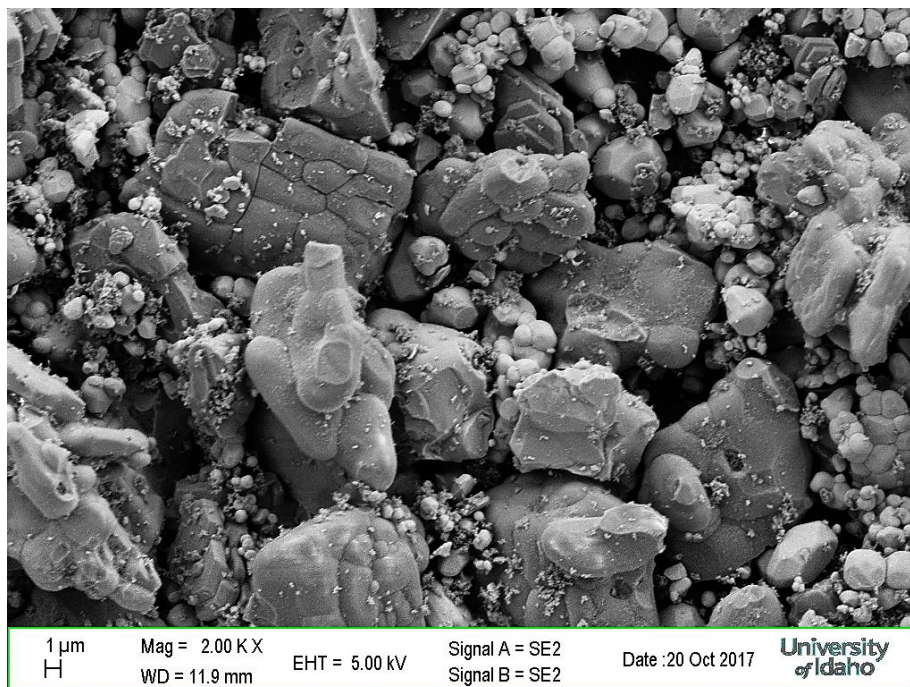
(a)



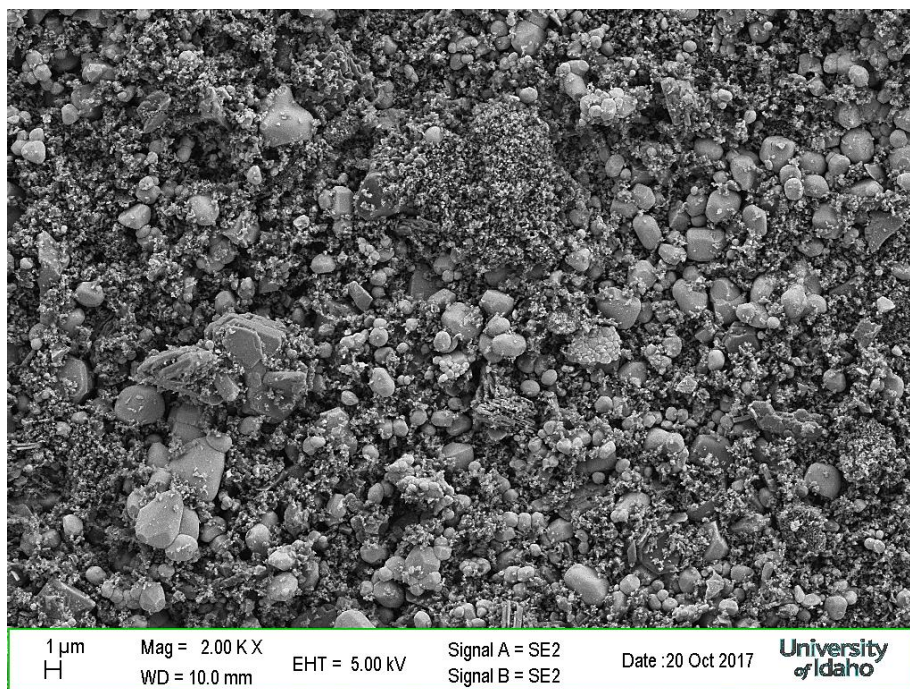
(b)



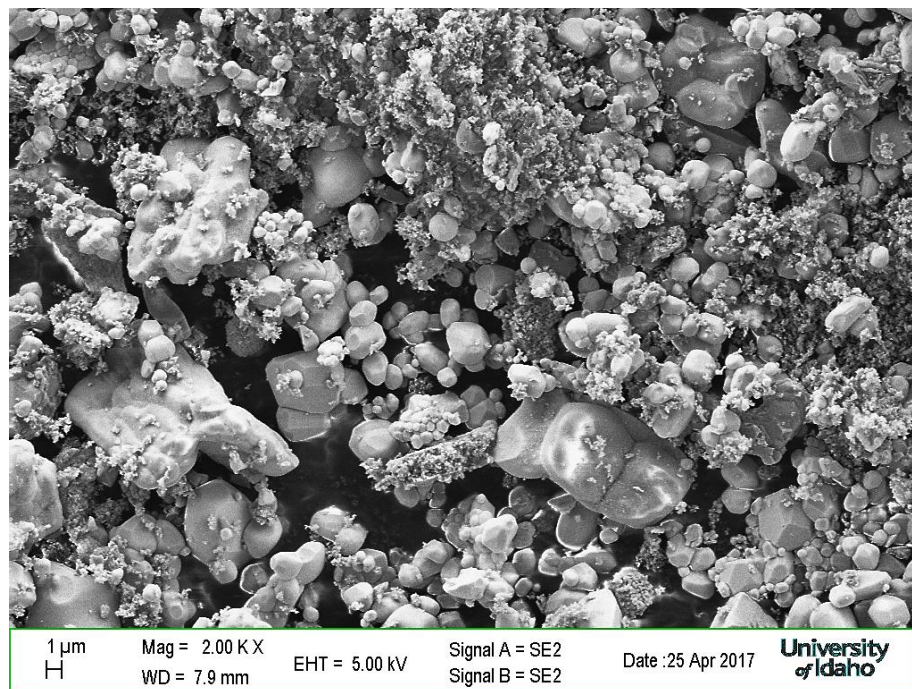
(c)



(d)



(e)



(f)

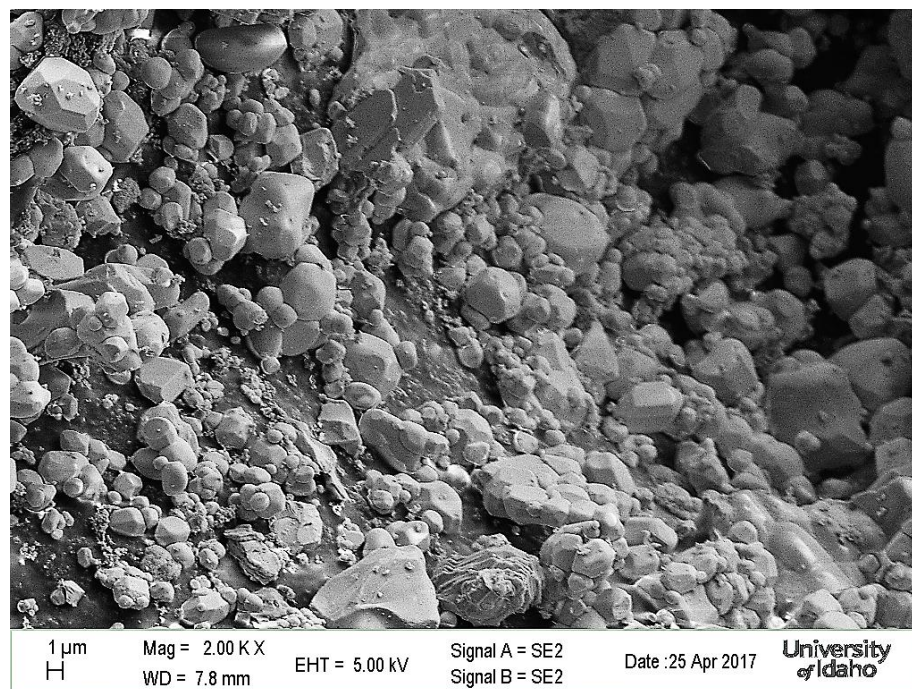


Figure 2-14. SEM images for (a) Original Sylvania phosphor; (b) phosphor heated at 600°C for 1 hour; (c) phosphor sonicated in 0.1M/0.25M NaCl/NaOCl solution for 5 minutes; (d) phosphor sonicated in 0.15M/0.375M NaCl/NaOCl solution for 5 minutes; (e) phosphor sonicated in 0.2M/0.5M NaCl/NaOCl solution for 5 minutes; (f) phosphor sonicated in 0.2M/0.5M NaCl/NaOCl solution for 15 minutes

2.4. Conclusion

Mercury in rare earth phosphors collected from used fluorescent lamps can be effectively reduced from more than 250 ppm to less than 10 ppm in a few minutes by simply using sodium hypochlorite solutions made from commercial bleach with an ultrasound-assisted leaching process and meet the USEPA standard for universal waste management. Based on the data, we can conclude that NaCl/NaOCl solutions of a higher concentration with a longer sonication time will increase the efficiencies of mercury removal from spent phosphors. In addition, solutions made from pure sodium hypochlorite solution have better efficiencies than the ones made from commercial bleach. It could possibly be attributed to the unknown chemical ingredients in the commercial bleach. The fluorescence spectra of the phosphors after mercury removal have similar spectra compared with the phosphors collected from new lamps. However, more investigation will be needed to determine the reusability.

The results suggest that recycling rare-earth phosphors, from phosphor collection to mercury removal, can all be accomplished within 5 minutes by using simple ultrasound-based techniques described in this study. This simple method of converting a hazardous material to potentially reusable rare earth phosphors should be of considerable interest to environmental conservation and critical materials management programs.

Acknowledgements

We would like to thank our colleagues Box Fox and Donna Beak for their professional opinions about this work. We also thank Anatech for running our mercury samples.

References

1. Critical Materials Strategy (2010). U.S. Department of Energy: 2010; pp 1-170.
2. Critical Materials Strategy (2011). U.S. Department of Energy: 2011; pp 1-190.
3. Schüler, D.; Buchert, M.; Liu, R.; Dittrich, S.; Merz, C. *Study on Rare Earths and Their Recycling* The Greens/EFA Group in the European Parliament 2011; pp 1-140.
4. *Environmental Impact Analysis: Spent Mercury-Containing Lamps (4th edition)* National Electrical Manufacturers Association: 2000; pp 1-9.
5. USEPA, Comments Related to Industry Source Reduction Efforts. Response to comments document. Final rule on hazardous waste lamps. USEPA, Ed. 1998; pp 1-22.
6. Aucott, M.; McLinden, M.; Winka, M., Release of Mercury from Broken Fluorescent Bulbs. *Journal of the Air & Waste Management Association* **2003**, 53 (2), 143-151.
7. Jang, M.; Hong, S. M.; Park, J. K., Characterization and recovery of mercury from spent fluorescent lamps. *Waste Management* **2005**, 25 (1), 5-14.
8. Raposo, C.; Windmüller, C. C.; Durão Júnior, W. A., Mercury speciation in fluorescent lamps by thermal release analysis. *Waste Management* **2003**, 23 (10), 879-886.
9. New Jersey Mercury Task Force Volume III: Sources of Mercury to New Jersey's Environment. Department of Environmental Protection, N. J., Ed. 2002; Vol. 3, pp 10-195.
10. UN Environment, Toolkit for identification and quantification of mercury releases: Reference Report and Guideline for Inventory Level 2 Version 1.4. UN Environment Chemicals Branch: 2017; pp 1-331.
11. Dang, T.; Frisk, T.; Grossman, M., Applications of surface analytical techniques for study of the interactions between mercury and fluorescent lamp materials. *Analytical and Bioanalytical Chemistry* **2002**, 373 (7), 560-570.

12. National Electrical Manufacturers Association Frequently Asked Questions About Compact Fluorescent Lamps. <http://www.nema.org/Policy/Environmental-Stewardship/Lamps/Frequently-Asked-Questions-FAQs/Pages/Frequently-Asked-Questions-About-Compact-Fluorescent-Lamps.aspx> (accessed 10/11/2017).
13. USEPA, Treatment Technologies for Mercury in Soil, Waste, and Water. USEPA 2007.
14. USEPA, FEDERAL REGULATIONS: Title 40: Protection of Environment, PART 268—LAND DISPOSAL RESTRICTIONS, Subpart D—Treatment Standards, §268.40.
15. USEPA, SW-846 Test Method 1311: Toxicity Characteristic Leaching Procedure. USEPA, Ed.
16. Fujiwara, K.; Fujinami, K. Mercury recovery apparatus. U.S. Patent: US6866814 B2, 2005.
17. Durao, W. A.; de Castro, C. A.; Windmoller, C. C., Mercury reduction studies to facilitate the thermal decontamination of phosphor powder residues from spent fluorescent lamps. *Waste Management* **2008**, 28 (11), 2311-2319.
18. Chang, T. C.; You, S. J.; Yu, B. S.; Chen, C. M.; Chiu, Y. C., Treating high-mercury-containing lamps using full-scale thermal desorption technology. *J Hazard Mater* **2009**, 162 (2–3), 967-972.
19. Pogrebnaia, V.; Pronina, N.; Strizhov, N.; Tsymbal, E.; Pol-uljakhova, N. Method of mercury recovery from lumi-nescent lamps. Patent: RU2116368, 1998.
20. Cogar, M. J. Lamp reclamation process. US Patent: US5106598 A, 1992.
21. Coskun, S.; Civelekoglu, G., Recovery of Mercury from Spent Fluorescent Lamps via Oxidative Leaching and Cementation. *Water, Air, & Soil Pollution* **2015**, 226 (6).

22. Romdhane, M. Extraction solide–liquide sous ultrasons—mise au point d’un capteur de puissance ultrasonore, Thèse, . Institut National Polytechnique de Toulouse, 1993.
23. Haunold, C. Extraction des pyrèthrine—analyse du procédé discontinu et de l’influence des ultrasons. Modélisation et mise en œuvre d’un procédé continu, Thèse,. Institut National Polytechnique de Toulouse, 1991.
24. Hiraide, M.; Mikuni, Y.; Kawaguchi, H., Solid–liquid extraction with an ammoniacal EDTA solution for the separation of traces of copper from aluminium. *Anal. Sci.* **1995**, *11* (4), 689-691.
25. Bang, J. H.; Suslick, K. S., Applications of Ultrasound to the Synthesis of Nanostructured Materials. *Advanced Materials* **2010**, *22* (10), 1039-1059.
26. Xu, H.; Zeiger, B. W.; Suslick, K. S., Sonochemical synthesis of nanomaterials. *Chemical Society Reviews* **2013**, *42* (7), 2555-2567.
27. Takahashi, T.; Takano, A.; Saiton, T.; Nagano, N.; Hirai, S.; Shimakage, K., Synthesis of red phosphor (Y₂O₃:Eu³⁺) from waste phosphor sludge by coprecipitation process. *Journal of the Mining and Materials Processing Institute of Japan* **2002**, *118*, 413-418.
28. Liu, Z.; Lai, Z.; Gong, M.; Wan, G. 一种再生灯用稀土三基色荧光粉的方法. Patent: CN101942298 A, 2011.
29. Twidwell, L. G.; Thompson, R. J., Recovering and recycling Hg from chlor-alkali plant wastewater sludge. *Journal of The Minerals Metals & Materials Society* **2001**, *53*, 15-17.
30. Said, A.; Mattila, O.; Eloneva, S.; Järvinen, M., Enhancement of calcium dissolution from steel slag by ultrasound. *Chemical Engineering and Processing: Process Intensification* **2015**, *89* (Supplement C), 1-8.

31. Hagenson, L. C.; Doraiswamy, L. K., Comparison of the effects of ultrasound and mechanical agitation on a reacting solid-liquid system. *Chemical Engineering Science* **1998**, *53* (1), 131-148.
32. Thompson, L. H.; Doraiswamy, L. K., Sonochemistry: Science and Engineering. *Ind. Eng. Chem. Res.* **1999**, *38* (4), 1215–1249.
33. Adewuyi, Y. G., Sonochemistry: Environmental Science and Engineering Applications. *Ind. Eng. Chem. Res.* **2001**, *40* (22), 4681–4715.
34. Chaturabul, S.; Srirachat, W.; Wannachod, T.; Ramakul, P.; Pancharoen, U.; Kheawhom, S., Separation of mercury(II) from petroleum produced water via hollow fiber supported liquid membrane and mass transfer modeling. *Chemical Engineering Journal* **2015**, *265* (Supplement C), 34-46.
35. Anacleto, A. L.; Carvalho, J. R., Mercury cementation from chloride solutions using iron, zinc and aluminium. *Minerals Engineering* **1996**, *9* (4), 385-397.
36. Ku, Y.; Wu, M.-H.; Shen, Y.-S., Mercury removal from aqueous solutions by zinc cementation. *Waste Management* **2002**, *22* (7), 721-726.
37. Noubactep, C., Elemental metals for environmental remediation: Learning from cementation process. *J Hazard Mater* **2010**, *181* (1), 1170-1174.
38. USEPA SW-846 Test Method 1311: Toxicity Characteristic Leaching Procedure. <https://www.epa.gov/hw-sw846/sw-846-test-method-1311-toxicity-characteristic-leaching-procedure> (accessed 10/13/2017).

Chapter 3: Selective Extraction of Rare Earth Elements from Spent Commercial Fluorescent Phosphors Using Supercritical Fluid Carbon Dioxide

Abstract

Supercritical carbon dioxide provides an effective medium for extraction of rare earth elements from phosphors collected from end-of-life fluorescent lamps. Without pretreatment, supercritical carbon dioxide extraction is only effective for removing europium and yttrium from the phosphors because they exist in oxide forms. To recover cerium, lanthanum, and terbium, which exist in phosphate or aluminate forms in the phosphors, a pretreatment procedure is required to facilitate their extraction. This paper describes a sodium peroxide calcination procedure which would decompose the phosphor matrices and convert the rare earths into their oxide forms prior to supercritical extraction. By utilizing a tri-n-butylphosphate-nitric acid complex, selective recovery of the rare earth elements from the pretreated phosphors can be achieved by supercritical CO₂ extraction. The extraction efficiencies are over 96% for all the rare earth elements using the supercritical extraction method.

3.1. Introduction

Rare earth elements (REEs) are used in a number of electronics and communication devices including lasers, magnets, wind turbines, cell phones, defense technologies, and phosphors for fluorescent light bulbs, TV screens and computer displays, etc.¹ Currently, only a handful of mines supply REEs to the entire world, and most of them are located in China. To alleviate the dependence on rare earth supplies from China or increase supply diversities, reopening the existing rare earth mines, seeking new rare earth ores or developing methods to recycle rare earth elements from end-of-life electronic wastes have become some of the approaches that are actively pursued by the U.S.A. Recycling rare earth elements from end-of-life products, including fluorescent light bulbs, magnets, batteries, electronics, etc., is one of the U.S. Department of Energy's strategies described in the "Critical Materials Strategy" report²⁻³. This approach is generally called urban mining. The advantages of urban mining include shorter operation period, relatively low cost, reduced amount of waste, and environmental friendliness. It provides a sustainable way of obtaining rare earth minerals. One of the most accessible sources containing rare earth elements in our day-to-day life is the phosphors coated on the inner wall of fluorescent lamps. From 2006 to 2008, approximately 7% of global consumption of rare earth metals was used in phosphors⁴. In the U.S. alone, more than 680 million fluorescent lamps are disposed annually, but most of them are not recycled⁵. A number of studies for recovering rare earth elements from the phosphors of end-of-life fluorescent lamps have been reported⁶⁻⁷.

The phosphor materials used in fluorescent lighting consist of 3 types of phosphors: red, green and blue phosphors, and therefore they are called tricolor or trichromatic phosphors. Red phosphors are usually in oxide forms, which can dissolve in acid solutions. Green and

blue phosphors have various forms, depending on what type of matrix in which rare earth metals are doped. There are generally 4 types of matrices: phosphate, aluminate, borate and silicate (Table 3-1). Phosphate and aluminate matrices are the most commonly used in the commercial fluorescent lamps⁸. These 2 matrices are much more stable than oxides, especially aluminate. Aluminate-based green and blue phosphors have been investigated and determined to be in spinel structures. This type of phosphors has the advantages of anti-ultraviolet aging, excellent thermal stabilities and high luminous efficiencies⁹. However, the stable structures also make extraction of rare earth metals doped in aluminate structures by conventional acid leaching considerably challenging¹⁰.

Table 3-1. Chemical formula for fluorescent phosphor materials

Phosphor	Red	Green	Blue
Phosphate matrix	$\text{Y}_2\text{O}_3:\text{Eu}^{3+}$	$\text{LaPO}_4:\text{Ce}^{3+}, \text{Tb}^{3+}$	$(\text{Ba}, \text{Sr}, \text{Ca})_5 (\text{PO}_4)_3 \text{Cl}:\text{Eu}^{2+}$
Aluminate matrix	$\text{Y}_2\text{O}_3:\text{Eu}^{3+}$	$\text{CeMgAl}_{11}\text{O}_{19}:\text{Tb}^{3+}$	$\text{BaMgAl}_{10}\text{O}_{17}:\text{Eu}^{2+}$
Borate matrix	$\text{Y}_2\text{O}_3:\text{Eu}^{3+}$	$\text{GdMgB}_5\text{O}_{10}:\text{Ce}^{3+}, \text{Tb}^{3+}$	$\text{Ca}_2\text{B}_5\text{O}_8\text{Cl}:\text{Eu}^{2+}$
Silicate matrix	$\text{Y}_2\text{O}_3:\text{Eu}^{3+}$	$\text{Y}_2\text{SiO}_3:\text{Ce}^{3+}, \text{Tb}^{3+}$	$\text{BaZrSi}_3\text{O}_9:\text{Eu}^{2+}$

Alkali fusion method is often used to decompose phosphors with stable structures and convert them to acid soluble species to improve leaching efficiency. Li et al. decomposed phosphors by calcining them with sodium hydroxide at 900 °C for 2 hours and reached a leaching efficiency close to 100%¹¹. Porob et al. converted phosphors into a mixture of oxides by heating them with sodium carbonate at 1000 °C¹². Zhang et al. performed 2-step acid leaching. Their results show that hydrochloric acid is better than sulfuric acid in the first acid leaching step, and sodium hydroxide is better than sodium carbonate in the alkali fusion process. The leaching rates for all rare earth metals reached over 97%¹³. Wu et al. investigated

the calcination of green phosphor ((Ce_{0.67}Tb_{0.33})MgAl₁₁O₁₉) using sodium peroxide system, and the phosphor was converted to the mixtures of Na₂CeO₃, Na₂TbO₃, MgO₂ and NaAlO₂. The optimal molten salt calcining conditions were found to be 650 °C, 50 min, and 1.5 : 1 of Na₂O₂-to-waste mass ratio¹⁴.

Compared to conventional solvent extraction methods, supercritical fluid extraction (SFE) provides an alternative way for recovering rare earth elements from spent fluorescent phosphors. In SFE, liquid solvents are replaced with supercritical fluid carbon dioxide (sc-CO₂), which can be recycled and reused after depressurization, and therefore the generation of secondary solvent wastes is greatly reduced. Supercritical carbon dioxide has the advantages of being non-flammable, inexpensive, easily accessible, and having moderate critical parameters. The nature of being able to dissolve materials like a liquid and diffuse like a gas also makes sc-CO₂ a very attractive option. Shimizu et al. demonstrated an SFE process by using a tri-n-butylphosphate-nitric acid (TBP-HNO₃) complex to extract the rare earth elements from fluorescent phosphors¹⁵. In their report, yttrium and europium, the rare earth elements in the red phosphor, could be effectively recovered. However, the REEs in non-oxide forms, such as lanthanide phosphates, showed very low extraction efficiencies.

In this paper, we report an SFE process for extracting rare earth elements from aluminate-based phosphors and commercial Sylvania brand fluorescent phosphor. The phosphors were pretreated via a sodium peroxide calcination process prior to SFE operation, and high extraction efficiencies were achieved. It is a selective extraction method for REEs when using a TBP-HNO₃ complex as the chelating agent in our SFE process. This simple batch extraction process using sc-CO₂ could achieve comparable results as the ones reported in the literature using multi-solvent systems. The SFE process described in this paper may

provide an environmentally sustainable and economically viable method for recycling rare earth elements from fluorescent lamps and other electronic wastes.

3.2. Experimental Section

3.2.1. Chemicals and materials

Green phosphor ($\text{Ce}_{0.63}\text{Tb}_{0.37}\text{MgAl}_{11}\text{O}_{19}$), blue phosphor ($\text{Ba}_{0.86}\text{Eu}_{0.14}\text{MgAl}_{10}\text{O}_{17}$) and Trichromatic phosphor (TRI), a mixture of the red ($\text{Y}_{1.92}\text{Eu}_{0.08}\text{O}_3$), green and blue phosphors, were purchased from Sigma-Aldrich. Sylvania fluorescent phosphor material was collected from end-of-life fluorescent lamps. Hydrogen peroxide (EMD Millipore, 30%) was used to digest phosphor materials; sodium peroxide (Na_2O_2 ; 95%) used to decompose phosphor materials was purchased from Alfa Aesar. All chemicals were used as received.

Based on a report by Shimizu et al.¹⁵, a TBP- HNO_3 adduct (complex A) was prepared by mixing an aliquot of TBP (Tri-*n*-butylphosphate, Sigma-Aldrich, 97%) with an equal volume of concentrated nitric acid (Macron Fine Chemicals, 70%) in a glass vial. This glass vial was shaken mechanically for 5 minutes and centrifuged at 4000 rpm for 10 minutes. The upper layer of the resultant mixture is the complex A. An aliquot of complex A and 0.25 aliquot of TBP were mixed to prepare another TBP- HNO_3 adduct, complex B.

3.2.2. Experimental apparatus

Inductively coupled plasma-mass spectroscopy (ICP-MS, Agilent 7700x) was used to quantify the amount of rare earth elements found in each solution. Fluorescence spectra were obtained using a fluorescence spectrometer (FluoroMax-3, Horiba). A schematic diagram of

the SFE apparatus is shown in Figure 1. The main parts consist of a liquid CO₂ tank (Matheson Tri-Gas), 2 parallelly connected syringe pumps (ISCO, model 260D, Japan), an injection cell (internal volume 15 cm³) and a reaction cell (internal volume 15 cm³) made of stainless steel AISI 316, a pressure gauge, a few needle valves (High Pressure Equipment Company), a micro-metering valve (Parker Autoclave Engineers) and a collection cell. As indicated in Figure 3-1, both the injection cell and reaction cell are on top of the hot plates with magnetic stir (Fisher Scientific) and are placed in the ovens to maintain 60°C. The output of the reaction cell is connected to a needle valve and a micro-metering valve, which controls the flow rate and back-pressure. 30 mL 0.1 M HNO₃ was used as the trap solution.

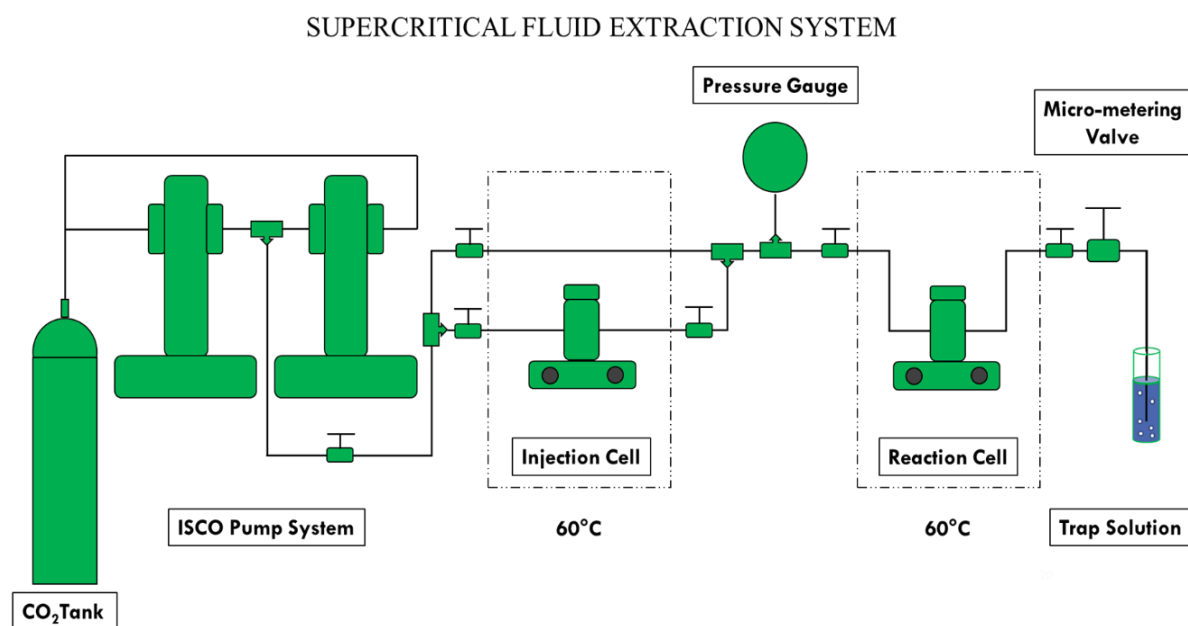


Figure. 3-1. Schematic diagram of the SFE system

3.2.3. Characterization of the phosphors

Our phosphor materials are from 2 sources. The one purchased from Sigma-Aldrich has been well processed by the merchant and does not contain any fragmented glass. However, the phosphor material collected from spent Sylvania lamps tends to contain moisture and small pieces of glass. As a result, drying and homogenization (manual mixing, sieving) were essential prior to performing the investigations. First, the Sylvania phosphor powder was collected from end-of-life Sylvania fluorescent lamps using sonication bath. Drying was carried out in an oven at 70°C for 24 hours. The Sylvania phosphor was then passed through 250 µm sieves and placed in a plastic bottle. The bottle was shaken mechanically for 3 hours to ensure the homogeneity. Finally, this bottle of processed phosphor material was stored in a desiccator. To estimate the metal content in the phosphors, whether purchased from Sigma-Aldrich or collected from Sylvania lamps, 100 mg of each of the materials was mixed with an appropriate amount of sodium peroxide to carry out alkali fusion under an elevated temperature. After the sodium peroxide treatment, acid digestion was performed on each of the alkaline slags by mixing 10 mL of concentrated HNO₃ and 10 mL of 30% H₂O₂. The solutions were heated, stirred and refluxed at 500 rpm and 80 °C for 24 hours to ensure all solid materials were completely dissolved. After dissolution, solutions were cooled, transferred and diluted in 100 mL volumetric flasks with deionized water. A 2% nitric acid solution, prepared with concentrated stock solution and deionized water, was used to further dilute the solutions for ICP analysis.

3.2.4. Sodium peroxide pretreatment of phosphors materials

To extract the rare earth elements in phosphate or aluminate-based phosphors, we pretreated the phosphor materials based on conditions from a report by Wu et al¹⁴ with modification. An aliquot of phosphor material and 1.5 aliquot of sodium peroxide were well mixed and placed in a nickel crucible. The crucible was then put into a tube furnace with a temperature of 650°C for 1-hour. The procedures for sodium peroxide pretreatment of waste phosphors are shown in Figure 3-2. After calcination, the treated phosphor was collected differently for different purposes. Normally we soak and wash the treated materials with deionized water to get rid of excess sodium peroxide and water-soluble species that are generated due to the decomposition of phosphor materials and then further anneal the washed materials at 700°C for 1 hour, but we also collected the samples without soaking and washing to conduct selectivity experiments.

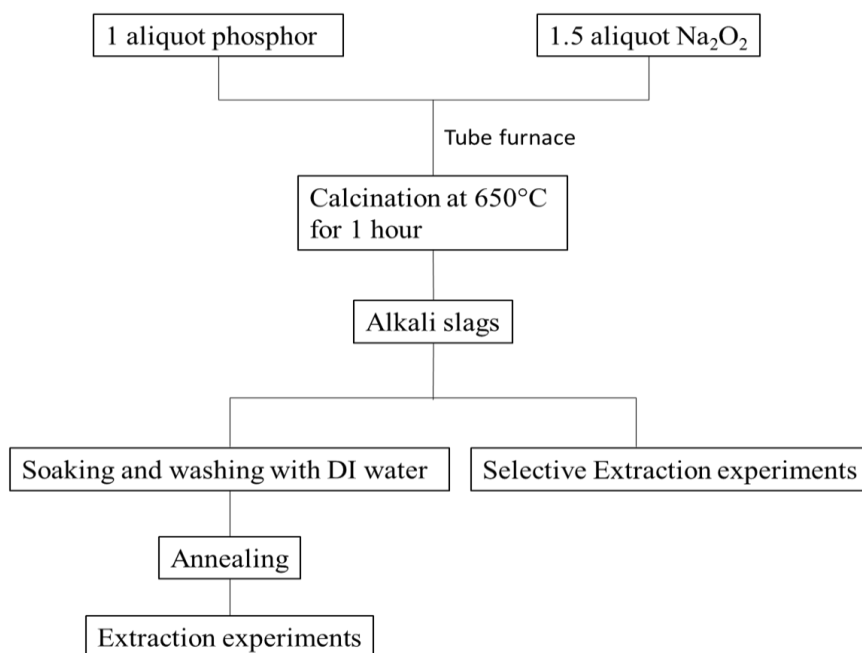


Figure. 3-2. Flowchart for sodium peroxide pretreatment

3.2.5. Extraction using TBP-HNO₃ adduct

To evaluate whether pretreatment of phosphor materials with sodium peroxide would improve the efficiencies of extraction, experiments were conducted under atmospheric pressure using the TBP-HNO₃ complex B as extractant. As shown in Table 3-2, in extraction experiments under atmospheric pressure, 10 mL of the TBP-HNO₃ complex B in a glass vial was preheated to 60°C in an oil bath, and 100 mg of the phosphor material was then added into the glass vial and stirred for 2 hours. Excessive amount of 0.1 M HNO₃ was used to back-extract the metal ions in the complex. The final solution was analyzed by ICP-MS.

Table 3-2. Extraction under atmospheric pressure

Adduct	10 mL TBP-HNO ₃ Complex B
Phosphor materials	Non-treated phosphors, treated-non-washed phosphors, treated-washed-annealed phosphors
Material size	100 mg
Temperature	60°C
Extraction time	120 min

For the extraction experiments under supercritical conditions, 2 mL of the TBP-HNO₃ complex B and 20 mg of the treated-washed-annealed phosphor material were placed in the reaction cell, and 10 mL of TBP was added into the injection cell as the extra eluent. Both cells were stirred and heated. 30 mL of 0.1 M nitric acid functioning as the trap solution was placed at the end of the system. Liquid CO₂ was pressurized to 3200 psi. When the temperature of the system reached 60°C, pressurized CO₂ was introduced into both cells and mixed with the TBP in the injection cell as well as the reaction mixture of TBP-HNO₃ complex B and phosphor material in the reaction cell. After 2 hours of static extraction, the terminal valve was opened to start the 2-hour dynamic extraction. The effluents from the reaction cell were directed into the trap solution through the micro-metering valve, which regulated the flow rate

of CO₂ as approximately 2 mL/min. Once the supercritical CO₂ came out of the tubing at atmospheric pressure, it was gasified and left the REE-TBP-HNO₃ complexes in the trap solution, which was later analyzed by ICP-MS. The conditions for extraction under supercritical conditions are listed in Table 3-3.

Table 3-3. Extraction under supercritical conditions

Adduct	2 mL TBP-HNO ₃ Complex B
Phosphor materials	Treated-washed-annealed phosphors
Material size	20 mg
Pressure	3200 psi
Temperature	60°C
Extraction time	Static stage = 120 min, Dynamic stage = 120 min

3.3. Results and discussion

3.3.1. Characterization and pretreatment of the phosphors

According to the estimates in the U.S. Department of Energy Critical Materials Strategy²⁻³, in lighting phosphors, yttrium has the highest average weight percentage, followed by cerium/lanthanum, terbium and europium. Green phosphors consist of terbium, lanthanum and/or cerium. Sometimes cerium has a higher weight percentage than lanthanum, and sometimes lanthanum is higher than cerium, all depending on what type of green phosphor is used in the tri-band combination. The percentage of each rare earth element also varies from manufacturer to manufacturer, but roughly follows similar trends.

The trichromatic phosphor (TRI) purchased from Sigma-Aldrich is a mixture of red, green and blue phosphors, which have chemical formulas of Y_{1.92}Eu_{0.08}O₃, Ce_{0.63}Tb_{0.37}MgAl₁₁O₁₉, and Ba_{0.86}Eu_{0.14}MgAl₁₀O₁₇, respectively. Lanthanum does not exist in

this purchased trichromatic phosphor, and the weight percentage of each element is unknown. As for the chemical composition and weight percentage of each element in the Sylvania fluorescent phosphor (SYL), we were not able to acquire the information since it could be commercially sensitive. As a result, we had to digest both phosphor materials to estimate the chemical composition and weight of each element in both phosphor materials. Alkali fusion and acid leaching were performed 3 times on both TRI and SYL phosphors. The results are shown in Table 3-4.

Table 3-4. Metal content of Sylvania and Trichromatic phosphor (mg g⁻¹ dry non-treated material)

	Ce	Eu	La	Tb	Y
SYL	50.3 ± 2.2	18.4 ± 0.4	46.3 ± 1.9	19.9 ± 0.5	219.0 ± 4.8
TRI	32.4 ± 1.9	26.2 ± 0.7	N/A	22.9 ± 0.6	254.6 ± 3.7
	Al	Ba	Ca	Mg	Sr
SYL	100.5 ± 13.3	3.2 ± 0.5	31.9 ± 2.3	2.1 ± 0.4	35.4 ± 3.2
TRI	204.9 ± 9.9	14.8 ± 3.4	N/A	24.6 ± 6.0	N/A

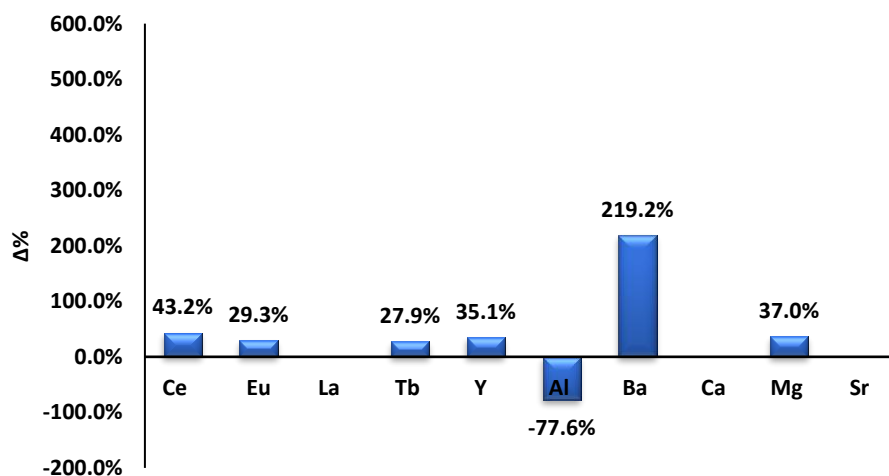
Due to the stable nature of green and blue phosphors, sodium peroxide was used on both materials to decompose their matrices. According to Wu et al.¹⁴, after calcinating with sodium peroxide, the waste phosphors will yield a mixture of rare earth compounds such as Na₂CeO₃, Na₂TbO₃, NaYO₂, La₂O₃, Tb₄O₇, Ce₂O₃ and non-rare earth compounds such as CaO, MgO, NaAlO₂, etc. We also observed excess sodium peroxide remained in the alkali slags. Therefore, we soaked the alkali slags with deionized water until the remnant sodium peroxide was completely consumed. The slurries were then washed to remove water-soluble undesired species. Finally, the slurries were annealed at 700°C for 1 hour to get the final product. After

the above process, the metal content of the pretreated phosphors was also analyzed. The results for treated-washed-annealed trichromatic phosphor (twa-TRI), treated-washed-annealed Sylvania phosphor (twa-SYL) and the comparisons with the non-treated phosphor materials are shown in Table 3-5, Figure 3-3.

Table 3-5. Metal content (mg g^{-1} dry material) for Trichromatic phosphor and Sylvania phosphor before and after sodium peroxide treatment. Δ stands for the weight difference before and after the treatment, and $\Delta \%$ stands for increase rate of weight.

	Ce	Eu	La	Tb	Y	Al	Ba	Ca	Mg	Sr
TRI	32.4 ± 1.9	26.2 ± 0.7	N/A	22.9 ± 0.6	254.6 ± 3.7	204.9 ± 9.9	14.8 ± 3.4	N/A	24.6 ± 6.0	N/A
twa-TRI	46.4 ± 0.8	33.9 ± 1.5	N/A	29.3 ± 2.3	344.0 ± 10.0	45.8 ± 2.6	47.2 ± 1.1	N/A	33.7 ± 4.7	N/A
Δ	14.0	7.7	N/A	6.4	89.4	-159.0	32.4	N/A	9.1	N/A
$\Delta \%$	43.2%	29.3%	N/A	27.9%	35.1%	-77.6%	219.2%	N/A	37.0%	N/A
SYL	50.3 ± 2.2	18.4 ± 0.4	46.3 ± 1.9	19.9 ± 0.5	219.0 ± 4.8	100.5 ± 13.3	3.2 ± 0.5	31.9 ± 2.3	2.1 ± 0.4	35.4 ± 3.2
twa-SYL	76.2 ± 4.1	27.1 ± 1.7	73.7 ± 0.3	27.6 ± 4.1	336.8 ± 5.8	43.6 ± 1.4	17.8 ± 1.5	79.6 ± 32.6	7.9 ± 0.3	78.7 ± 0.8
Δ	26.0	8.7	27.3	7.7	117.8	-56.9	14.6	47.6	5.8	43.4
$\Delta \%$	51.7%	47.5%	59.0	38.6%	53.8%	-56.6%	453.7%	149.1%	280.4%	122.7%

(a) **Weight increase (twa-TRI)**



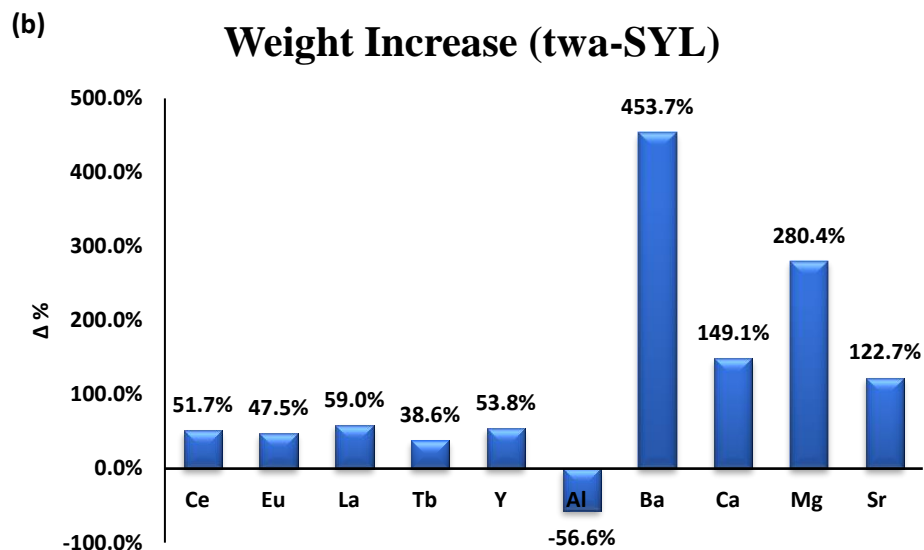


Figure 3-3. (a) The weight increase rate for each metal in treated-washed-annealed trichromatic phosphor. (b) The weight increase rate for each metal in treated-washed Sylvania phosphor

Compared to the non-treated phosphors, the concentrations of most metals in the pretreated phosphors increased except aluminum, in both Sylvania and Trichromatic phosphors. This means the stable aluminate-based phosphors were decomposed and aluminum formed water-soluble species after the pretreatment. In order to characterize and see the influence of the pretreatment on the phosphors, the fluorescent spectroscopy and SEM were employed on the phosphor materials before and after the pretreatment. An excitation wavelength of 254 nm was used when taking fluorescence spectra of fluorescent phosphors. Fluorescence spectroscopy for the purchased blue and green phosphors were also taken so we could better locate the peaks for each phosphor in the Trichromatic phosphor. The overlap of the spectra of the Trichromatic, green and blue phosphors are shown Figure 3-4. The peak around 508nm is the peak of second order Ryleigh scattering of the excitation wavelength. The peaks for the green phosphor are around 557nm, 598nm and 636. The blue phosphor is 460nm. As a result, the peak for red phosphors in Sylvania and Trichromatic phosphor can be

easily determined, which is around 625nm. Figure 3-5(a) are the spectra for the original and the pretreated Trichromatic phosphor. As we can see, after the treatment, all the peaks disappeared except the peak of second order Ryleigh scattering. It means the phosphor materials, including the green and blue phosphors with stable structures, had been decomposed, and the cerium, lanthanum and terbium were transformed into oxides¹⁴, which caused the change of fluorescence emission. The spectra for the original and the pretreated Sylvania phosphor are shown in Figure 3-5(b), which are similar to Figure 3-5(a). The scanning electron microscopy (SEM) was used to evaluate the change of particle sizes and morphologies of the phosphor materials before and after the treatment. TRI, twa-TRI, SYL and twa-SYL phosphors are shown in Figure 3-6, 3-7, 3-8 and 3-10, respectively. Obviously, the particles of the phosphors became fragmented after the application of sodium peroxide calcination and 700°C annealing.

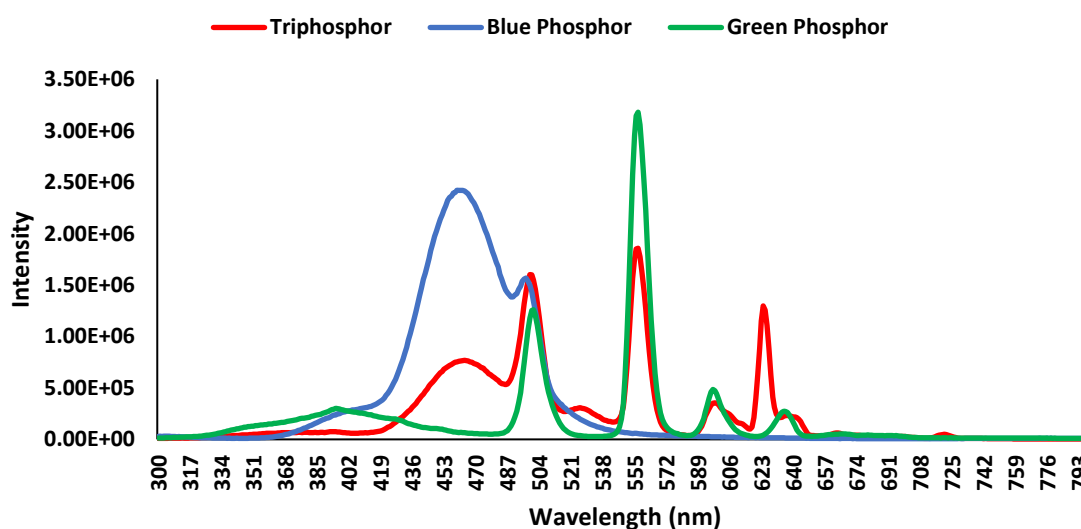


Figure 3-4. The fluorescence spectra for the Trichromatic phosphor, green phosphor and blue phosphor.

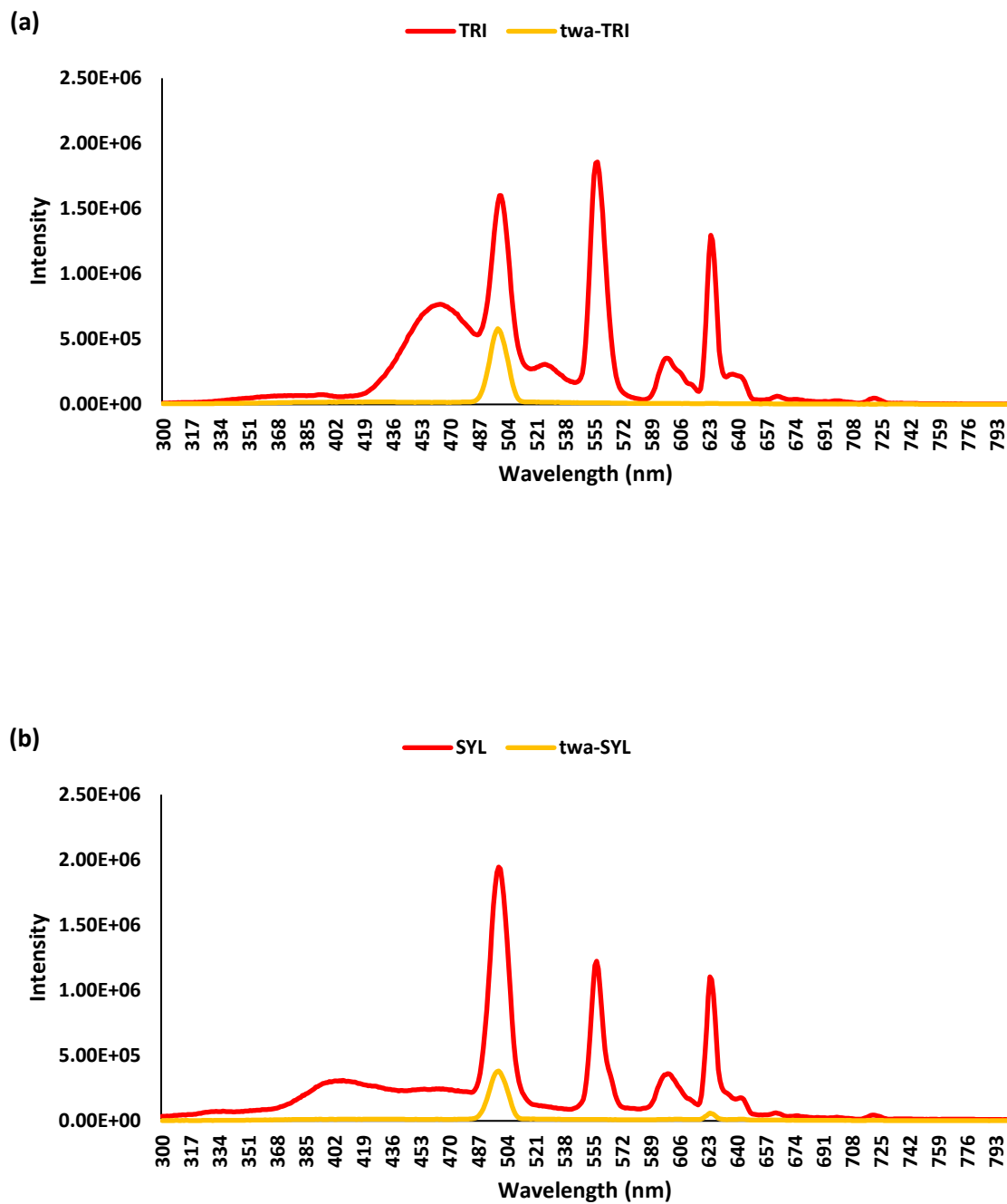


Figure 3-5. Fluorescent spectra before and after pretreatment for (a) Trichromatic phosphor (b) Sylvania phosphor

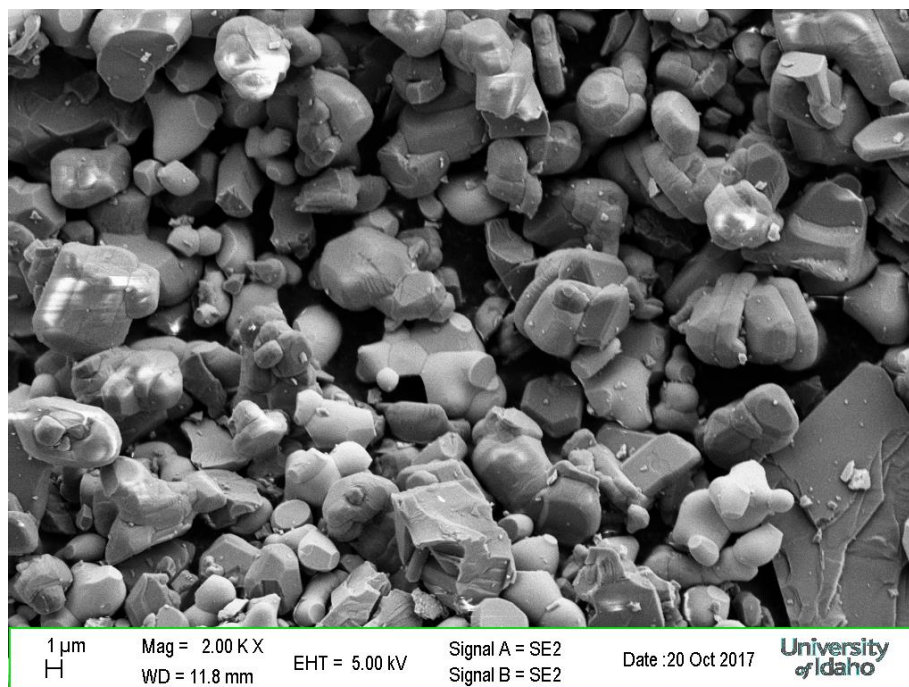


Figure 3-6. The SEM micrograph of original Trichromatic phosphor.

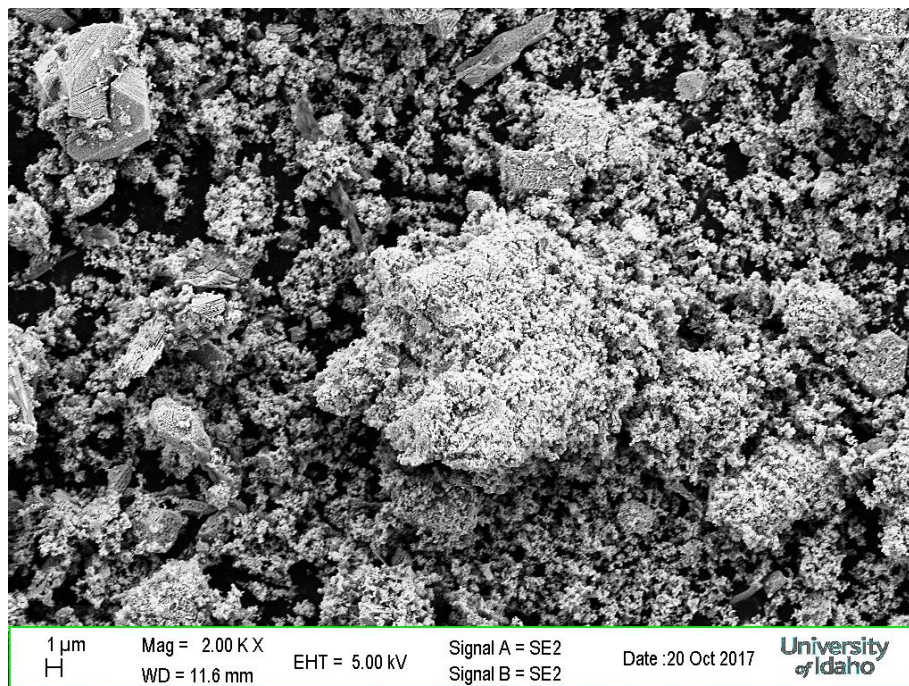


Figure 3-7. The SEM micrograph of pretreated Trichromatic phosphor.

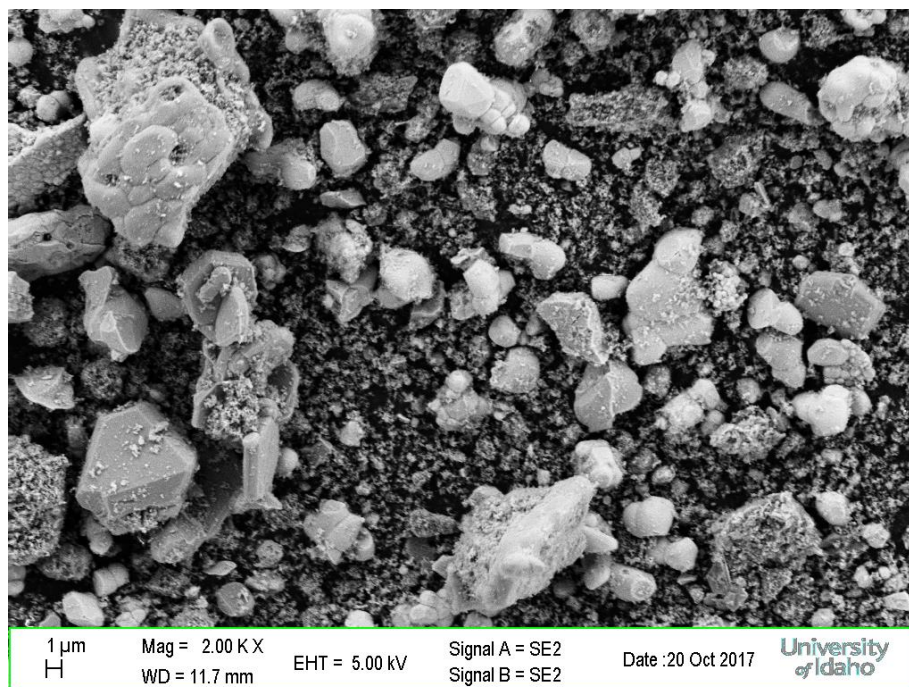


Figure 3-8. The SEM micrograph of original Sylvania phosphor.

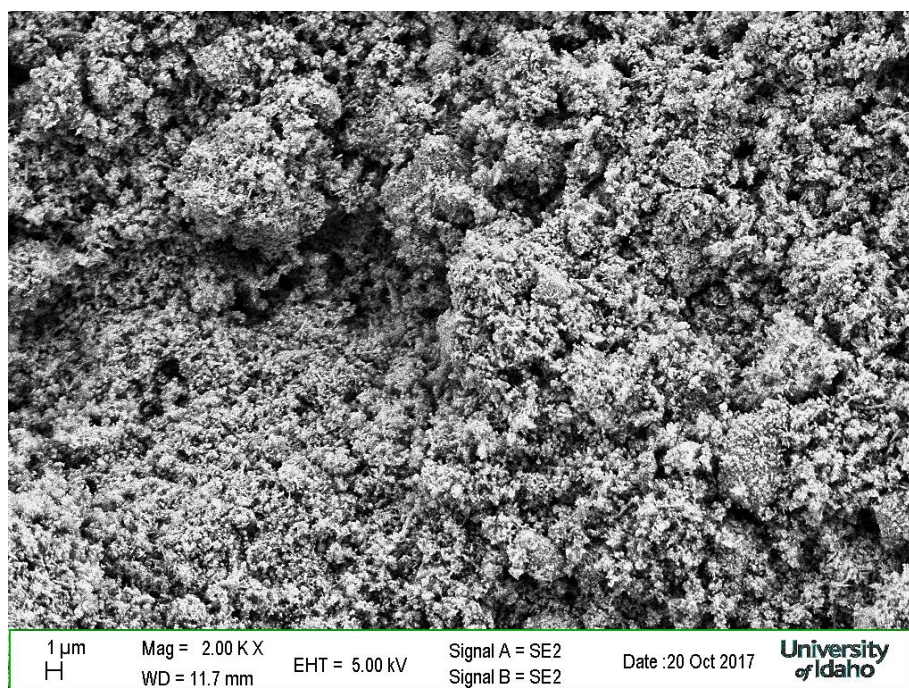
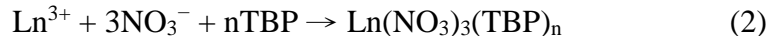
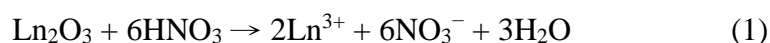


Figure 3-9. The SEM micrograph of pretreated Sylvania phosphor.

3.3.2. TBP-HNO₃ complex preparation

Due to the nonpolar nature of carbon dioxide, direct application of supercritical carbon dioxide (sc-CO₂) to extract rare earth metals from waste phosphors is not likely. Therefore, tributyl phosphate-nitric acid (TBP-HNO₃), a complex commonly used for extracting uranium and lanthanides, was chosen for our investigation. TBP, an amphiphilic species functioning like surfactants, has 3 non-polar ends, which make it highly soluble in sc-CO₂ and a polar end, which can form hydrogen bonding with nitric acid that can pick up rare earth metal ions. Conventionally, TBP-HNO₃ adduct prepared by mixing 1 aliquot of TBP and 1 aliquot of concentrated HNO₃ to make complex A. Based on Shimizu et al.'s report, the extraction reactions of lanthanide oxides by TBP-HNO₃ complex can be expressed by Eqs. (1) and (2).



The water generated from the first reaction will form small droplets, which will further affect the extraction efficiencies. Therefore, additional ¼ aliquot of TBP was added to 1 aliquot of complex A to make complex B. This additional amount of TBP will make extraction of lanthanide oxides more efficient.

3.3.3. Extraction of rare earth elements from fluorescent phosphor materials under atmospheric conditions and selectivity

Prior to supercritical extraction, we performed extraction experiments under atmospheric conditions, as described in sec. 2.3., on the original phosphors, treated-non-washed phosphors and treated-washed phosphors by using complex B. The reason we

performed extraction experiments on treated-non-washed phosphors was to leave as much impurities and undesired metals as possible in the materials and see if this TBP-HNO₃ adduct could achieved selective extraction. Our results for both Trichromatic phosphor and Sylvania materials are shown in Figure 3-6 and Figure 3-7. Due to the change of metal concentrations of each metal in the phosphor materials before and after pretreatment, our definitions of extraction efficiency are slightly different for original, treated-non-washed and treated-washed materials. The definitions are as follows:

For original and treated-non-washed phosphors-

$$\text{Efficiency [\%]} = \frac{\text{Metal extracted from original or treated-non-washed phosphor}}{\text{Metal of original phosphor loaded}} \times 100$$

For treated-washed phosphors-

$$\text{Efficiency [\%]} = \frac{\text{Metal extracted from treated-washed-annealed phosphor}}{\text{Metal of treated-washed-annealed phosphor loaded}} \times 100$$

Figure 3-10 shows that when extraction experiments were performed on original Trichromatic phosphor (TRI) with complex B, only europium and yttrium had noticeable yields. As expected, the extraction efficiencies for cerium, and terbium were next to nothing. It is understandable since europium and yttrium in red phosphors are in oxide forms while cerium and terbium are doped in relatively stable green phosphors. In addition, most of the europium in a phosphor material is contained in the red phosphor, and the rest of the europium content is in the blue phosphor, which is stable and relatively challenging to be extracted without pretreatment. Consequently, only 66.9% of europium was extracted.

When extraction experiments were performed on treated-non-washed Trichromatic phosphor (tnw-TRI), all rare earth metals could be extracted out, including cerium and terbium in the green phosphor. In addition, only magnesium had a noticeable yield among all the non-rare earth metals. However, the extraction efficiencies of all the rare earth elements were only between 40.7% and 44.5%. It is noteworthy that even the yields of europium and yttrium were not comparable with the yields of non-treated Trichromatic phosphor. Here are some explanations: (1) After the treatment of sodium peroxide at 650°C for 1 hour, there was still excess sodium peroxide leftover. The amount was hard to estimate, but it lowered the weight percentage of rare earth metals in the phosphor material. As a result, when we took a certain amount of treated phosphor material, there was less rare earth metal content than we expected. (2) Sodium peroxide, which tends to react with acids, might have reacted with the nitric acid in the TBP-HNO₃ complex and consumed the extraction capacity. (3) The matrices of green and blue phosphors might have been decomposed through alkali fusion, but cerium, lanthanum, terbium and the europium in the blue phosphor might not have been completely transformed into leachable species. Due to the above reasons, the Na₂O₂-treated phosphor material was soaked in deionized water to consume all the Na₂O₂ leftover after calcination and washed to get rid of undesired metals and impurities. The slurry was then annealed at 700°C for 1 hour.

Results shows the extraction efficiencies for the treated-washed-annealed Trichromatic phosphor (twa-TRI) improved significantly. The yields of europium and yttrium achieved to > 99%, and the yields of the other rare earth metals also improved significantly. For non-rare earth metals, same as the results for treated-non-washed phosphor, only magnesium had a noticeable yield, and the others remained negligible. The same set of

experiments were performed on Sylvania phosphors and similar results were obtained (Figure 3-11). Therefore, we believe the pretreatment procedure could help supercritical extraction of cerium, lanthanum and terbium and part of the europium out of green and blue phosphors.

From our results, we noticed that the extraction efficiencies for the non-rare earth metals were usually insignificant except magnesium. Thus, we carried out acid extraction experiments under the same conditions on Sylvania phosphor, but only replaced TBP-HNO₃ complex with 7M HNO₃. The results in Figure 3-12 show that significant extraction yields of the non-rare earth metals in the phosphors could be achieved via acid extraction. Therefore, we could conclude that TBP-HNO₃ complexes are in favor of the extraction of rare earth elements, which helps achieve selective extraction. This phenomenon could possibly be attributed to the following reasons: 1. Rare earth metals have great capability to form complexes with TBP-HNO₃, but the non-rare earth metals in the phosphor materials do not have this capability to form strong complexes. As a result, selective extraction was achieved. 2. Rare earth metals have very good solubility in TBP-HNO₃ complex, but the non-rare earth metals in the phosphors can only dissolve in TBP-HNO₃ complex to a very limited extent. However, compared to the other non-rare earth metals, magnesium might have a relatively greater solubility in TBP-HNO₃ complex. Consequently, a noticeable yield of magnesium was observed. Figure 3-13 shows our measurement of the solubility for relevant metal oxides in TBP-HNO₃ complex. As expected, rare earth oxides have much higher solubility than non-rare earth oxides. Among the non-rare earth oxides, magnesium oxide has the highest solubility followed by calcium oxide and aluminum oxide, which is consistent to the results in Figure 3-10 and Figure 3-11.

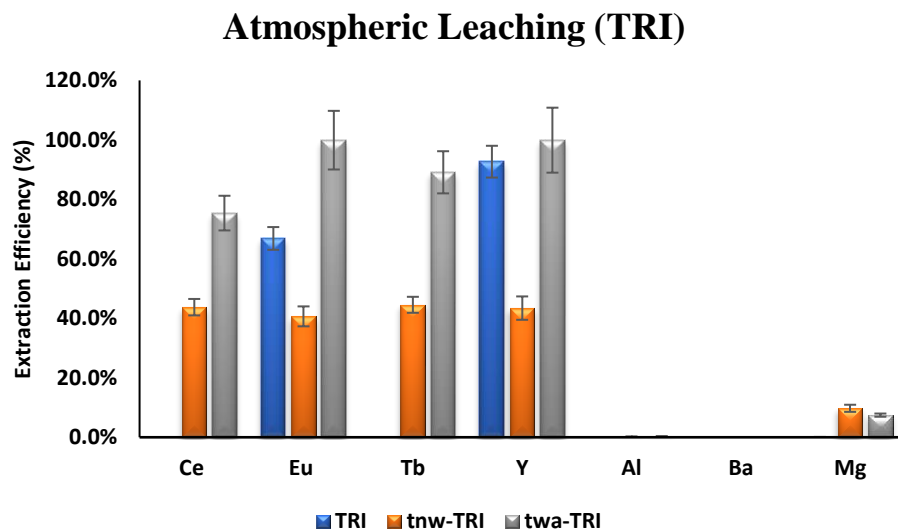


Figure 3-10. TBP-HNO₃ extraction under atmospheric conditions for original Trichromatic phosphor (TRI), treated-non-washed Trichromatic phosphor (tnw-TRI), and treated-washed-annealed Trichromatic phosphor (twa-TRI).

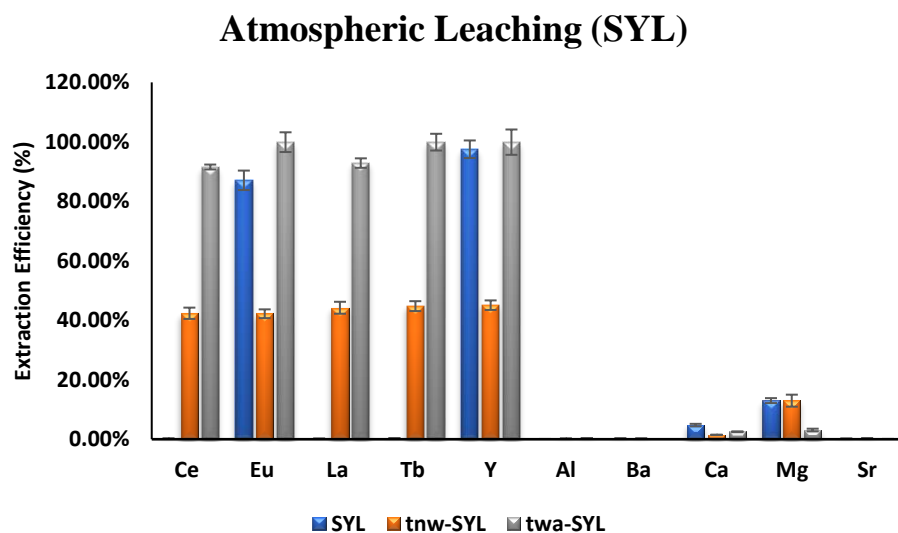


Figure 3-11. TBP-HNO₃ extraction under atmospheric conditions for original Sylvania phosphor (SYL), treated-non-washed Sylvania phosphor (tnw-SYL), and treated-washed-annealed Sylvania phosphor (twa-SYL).

Acid leaching

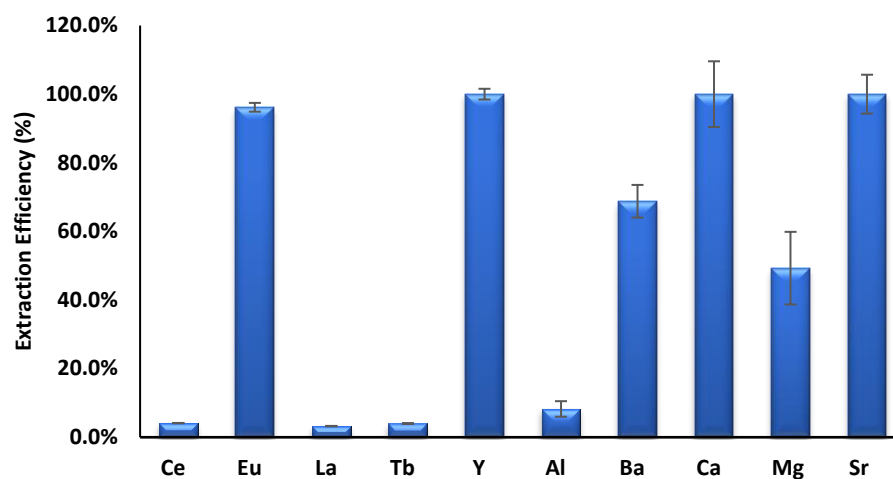


Figure 3-12. Acid leaching on Sylvania phosphor with 7M HNO₃ at 60°C for 2 hours.

Solubility

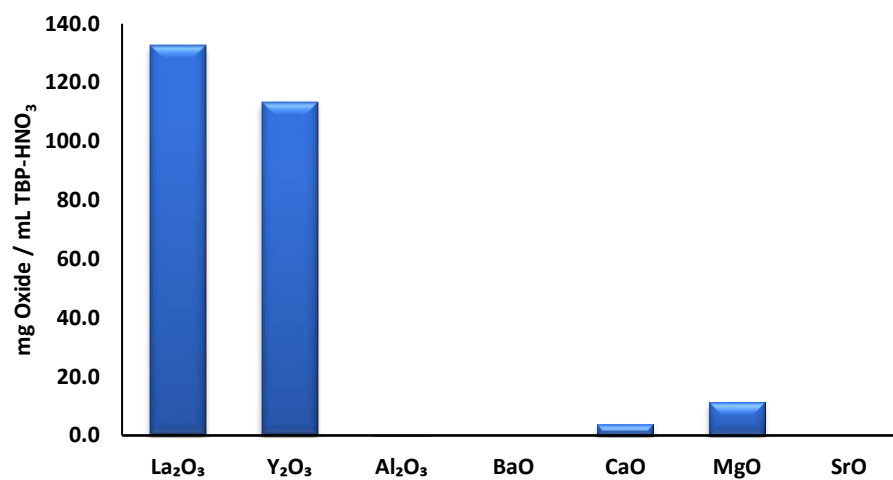


Figure 3-13. Solubility of rare earth oxides and non-rare earth oxides in TBP-HNO₃ adduct (mg·mL⁻¹) at 60°C

3.3.4. Extraction of rare earth elements from fluorescent phosphor materials via supercritical CO₂

Based on the results on Sec. 3.3.3., obviously, sodium peroxide pretreatment can help extraction of rare earth elements out of green and blue phosphors. Therefore, supercritical fluid extraction was performed on the treated-washed-annealed phosphor materials. The conditions and procedure were as described in Sec. 3.2.5. Figure 3-13 shows the results for supercritical extraction of the treated-washed-annealed Trichromatic phosphor and treated-washed-annealed Sylvania phosphor. As we can see, compared to the results of extraction under atmospheric conditions, the extraction efficiencies for all the rare earth metals improved to be > 99% for both phosphor materials. As for the non-rare earth metals, the yield for aluminum increased in twa-TRI, and the yield for magnesium increased dramatically in both twa-TRI and twa-SYL. This phenomenon could have been attributed to 2 factors: 1. aluminum and magnesium ions were able to form weak but relatively stronger complexes with the mixture of TBP-HNO₃ and sc-CO₂ than the other non-rare earth metals; 2. the TBP in the injection cell served as a continuous supply of ligand, which was steadily introduced to the reaction cell via sc-CO₂ during dynamic extraction stage and eluted aluminum and magnesium complexes out of the reaction cell to reach a dynamic equilibrium. It is noteworthy that even though the extraction efficiencies for aluminum and magnesium look significant, but the absolute values of Al and Mg are only 11.4 and 59.9 ppm for twa-TRI, 0.32 and 6.7 ppm for twa-SYL. Compared the rare earth elements' several hundred ppm of concentration, the extraction may be considered selective for the REEs.

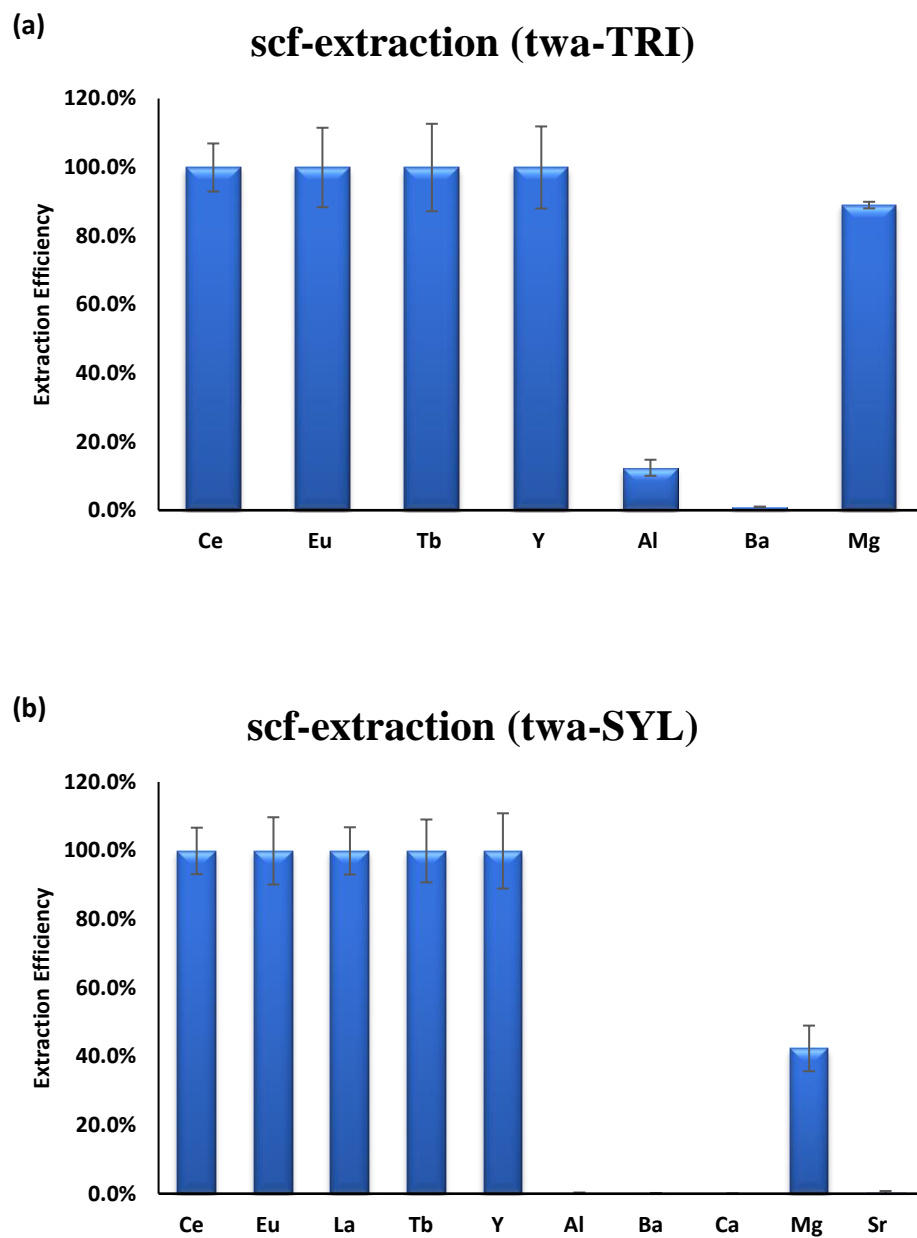
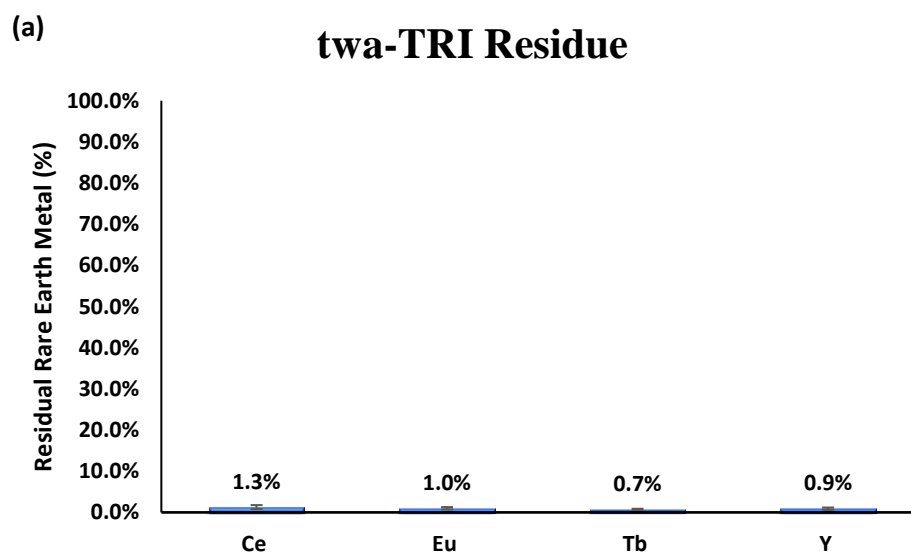


Figure 3-14. Supercritical extraction efficiencies for (a) treated-washed-annealed Trichromatic phosphor (b) treated-washed-annealed Sylvania phosphor

3.3.5. Mass balance of rare earth elements

The solid residue after sc-CO₂ extraction was analyzed for its rare earth content to ensure material balance of the extraction process. The results are shown in Figure 3-14. In the TRI residues, the Ce, Eu, Tb, and Y contents (weight %) were all less than 1.3% indicating virtually quantitative extraction of these rare earths (>98.7%) from the treated sample by the sc-CO₂ process; in the SYL residues, the rare earth contents varied from 3.3% for La to 1.0% for Tb. These results also indicate near total extraction of the REEs from the treated phosphor by the sc-CO₂ process.



twa-SYL Residue

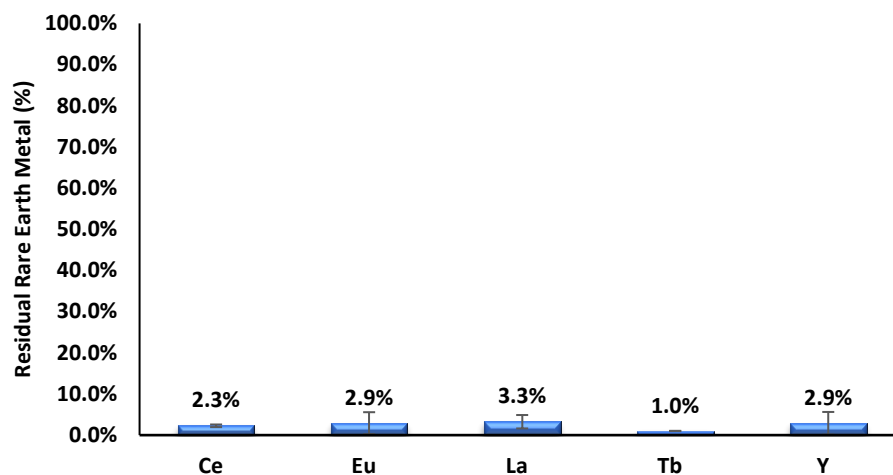


Figure 3-15. (a) The weight percent of the remaining rare earth elements in the Trichromatic phosphor residue after Sc-CO₂ extraction. (b) The weight percent of the remaining rare earth elements in the Sylvania phosphor residue after Sc-CO₂ extraction.

3.4. Conclusion

Supercritical carbon dioxide could be used to extract rare earth metals out of waste phosphor materials and realize high extraction efficiencies by using TBP-HNO₃ adduct if the phosphors are pretreated. It is important to wash and anneal the sodium peroxide-calcinated phosphor materials to raise the REE concentrations and to completely transform the rare earth metals into extractable species. Under atmospheric conditions, decent yields of REEs and high degree of selective extraction can be achieved through using TBP-HNO₃ adducts. Under supercritical conditions, extraction efficiencies of REEs can be further improved due to the continuous extraction process though it will also increase the yields of undesired elements such as magnesium and aluminum. How to achieve high extraction efficiencies of rare earth metals without extracting non-rare earth metals will be an important topic for further investigation.

Acknowledgement

This research was supported by Idaho National Laboratory. We are thankful to our colleagues Bob Fox, Donna Beak, Mary Case and Clive Yen, who provided expertise, technique support or professional opinions that greatly assisted the research. We have to express our appreciation to Leslie Backer for taking time out of her busy schedule to run ICP analysis for us.

Reference

1. Binnemans, K.; Jones, P. T.; Blanpain, B.; Van Gerven, T.; Yang, Y.; Walton, A.; Buchert, M., Recycling of rare earths: a critical review. *Journal of Cleaner Production* **2013**, *51*, 1-22.
2. Critical Materials Strategy (2010). U.S. Department of Energy: 2010; pp 1-170.
3. Critical Materials Strategy (2011). U.S. Department of Energy: 2011; pp 1-190.
4. Goonan, T. G. *Scientific Investigations Report : Rare Earth Elements—End Use and Recyclability*; 2011; pp 1-22.
5. *Environmental Impact Analysis: Spent Mercury-Containing Lamps (4th edition)* National Electrical Manufacturers Association: 2000; pp 1-9.
6. Binnemans, K.; Jones, P. T., Perspectives for the recovery of rare earths from end-of-life fluorescent lamps. *Journal of Rare Earths* **2014**, *32* (3), 195-200.
7. Tunsu, C.; Petranikova, M.; Gergorić, M.; Ekberg, C.; Retegan, T., Reclaiming rare earth elements from end-of-life products: A review of the perspectives for urban mining using hydrometallurgical unit operations. *Hydrometallurgy* **2015**, *156*, 239-258.
8. Wu, Y.; Yin, X.; Zhang, Q.; Wang, W.; Mu, X., The recycling of rare earths from waste tricolor phosphors in fluorescent lamps: A review of processes and technologies. *Resources, Conservation and Recycling* **2014**, *88*, 21-31.
9. Zhao, Z. Q., Rare earth luminescent material industry and development trend of foreign. *Expert Opinion* **2010**, *10*, 10-17.
10. Otto, R.; Wojtalewicz-Kasprzak, A. Method for recovery of rare earths from fluorescent lamps. US20120027651 A1, 2012.

11. Li, R. Q.; Wu, Y. F.; Zhang, Q. J.; Wang, W. In *Extraction of rare earth from waste three primary colors fluorescent powder in high temperature alkali fusion method*, Proceedings of CCATM' 2012 international conference & exhibition on analysis & testing of metallurgical process & materials, 2012; pp 795-799.
12. Porob, D. G.; Srivastava, A. M.; Nammalwar, P. K.; Ramachandran, G. C.; Comanzo, H. A. Rare earth recovery from fluorescent material and associated method. US8137645 B2, 2012.
13. Zhang, S.-G.; Yang, M.; Liu, H.; Pan, D.-A.; Tian, J.-J., Recovery of waste rare earth fluorescent powders by two steps acid leaching. *Rare Metals* **2013**, *32* (6), 609-615.
14. Wu, Y.; Wang, B.; Zhang, Q.; Li, R.; Yu, J., A novel process for high efficiency recovery of rare earth metals from waste phosphors using a sodium peroxide system. *RSC Advances* **2014**, *4* (16), 7927-7932.
15. Shimizu, R.; Sawada, K.; Enokida, Y.; Yamamoto, I., Supercritical fluid extraction of rare earth elements from luminescent material in waste fluorescent lamps. *The Journal of Supercritical Fluids* **2005**, *33* (3), 235-241.

Chapter4: The Influence of Ultrasound on Acid Leaching of Rare Earth Elements from the Phosphors of End-of-Life Fluorescent Lamps

Abstract

Extractions of Rare Earth elements from fluorescent phosphors with nitric acid under the influence of ultrasound were systematically investigated with respect to various parameters including sonication time, temperature, and acid concentration. Using 11M HNO₃ at 80°C with 1-hr sonication, extraction yields over 99% for cerium, europium, lanthanum and yttrium as well as 93% for terbium could be achieved. Europium and yttrium are easily extracted by nitric acid under sonication whereas cerium, lanthanum, and terbium require longer extraction times. The rates of extraction of Ce, La, and Tb appear to follow first order kinetics. The activation energies of Ce, La, and Tb were determined to be 56.9, 58.7, and 56.1 kJ/mol, respectively. Ultrasound-assisted pretreatment of fluorescent phosphors followed by acid leaching of the REEs under different conditions were also investigated. Some information about the fluorescence spectra and SEM micrographic morphologies of the treated phosphors is also given.

4.1. Introduction

Rare earth elements (REEs) have numerous industrial applications and are essential for modern societies. They drive our new technologies and shape our lifestyles. Rare earth elements are used not only in defense technologies such as stabilizer material in rocket nose cones, and laser crystals specific to spectral characteristics for military communications, but also in consumer electronics, including phosphors for TV screen, computer display and fluorescent light bulbs, batteries, cell phones, electric vehicles, etc. China has been the biggest supplier of rare earth elements since the late 1990s. According to the estimates made by the U.S. Geological Survey, there are approximately 130 million metric tons of worldwide rare earth reserves. China owns the highest proportion of these reserves, which are estimated at some 44 million metric tons¹. With the attempt to develop its own industry for the 17 REE minerals and raise their prices, China imposed restrictions on exports of REEs in 2009, which resulted in escalated concerns about the future accessibility of these elements. Consequently, industrial countries such as Japan, the United States, and countries of the European Union face tighter supplies and higher prices for rare earth elements. Although China dropped its restrictions after losing the WTO case in 2015², recycling of rare earth elements from end-of-life electronic products has become a new research area of considerable interest in recent years.

Fluorescent lamps are the most accessible source of rare-earth-containing end-of-life electronic products in our daily life. The white powder coated on the inner wall of fluorescent lamps is a mixture of 3 types of rare-earth-containing phosphors, i.e., red, green, and blue phosphor, to produce visible light. They usually come in different chemical forms including oxides, phosphates, silicates or aluminates (Table 1), which generally contain cerium,

europium, terbium, yttrium with or without lanthanum, depending on the brand of fluorescent lamps and what type of green phosphor is employed³⁻⁴.

Table 4-1. Rare-earth-containing phosphors

Phosphor type	Possible compositions	Wavelength
Red	$\text{Y}_2\text{O}_3:\text{Eu}^{3+}$	611 nm
Green	$\text{CeMgAl}_{10}\text{O}_{17}:\text{Tb}^{3+}$; $\text{LaPO}_4:\text{Ce}^{3+}\text{Tb}^{3+}$; $(\text{Ce,Tb})\text{MgAl}_{11}\text{O}_{19}$	546 nm
Blue	$\text{CaMgSi}_2\text{O}_6:\text{Eu}^{2+}$; $\text{BaMgAl}_{10}\text{O}_{17}:\text{Eu}^{2+}$	450 nm

As shown in Table 1, red phosphors are usually in the form of oxides. Green and blue phosphors are usually in the forms of phosphates, silicates or aluminates. In general, rare earth oxides can dissolve in acid solutions with or without heating. When rare earth metals, however, are doped in phosphate, silicate or aluminate matrices, they are more difficult to be extracted by conventional acid leaching processes due to their relatively stable chemical structures. Therefore, europium and yttrium tend to be easy to be leached out by acid solutions, but acid leaching of cerium, lanthanum, and terbium are much more challenging. As a result, new activation methods are required to extract cerium, lanthanum, and terbium from fluorescent phosphors.

The influence of ultrasound on rate enhancement of chemical reactions accompanied with higher production yields, in homogeneous or heterogeneous systems, is well known in the literature⁵. Ultrasound is sound at frequencies greater than the upper frequency limit of human hearing range (approximately 20 kHz). At atmospheric pressure, ultrasonic waves have wavelengths of 1.90 cm and less in air or 7.42 cm and less in water. Whether in air or in water, the wavelength is much greater than the bond length between atoms in the molecule.

Thus, the sound wave will not cause any change on the vibrational energy of the bond, and therefore will not directly increase the internal energy of a molecule. That is, the chemical effects of ultrasound on chemical reactions do not result from a direct interaction of the ultrasonic sound wave with the molecules in the solution, Instead, the effects arise from acoustic cavitation⁶⁻⁷.

Ultrasound travels in media as longitudinal waves and forms areas of high and low pressure known as compression and rarefaction phases, respectively. Air molecules dissolved in the solution nucleate around particles to form bubbles during rarefaction phases. When a solution is irradiated with ultrasound, these bubbles grow during the rarefaction phases. On the compression phases, however, the high external pressure squeezes the bubbles as well as the matters inside, and cause the bubbles to shrink. The bubbles grow a little more during the rarefaction phase of the sound wave than they shrink during the compression phase. This process of growth and compression proceeds for a few cycles until the external pressure dominates and the bubbles collapse^{5, 8}. The formation, growth, and collapse of the bubbles is well-known as the cavitation phenomenon, and the bubbles are called cavitation bubbles. Cavitation bubbles resemble tiny chemical facilities, in which chemical species interact with each other under extremely high temperature and pressure. According to the reports of Suslick et al., the temperature and pressure inside cavitation bubbles can reach as high as 5000°C, and 1000 atm^{9,10}. Therefore, acoustic cavitation provides unique environments for chemical reactions. Application of ultrasonic radiation to solutions generates not only chemical but also physical effects. With liquids containing solids, similar phenomena also occur with exposure to ultrasound. Upon collapse of cavitation bubbles, shock waves and microjets are produced. These shockwaves and microjets can break brittle materials into fragments, deform

ductile materials and exfoliate layered materials¹¹⁻¹⁴. Liquid-powder suspensions produce high velocity interparticle collisions. These collisions can change the surface morphology, composition, and reactivity¹¹. Moreover, the nature of ultrasound provides chemical reactions with high speed and frequency of agitation compared to the conventional magnetic stirring method. As a result, sonication has been used in various fields such as food processing, waste water treatment, nanomaterial synthesis, extraction, etc.

The effects of ultrasound in solutions have been applied in many different fields. In the field of sonochemistry, different results usually come with different parameters, such as frequency, power, solution, temperature, sonication times. In this paper, we will demonstrate enhancement of acid leaching of rare earth elements from end-of-life fluorescent phosphors using nitric acid with ultrasonic assistance and discuss the effects of various acid concentrations, sonication time, and temperature.

4.2. Experimental Section

4.2.1. Waste phosphor materials, chemicals

Sylvania fluorescent phosphor material was collected with ultrasonic assistance from end-of-life fluorescent lamps, in which fluorescent lamps were cut into sections and immersed into the water of a sonication bath (Fisher Scientific FH60H, 100-Watt, 42 kHz). After 30-60 seconds of sonication, the white rare earth phosphor coating was totally removed from the inner wall of the lamp with gentle shaking. After rinsing, the phosphor material in water was collected and dried. The material was dried in an oven at 70°C for 24 hours. The Sylvania phosphor was then passed through 250 μm sieves and placed in a plastic bottle. The bottle

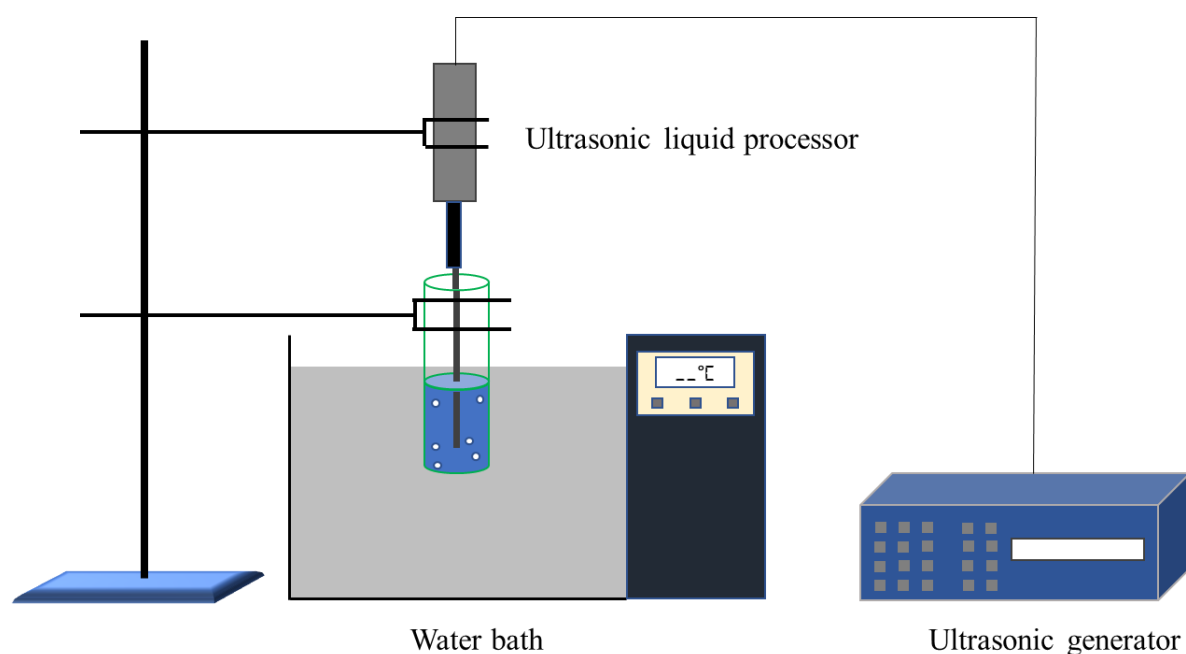
was shaken mechanically for 3 hours to ensure the homogeneity. Finally, this bottle of processed phosphor material was stored in a dessicator. To estimate the metal content in the phosphor, samples of 100 mg of the material was mixed with an appropriate amount of sodium peroxide to carry out alkali fusion under an elevated temperature. After the sodium peroxide calcination, acid digestion was performed on the alkaline slags by mixing 10 mL of concentrated HNO_3 and 10 mL of 30% H_2O_2 (Fisher Scientific). The solutions were heated, stirred and refluxed at 80 °C and 500 rpm for 24 hours to ensure all solid materials were completely dissolved. After dissolution, solutions were cooled, transferred and diluted in 100 mL volumetric flasks with deionized water. A 2% nitric acid solution, prepared from concentrated stock solution and deionized water, was used to further dilute the solutions for ICP analysis. Concentrated nitric acid (Macron Fine Chemicals, 70%) was used to prepare various concentrations of nitric acid solutions. A 12M sodium hydroxide solution was prepared using sodium hydroxide pallets (mallinckrodt chemicals).

4.2.2. Experimental set-up, instruments and experiment methods

In ultrasonically-assisted extraction experiments, samples of 100 mg Sylvania phosphor material and 20 mL nitric acid solutions of the designated concentrations were put into 50-mL centrifuge tubes. The centrifuge tubes were placed in a water bath at a designated temperature. An ultrasonic liquid processor (Sonics, VCX130, 20kHz, 130 Watt) was inserted into the centrifuge tube and sonicate the reaction mixture. The parameters are shown in Table 4-1. The experimental setup for sonication was illustrated in Figure 4-1.

Table 4-2. Extraction under ultrasonic conditions

Extractant	1M, 3M, 5M, 7M, 9M, 11M HNO ₃
Phosphor materials	Sylvania fluorescent phosphor
Material size	100 mg phosphor + 20 mL HNO ₃ solution
Frequency	20kHz
Amplitude	80%
Pulse	8 seconds on, 2 seconds off
Temperature	30°C, 40°C, 60°C, 70°C, 80°C
Sonication time	10, 20, 30, 40, 60 min

**Figure 4-1.** Experimental set-up for sonication experiments.

A few extraction experiments under traditional agitation conditions were performed as the control group. In the control experiments, samples of 100 mg Sylvania phosphor material and 20 mL nitric acid solutions of the designated concentrations were put into 30-mL glass vials. These vials were put into an oil bath at a designated temperature and stirred magnetically. After the experiments, the solutions were allowed to cool down and centrifuged at 3300 rpm for 10 minutes. The supernatants were then collected and sent for ICP analysis.

The parameters for extraction under ultrasonic conditions a traditional agitation conditions are as follows:

Table 4-3. Extraction under traditional agitation conditions

Extractant	1M, 3M, 5M, 7M, 9M, HNO ₃
Phosphor materials	Sylvania fluorescent phosphor
Material size	100 mg phosphor + 20 mL HNO ₃ solution
Stir speed	500 rpm
Temperature	60°C, 80°C
Sonication time	10, 20, 30, 40 min

For ultrasound-assisted pretreatment of phosphor experiments, the process was carried out in the similar fashion as the ultrasonic-assisted extraction experiments. A sample of 1000 mg Sylvania phosphor material and 20 mL reagent (H₂O, H₂O₂, 12M NaOH, etc.) were put into a 50-mL centrifuge tube. This centrifuge tube was then placed in a water bath at 60°C or 80°C and sonicated with an ultrasonic liquid processor. After sonication, the solution was allowed to cool down and centrifuged at 3300 rpm for 10 minutes. The supernatants and the precipitates were collected separately. The supernatants were analyzed using ICP-MS. The precipitates were used for extraction experiments. The parameters for the pretreatment under ultrasonic conditions are as follows:

Table 4-4. Pretreatment under ultrasonic conditions

Reagents	DI H ₂ O, 30% H ₂ O ₂ , 12M NaOH
Phosphor materials	Sylvania fluorescent phosphor
Material size	1000 mg phosphor + 20mL reagent
Frequency	20kHz
Amplitude	80%
Pulse	8 seconds on, 2 seconds off
Temperature	60°C, 80°C
Sonication time	60 min

After all the experiments, all the solutions were analyzed using ICP-MS (Agilent 7700x). Florescence spectra for the solid residues were obtained by a fluorescence spectrometer (FluoroMax-3, Horiba).

4.3. Results and discussion

It is well-known that particle size, temperature, solvent concentration, solid to liquid ratio and agitation method are generally the most important factors to be considered when a chemical reaction, including solvent extraction, is carried out. The particle size of a substance has a significant effect on extraction efficiency. Smaller particle size of a material gives a larger contact surface area with the solvent, which will have a higher collision probability among the reactants and a better mass transfer rate. As we mentioned earlier, when cavitaional bubbles implode, shockwaves and microjets are generated. They are able to break brittle materials into fragments. Thus, ultrasound provides a great tool for ultrasonic vibration machining, which breaks big particles into smaller ones. In addition to the above factors, some other factors are as important in the field of sonochemistry. These parameters include sonication time, reaction temperature, hydrostatic pressure, ultrasonic frequency, acoustic power, the nature of dissolved gases and the physicochemical properties of the solvent., etc. The best extraction efficiency comes from the optimal combination of numerous factors. Thus, we conducted investigation to achieve the optimal condition. Due to our availability of equipment, an ultrasonic generator with only one default frequency of 20 kHz and 130 watts (Sonics, VCX130) was employed. Also, because of the corrosion issue of the ultrasonic liquid

processor, we mainly used nitric acid and sodium hydroxide solutions as our primary reagents of investigation.

4.3.1. Characterization of the phosphor

Due to the fact that we were not able to acquire the information of rare earth metal content of Sylvania fluorescent phosphor, acid digestion had to be performed on the phosphor material to estimate the chemical composition and weight percentage of each element in the phosphor material. Alkali fusion and acid leaching were carried out 3 times. The relative standard deviation of each rare earth element doesn't exceed 6%. The results are shown in Table 4-5. Our estimates for europium, terbium and yttrium are very close to those in the report from the U.S. Department of Energy³⁻⁴, which are the average of values given by lighting manufacturers in communications with DOE staff. However, our estimates of cerium and lanthanum are somewhat different. The reason can be attributed to the composition of green phosphor. The weight percentages of cerium and lanthanum vary from one manufacturer to another. Based on the DOE report, the sum of cerium and lanthanum in different types of green phosphors make up approximately 28.5%, and the sum of cerium and lanthanum in our estimate is 27.3%. Therefore, our estimate is fairly accurate.

Table 4-5. Rare earth metal content of Sylvania phosphor (mg. g⁻¹ dry phosphor material)

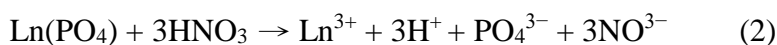
Sylvania phosphor	Ce	Eu	La	Tb	Y
Weight (mg. g ⁻¹)	50.3	18.4	46.3	19.9	219.0
Weight percentage (%)	14.2%	5.2%	13.1%	5.6%	61.9%
USDOE estimates (%)	6.5%	4.5%	22.0%	5.0%	62.0%

Therefore, the definition of extraction efficiency in this study is as follows:

$$\text{Efficiency [\%]} = \frac{\text{Metal extracted from phosphor (mg)}}{\text{Metal content of phosphor loaded (mg)}} \times 100$$

4.3.2. Comparison of extraction with ultrasonic and without ultrasonic influence

Shimizu et al. reported the dissolution yields of Y, Eu, La and Ce when a quantity of 20 mg of the luminescent material was dissolved in concentrated HNO₃ for 120 min at 313 K, which were 20.1, 23.6, 0.6 and 0.4%, respectively¹⁵. Based on this report, the dissolution and extraction reactions of lanthanide oxides and lanthanide phosphate of luminescent material can be expressed by the equation (1) and (2), respectively¹⁵:



Europium and yttrium are in their oxide forms, and lanthanide oxides tend to dissolve in acid solutions very easily. Therefore, they had higher yields than lanthanum and cerium which exist in their phosphates in their study. To assess the influence of ultrasound, an extraction was performed on 100 mg Sylvania phosphor material with 20 mL 9M HNO₃ for 40 minutes at 40°C (313 K) under ultrasonic influence. The dissolution yields for Eu and Y were over 99.9% and 9.2, 9.9 and 8.8% for Ce, La and Tb, respectively. Compared to Shimizu et al.'s results, under sonication we obtained higher yields with a lower concentration of HNO₃ and shorter time.

In order to further evaluate the effects of sonication, experiments for extraction of rare earth elements from fluorescent phosphors with 9M nitric acid solution at 60°C were conducted. The first set was agitated by conventional magnetic stirring at 500 rpm in a 60°C oil bath for 40 minutes while the other set was agitated with an ultrasonic liquid processor with a 20kHz frequency in a 60°C water bath. The results are shown in Figure 4-2.

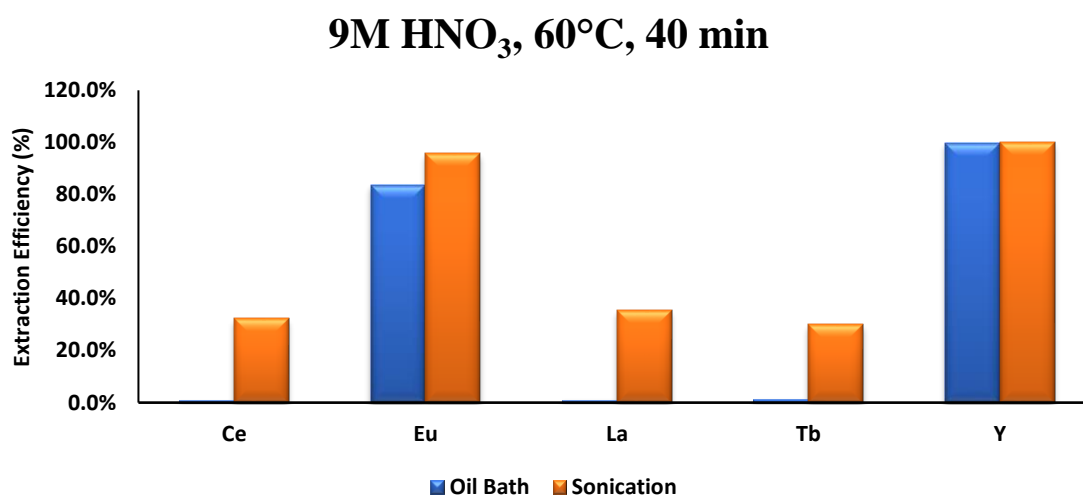


Figure 4-2. Extraction efficiencies of rare earth elements from fluorescent phosphors with and without sonication.

In fluorescent phosphors, europium and yttrium of red phosphors are usually in their oxide forms, which can easily dissolve in acid solutions, whether weak or strong, while the europium in blue phosphors and the cerium, lanthanum and terbium in green phosphors, which are doped in phosphate or aluminate matrices, are known to be challenging to be extracted through conventional solvent extraction methods. As expected, with conventional magnetic stirring agitation, 80% or more of the europium and yttrium could be leached by 9M HNO₃, but the efficiencies for cerium, lanthanum and terbium were next to nothing. However, when

extraction experiments were conducted under the influence of ultrasound, cerium, lanthanum and terbium were extracted, and the efficiencies ranged from 30.0% to 35.4%. With ultrasound, the efficiencies for europium and yttrium did not improve much, but for cerium, lanthanum and terbium, they improved over 30%. Indeed, the ultrasonic liquid processor vibrates 20000 times per second, but magnetic stirring at 500 rpm is only 8.3 round per second, in which the agitation rate of the ultrasonic liquid processor is 2400 times greater, not to mention the sonochemical effects ultrasound can offer. Therefore, extraction under ultrasonic influence significantly enhanced the extraction of rare earth metals from fluorescent phosphors.

4.3.3. Sonication time effect

The sonication time has to be carefully considered when using ultrasound. With insufficient sonication time, desired results might not be obtained; an excess of time can cause not only a waste of energy and time, but also damage to the quality of the solute since sonofragmentation is one of the sonochemical effects that ultrasonic cavitation can offer¹⁶⁻¹⁷. To achieve an optimal sonication time is an important topic. Therefore, sonication time is one of the most crucial factors when it comes to taking advantage of ultrasound effects, and it has also been discussed by many researchers in various fields¹⁸⁻²². Whether and how sonication time could influence the efficiencies of ultrasonic extraction of rare earth metals from fluorescent phosphors is critical. Figure 4-3 shows the results for extraction of rare earth metals from Sylvania fluorescent phosphors under sonication at 30°C for different lengths of sonication time. As expected, the yields of europium and yttrium are over 99.9% since they

are in their oxide forms. For the rest of the rare earth metals, the yields are not significant. However, the yields gradually increase as the sonication time increases. Obviously, extended sonication times are of help to extraction of rare earth metals from fluorescent phosphors.

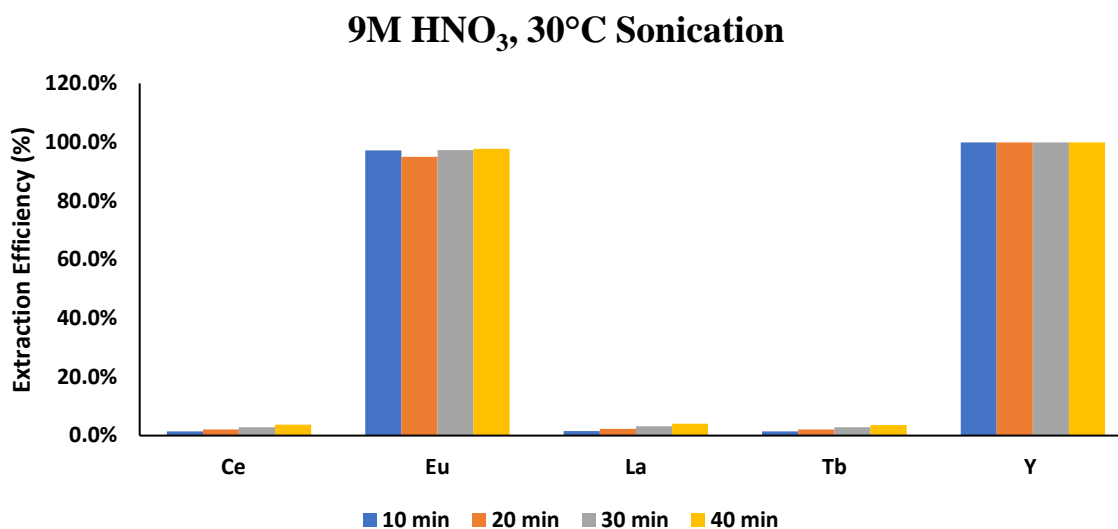


Figure 4-3. Extraction efficiencies of rare earth elements from phosphors with 9M HNO₃, sonication at 0°C for 10, 20, 30, 40 min.

4.3.4. Temperature effect

Temperature is an important parameter in solvent extraction. Conventionally, the higher the temperature of a reaction mixture, the higher the kinetic energy of the reactant particles and thus the higher the yield. However, it is not always the case. Some researchers have discovered that the solution temperature has no effect on the calcium extraction efficiency²³⁻²⁴. As a result, the influence of temperature on extraction of rare earth metals from fluorescent phosphors during sonication was investigated.

With the irradiation of ultrasound, the temperature of a receptive solution usually gradually increases due to the absorption of acoustic energy. Based on our measurement,

sonication of a 20-mL aqueous solution with a 20 Hz, 130-Watt ultrasonic liquid processor at room will cause the temperature of the solution increase to 60°C in 5 minutes, 70°C in 10 minutes and fluctuates around 70°C for extended sonication times as shown in Figure 4-4. The temperature of solution is also very susceptible to the ambient temperature and drops very quickly once sonication stops. A temperature drop of approximately 20°C occurred in 5 minutes in this case.

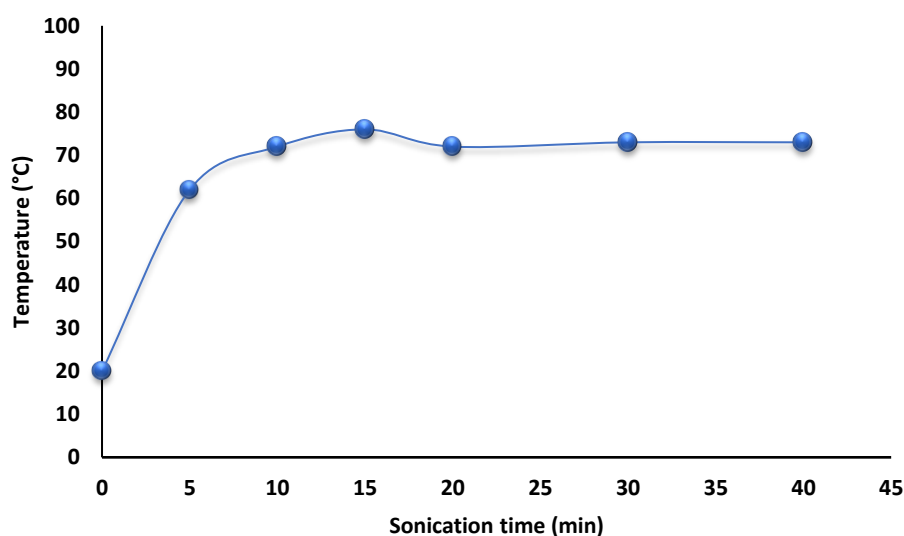


Figure 4-4. The temperature changes of a 20-mL aqueous solution vs sonication time.

Extraction using 9M HNO₃ solution under sonication for different lengths of sonication times without water bath was carried out. The results are shown in Figure 4-5. The only difference in condition between this experiment and the experiment in Section 4.3.3 is temperature control. The results in Figure 4-5 further confirm the effect of sonication time. The yield of each element increases as sonication time increases. Compared to the results in Figure 4-2, yields of europium and yttrium are highly comparable, which is understandable

and predictable since europium and yttrium are in their oxide forms, and thus they can be easily extracted. However, the yields for the rest of the metals are much higher when temperature was not controlled by the water bath. The possible explanation could be 1) with the 30°C water bath, the increase of temperature and cavitation phenomenon caused by the acoustic energy of ultrasound could be dispersed and weakened by the water bath, so the ultrasonic liquid processor became a high-speed mechanical stirrer with little sonochemical effects. It resembles the conventional extraction method using a magnetic stirring, but at a much higher speed. As a result, a great amount of the europium and yttrium dissolved in the acid solution, but cerium, lanthanum and terbium could hardly be extracted; 2) without the 30°C water bath, the acoustic energy was used to produce cavitation and increase the temperature in the solution, and therefore, the yields of cerium, lanthanum and terbium increase by the duration of ultrasonic radiation.

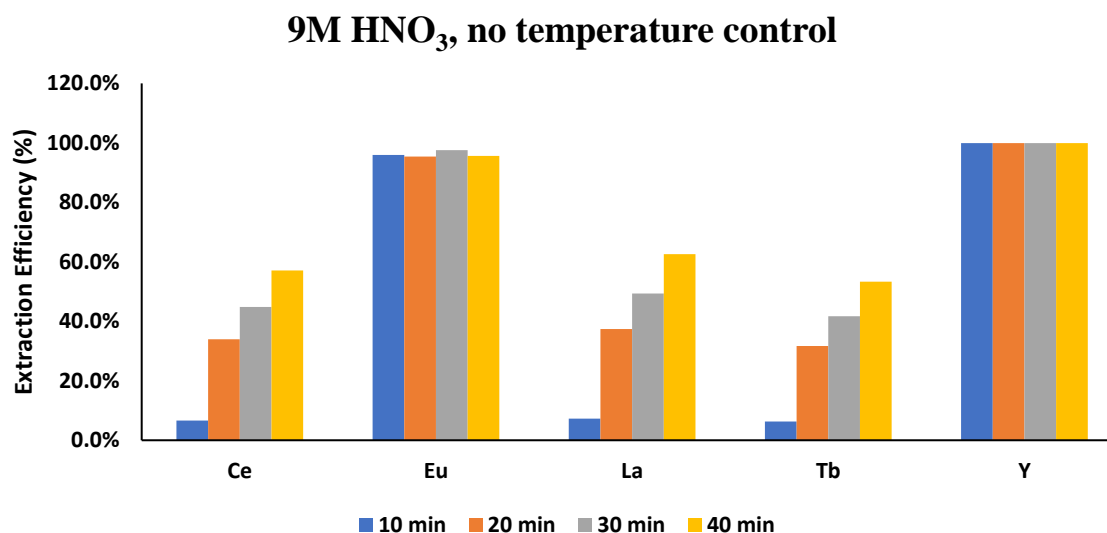


Figure 4-5. Extraction efficiencies for sonication of Sylvania phosphor with 9M HNO₃ for 10, 20, 30, 40 min without temperature control.

Experiments using 9M HNO₃ solution under sonication influence for 40 minutes in the water bath at different temperatures were also performed. The results in Figure 4-6 indicate that under lower temperatures such as 30°C and 40°C, the extraction efficiencies of europium and yttrium are comparable to the ones at higher temperatures. For the efficiencies of cerium, lanthanum and terbium, the efficiencies are also improved as the temperature increases. It is noteworthy that the results of extraction efficiencies for sonication of Sylvania phosphor with 9M HNO₃ for 40 min without temperature control (Figure 4-5) are comparable to the results obtained at 70°C, which is consistent with our measurement of temperature change under sonication (refer to Figure 4-4). That is, after 40-min of sonication, the temperature can reach up to approximately 70°C.

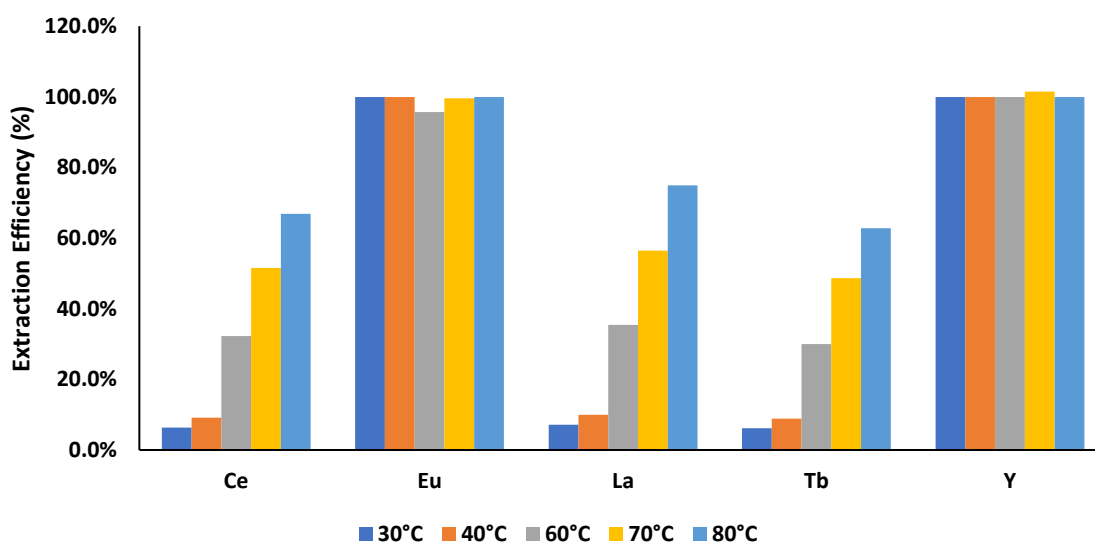


Figure 4-6. Extraction efficiencies for sonication of Sylvania phosphor with 9M HNO₃ for 40 min at 30°C, 40°C, 60°C, 70°C, 80°C.

Based on the results for temperature effect, we have concluded that using water bath to control the ambient temperature of reactions during the sonication process is more favorable

for us to manage the extraction experiments. It provides a more stable reaction environment, which makes the results more reproducible.

4.3.5. Solvent concentration effect

Solvent concentration is important for extraction process. In general, when concentration is too low, the yield might not achieve our expectation; when concentration is too high, all the metal content including undesirable impurities might be all leached out. However, due to the chemical properties of different elements, some elements can only be leached within a certain range. For example, when extracting calcium from steelmaking slag, an ammonium salt concentration higher than 1M will begin to dissolve other impurity species from the slag²⁴; in supercritical CO₂ extraction from nitric acid solution, uranyl ions can only be quantitatively extracted into the sc-CO₂ phase above 1 M HNO₃, and the extraction of trivalent lanthanide ions such as Eu³⁺ as well as trivalent actinides such as Am³⁺ only occurs above 5 M HNO₃²⁵. As a result, HNO₃ solutions of various concentrations were employed to perform extraction of rare earth metals from fluorescent phosphors at 80°C under 40 min of ultrasonic influence. As shown in Figure 4-7, over 99.9 % of europium and yttrium could be leached under this condition even when the concentration of HNO₃ was low. However, cerium, lanthanum and terbium could hardly be leached with 1M HNO₃. With the concentration of HNO₃ increasing, the yields were gradually improved. Based on the results from the previous sections, in order to extract all the rare earth metals from fluorescent phosphors, high temperature, high acid concentration and extended sonication time will be required. An

experiment employing 11 M HNO₃ at 80°C for 1 hour was carried out. In Figure 4-8, the extraction efficiency for terbium was 93.4% and the rest were over 99.9%.

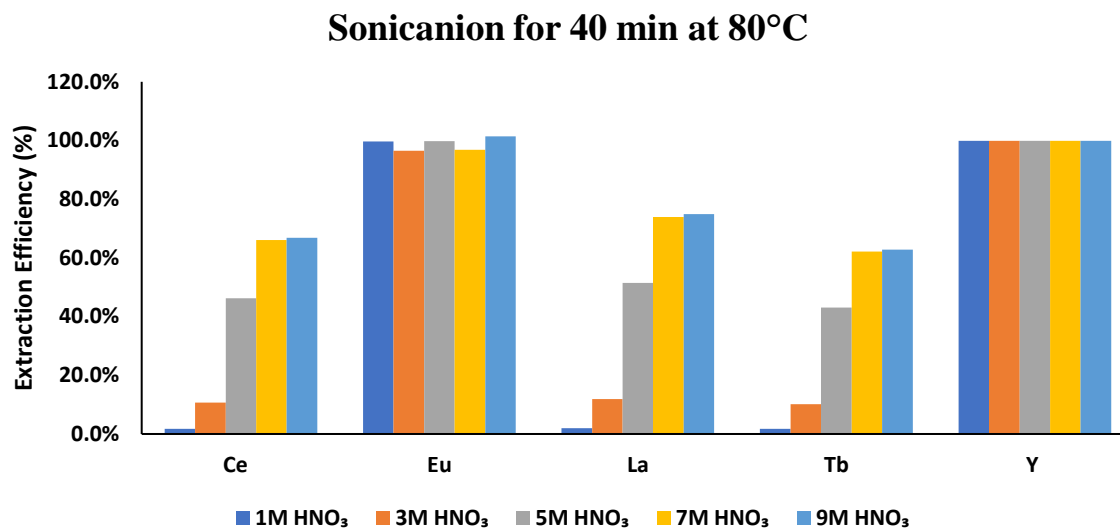


Figure 4-7. Extraction efficiencies for sonication of Sylvania phosphor at 80°C for 40 min at with 1M, 3M, 5M, 7M, 9M HNO₃ solutions.

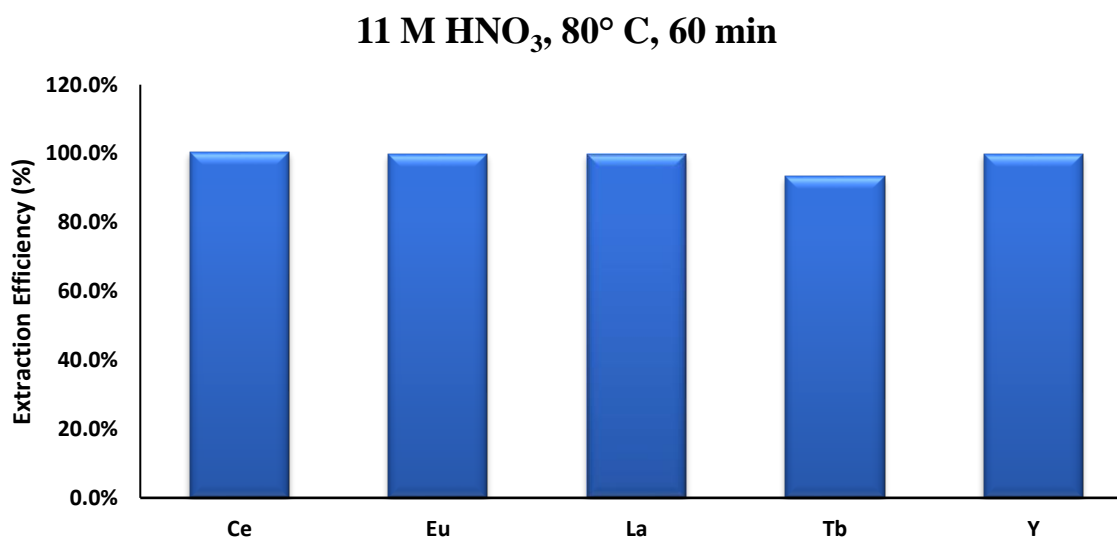


Figure 4-8. Extraction efficiency of rare earth metals from fluorescent phosphors with 11M HNO₃ at 80°C for 1 hour.

4.3.6. Kinetics Study

The rates for the extraction of cerium, europium, lanthanum, terbium and yttrium from the Sylvania fluorescent phosphor material with 9M HNO₃ solution at 60°C under sonication and in an oil bath without ultrasound were carried out and compared. Due to the fact that europium and yttrium are very easily extracted at low temperature even with low concentrations of nitric acid, the investigation of their kinetics is not discussed here.

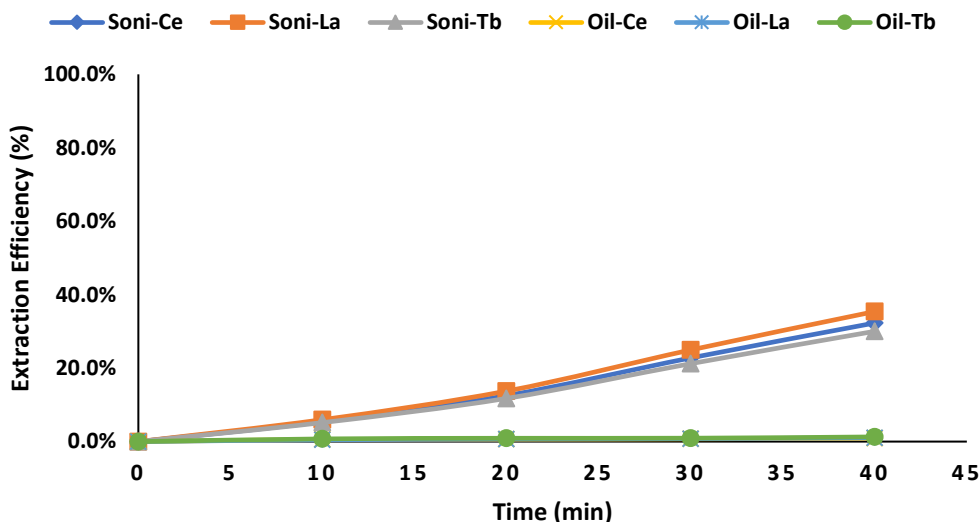


Figure 4-9. Influence of ultrasound on the yield and kinetics of the extraction of cerium, lanthanum and terbium from fluorescent phosphors with 9M HNO₃ solution at 60°C. (Results obtained from sonication experiments are prefixed with Soni-; results obtained from oil bath experiments are prefixed with Oil-.)

From the results given in Figure 4-9, we can see that the extraction rates of the REEs by 9 M nitric acid at 60°C are obviously accelerated under ultrasonic influence. Consequently, a more comprehensive kinetics study for the extraction of cerium, lanthanum, and terbium from the Sylvania fluorescent phosphor material with 9M HNO₃ solution at 30°C, 40°C, 60°C,

70°C, 80°C (313, 333, 343 and 353K) were investigated. The data for 30°C and without temperature control were also used to compared.

The time-dependent REE extraction data were analyzed by Microsoft-Excel software to obtain possible kinetics information. Based on the curve fitting for the initial rates of each element, these extraction reactions are best fitted exponentially from 40°C to 80°C, with an average coefficient of determination R^2 approximately 0.98. The exponential fitting appears to be better at higher temperatures. The R^2 values for exponential fitting are given in Table 4-6 and Figure 4-10:

Table 4-6. Coefficient of determination (R^2) for extraction of cerium, lanthanum, and terbium from fluorescent phosphor with 9M HNO_3 solution under sonication without temperature control and at 30°C, 40°C, 60°C, 70°C, 80°C (303, 313, 333, 343 and 353K).

	R^2 (Ce)	R^2 (La)	R^2 (Tb)
No temp control	0.973	0.9722	0.9733
303K	0.855	0.857	0.845
313K	0.9659	0.959	0.9562
333K	0.9709	0.9691	0.9737
343K	0.9853	0.9827	0.9876
353K	0.9899	0.9891	0.9901

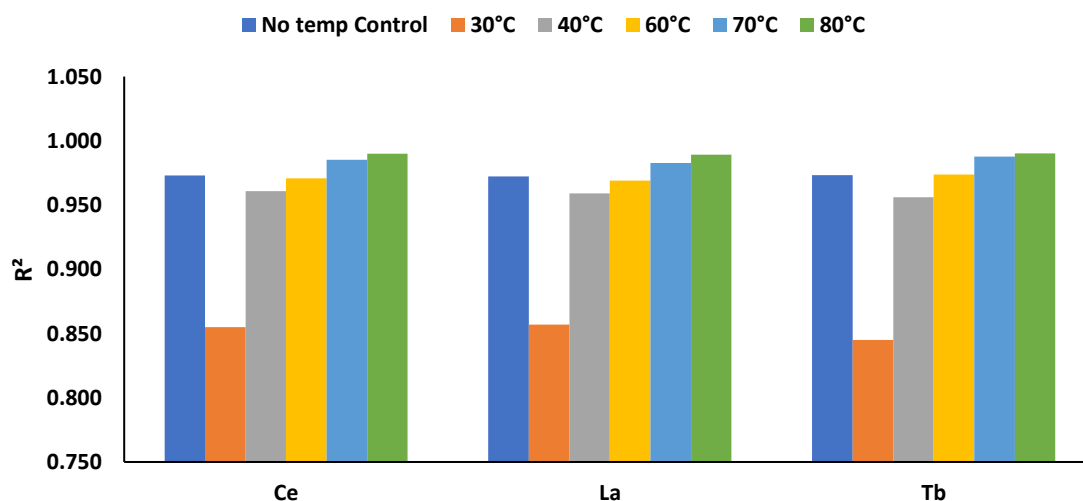


Figure 4-10. R^2 for extraction of cerium, lanthanum, and terbium at various temperatures.

According to the data, we can see that the R^2 for 30°C is relatively lower compared to the other groups. It means the curve of 30°C does not fit well exponentially; however, when it was fitted linearly, with the values of R^2 - 0.8491 for Ce, 0.8504 for La, 0.8393 for Tb, do not seem to fit well either. As for the other temperature groups, the kinetics analysis suggests that the REE leaching process probably follows first order reaction. The rate law of first order reaction is as follows:

$$[A]_t = [A]_0 e^{-kt} \quad (1)$$

where $[A]_0$ and $[A]_t$ are the initial concentrations of the loaded rare earth elements and the remaining concentrations of the rare earth elements, respectively. The value t represents the extraction time. Through curve fitting using the initial reaction rate approach, the rate constants k (in min^{-1}) of each element at different temperatures are given in Table 4-7 and figure 4-11.

Table 4-7. Rate constant k of extraction of cerium, lanthanum and terbium with 9M HNO_3 under sonication without temperature control and at 303, 313, 333, 343 and 353K (30°C, 40°C, 60°C, 70°C and 80°C).

	k (Ce)	k (La)	k (Tb)
No temp control	0.022	0.026	0.02
303K	0.001	0.002	0.001
313K	0.002	0.002	0.002
333K	0.01	0.011	0.009
343K	0.01	0.021	0.017
353K	0.029	0.036	0.026

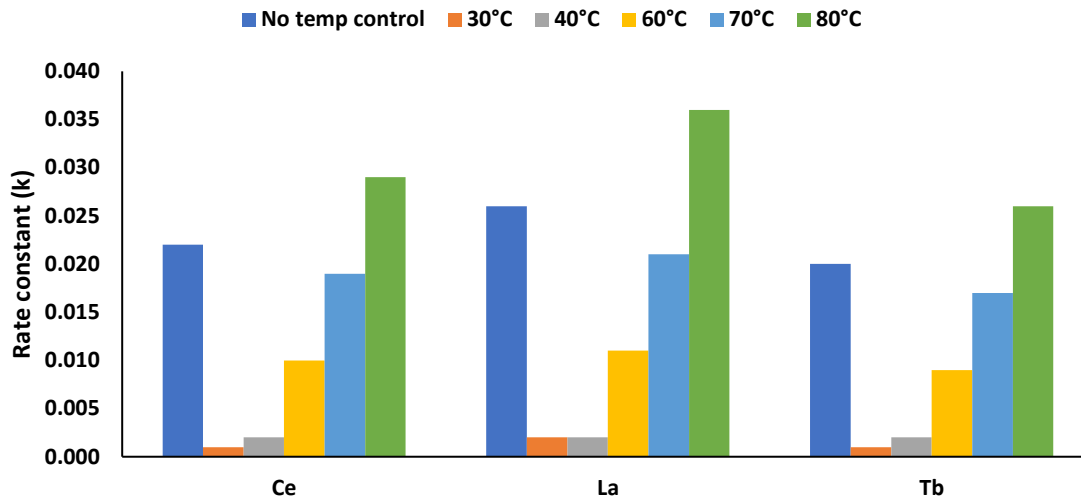


Figure 4-11. Rate constant of extraction of cerium, lanthanum and terbium with 9M HNO₃ under sonication without temperature control and at 303, 313, 333, 343 and 353K (30°C, 40°C, 60°C, 70°C and 80°C).

The data show that the rate constant values for all 3 elements increased as temperature increased, which implies the extraction process is temperature-dependent. In addition, compared to the other temperature-controlled groups, the k values of no-temperature-control group are close to those of the 70°C group, which is consistent with the results in section 4.3.4: after 40 minutes of sonication, the temperature of a 20 mL of aqueous solution will increase to approximately 70°C. Due to the low R^2 and k values of the 30°C curve, this group will not be discussed in the following kinetics study. The plots for the initial rate of reaction at 40°C, 60°C, 70°C, 80°C and without temperature control are presented in Figure.4-12 (a)-(e), respectively.

To evaluate the temperature dependence of the rate constants of the extraction of cerium, lanthanum, and terbium from the Sylvania fluorescent phosphor, Arrhenius equation is then used, which is as follows:

$$k = A \cdot \exp(-E_a/R \cdot T) \quad (2)$$

where k is the rate constant, A is a constant, E_a is the activation energy, R is the universal gas constant ($8.314 \times 10^{-3} \text{ kJ mol}^{-1}\text{K}^{-1}$), and T is the absolute temperature (in Kelvin).

Equation (2) can be rewritten as

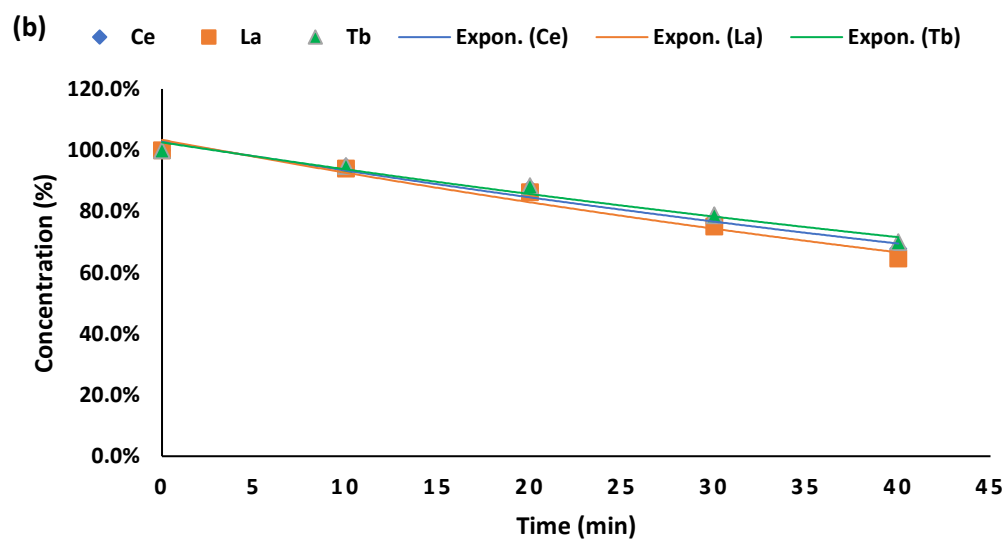
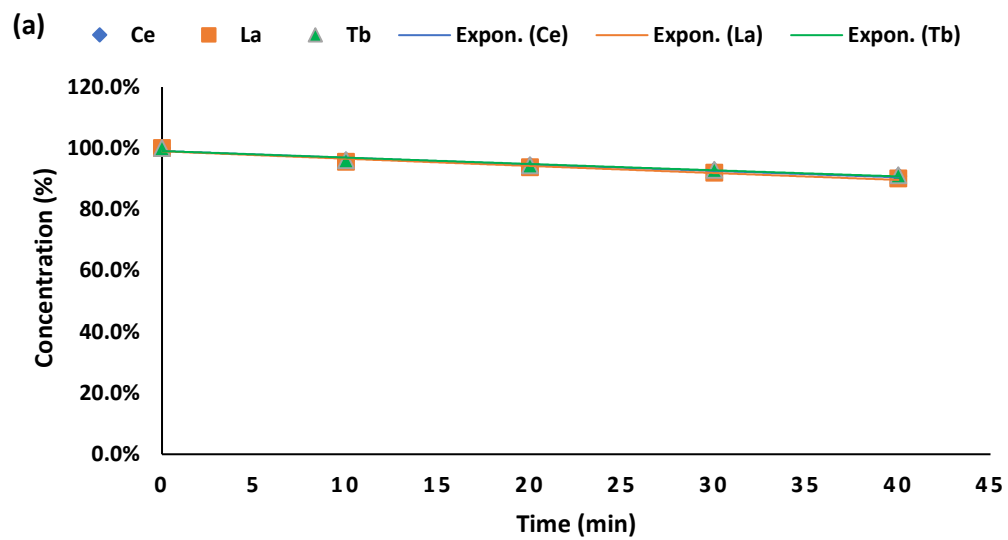
$$\ln k = -(E_a/R) (1/T) + \ln A \quad (3)$$

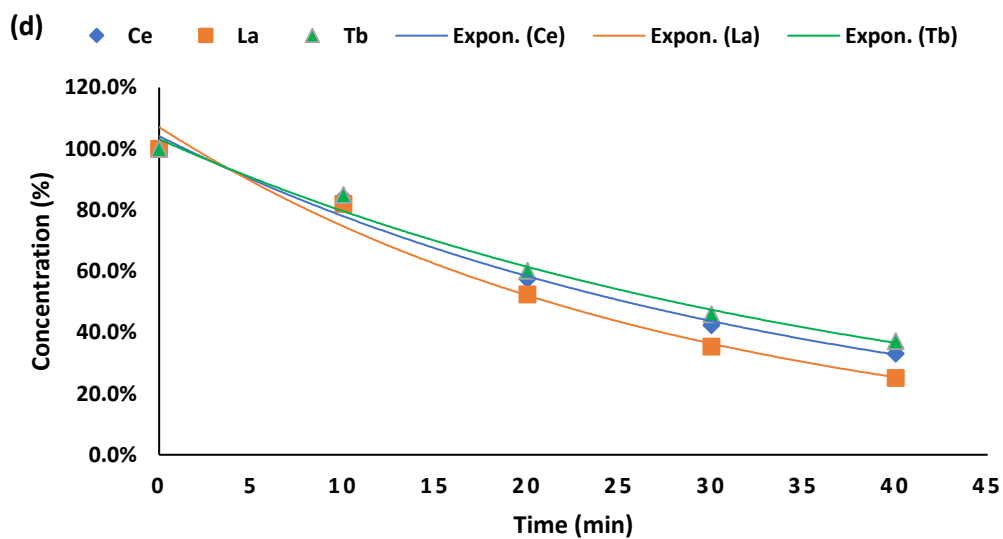
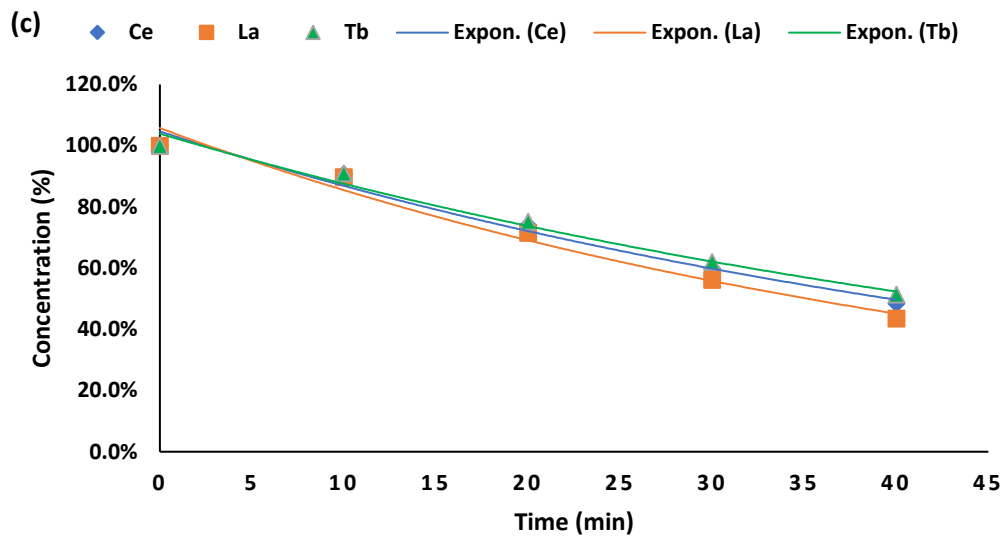
The Arrhenius plots of Ce, La and Tb for the extractions are shown in Figure 4-13. All the plots of Ce, La and Tb for the equation show linear relationships ($R^2 > 0.99$). These results indicate that the extraction efficiency increased as the temperature increased from 313 to 353 K. The slope of the curves is $-(E_a/R)$. Based on the slope of each curve from the plots, the activation energies for Ce, La and Tb are calculated and given in the following table:

Table 4-8. Slopes of Arrhenius plots and activation energies for Ce, La and Tb

	Ce	La	Tb
$-E_a/R$	-6848.1	-7059.3	-6747.5
$E_a \text{ (kJ} \cdot \text{mol}^{-1}\text{)}$	56.9	58.7	56.1

Shimizu et al. reported that the activation energies for acid leaching of Y and Eu from spent fluorescent phosphors using TBP-HNO₃ complex were 31 ± 6 and $42 \pm 11 \text{ kJ} \cdot \text{mol}^{-1}$, respectively¹⁵. Since Ce, La and Tb are imbedded in phosphate or aluminate matrices, it is very reasonable that they have higher activation energies relative to Y and Eu, which are known to exist as oxides in fluorescent phosphors.





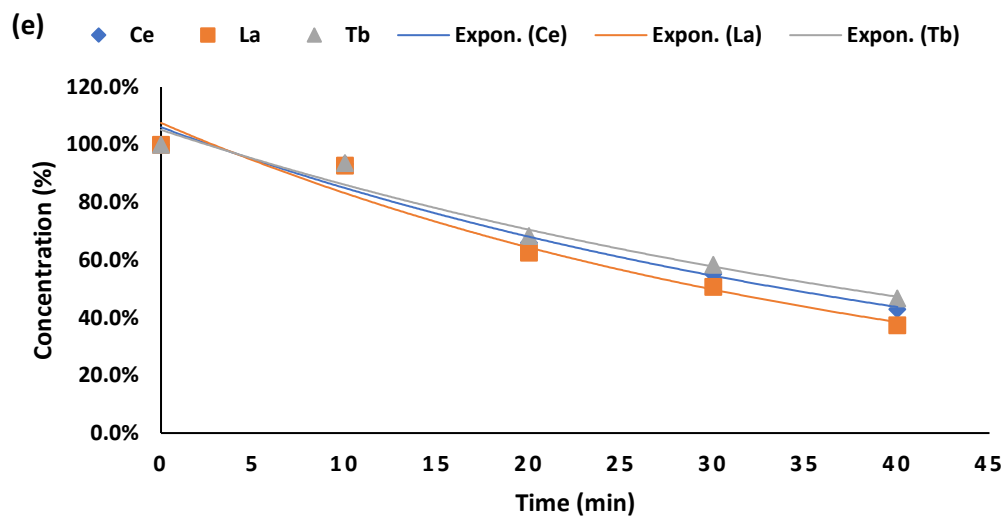


Figure 4-12. Extraction of rare earth elements in luminescent materials at (a) 313, (b) 333 (c) 343 and (d) 353 K. (e) No temperature control. Time—0 indicates the start of the ultrasonic extraction.

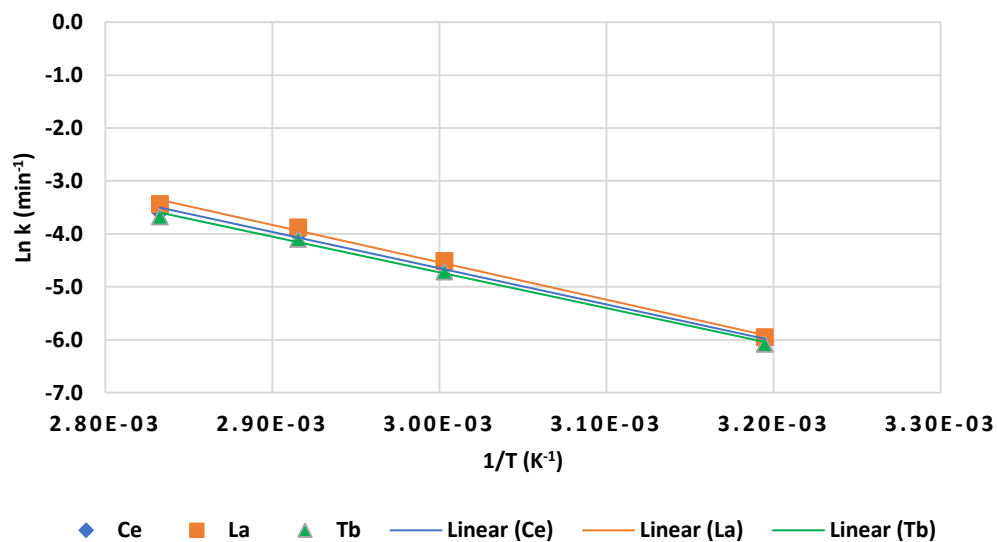
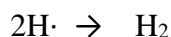


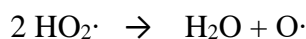
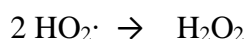
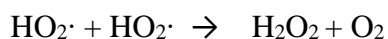
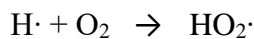
Figure 4-13. Arrhenius plots for the dissolution reactions of Ce, La and Tb with 9M HNO₃ under sonication at 313, 333, 343 and 353 K.

4.3.7. Ultrasonically-assisted pretreatment of fluorescent phosphors using H₂O and NaOH solutions

Alkali fusion method has been used to decompose phosphors with stable structures to improve leaching efficiency, in which phosphors are usually treated with strong oxidizing agents under elevated temperatures. For example, Li et al. decomposed phosphors by calcining them with sodium hydroxide at 900 °C for 2 hours and reached a leaching efficiency close to 100%²⁶. Porob et al. converted phosphors into a mixture of oxides by heating them with sodium carbonate at 1000 °C²⁷. Zhang et al. performed 2-step acid leaching and the results show that sodium hydroxide is better than sodium carbonate in the alkali fusion process. The acid leaching rates for all REEs reached over 97%²⁸. Wu et al. investigated the calcination of green phosphor using sodium peroxide system, and the optimal molten salt calcining conditions were found to be 650 °C, 50 min, and 1.5 : 1 of Na₂O₂-to-waste mass ratio²⁹, and over 99.9% recovery rate of rare earth elements was achieved.

Irradiation of aqueous solutions with ultrasound can cause sonolysis and generate highly reactive species such as hydrogen atoms and hydroxyl radicals. These radicals can attack solute molecules or combine to form H₂, H₂O₂ or water. The most common reaction upon sonolysis of water is dimerization of the hydroxyl radical to produce hydrogen peroxide³⁰⁻³¹. If oxygen molecules exist in the solution, oxygen atoms can also be produced³². Makino et al. first proved the formation of hydrogen atoms and hydroxyl radicals in the sonolysis of water through electron spin resonance (ESR) and spin-trapping studies in 1983³³. The reactions induced by ultrasound are as follows:





Since ultrasound can generate extreme chemical environment and strong oxidizing agent H_2O_2 , pretreatment of phosphors with water or even hydrogen peroxide seem to be an alternative way to decompose the phosphors. Phosphors samples were sonicated with deionized water and 12M sodium hydroxide at 60°C and 80°C for 1 hour. The pretreatment procedures were followed by nitric acid leaching. In order to better evaluate the efficiencies of sonication pretreatment, oil bath and 1M HNO_3 were employed to minimize the effect of solvent concentration and avoid the influence of sonication. The results are shown in Figure 4-14. Compared to the non-treated phosphor, all the pretreated phosphors, whether with water or NaOH, the efficiencies were all improved, especially the one pretreated with NaOH at 80°C (NaOH-soni-1hr- 80°C). This outcome for the pretreatment is also consistent with the conclusion of section 4.3.2.- sonication at higher temperatures will have a higher impact on the reaction. The improvement of efficiencies for cerium, lanthanum and terbium from the water-treated phosphors was not significant though, approximately 2%. When acid leaching was performed with 9M HNO_3 at 80°C under ultrasound influence, with the assistance of concentration, temperature and sonication effects, the efficiencies were further improved. The efficiencies for cerium, lanthanum and terbium of the phosphors pretreated with sodium hydroxide, whether treated at 60°C or 80°C , still outperformed the others (Figure 4-15). In

addition, compared to non-treated phosphors, the NaOH-treated phosphors had higher yields under the same extraction condition (refer to Figure 4-7.)

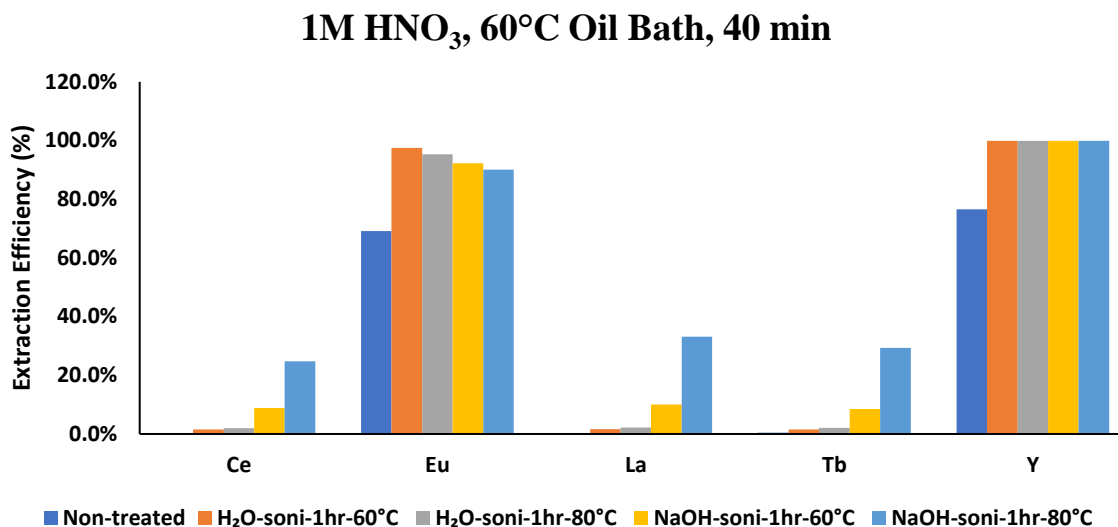


Figure 4-14. Acid leaching of non-treated, H₂O and NaOH treated phosphors with 1M HNO₃ in an oil bath at 60°C for 40 minutes, where H₂O-soni-1hr-60°C represents the phosphor material was pretreated by sonication at 60°C with H₂O for one hour; NaOH-soni-1hr-60°C represents the phosphor material was pretreated by sonication at 60°C with NaOH for one hour and so on.

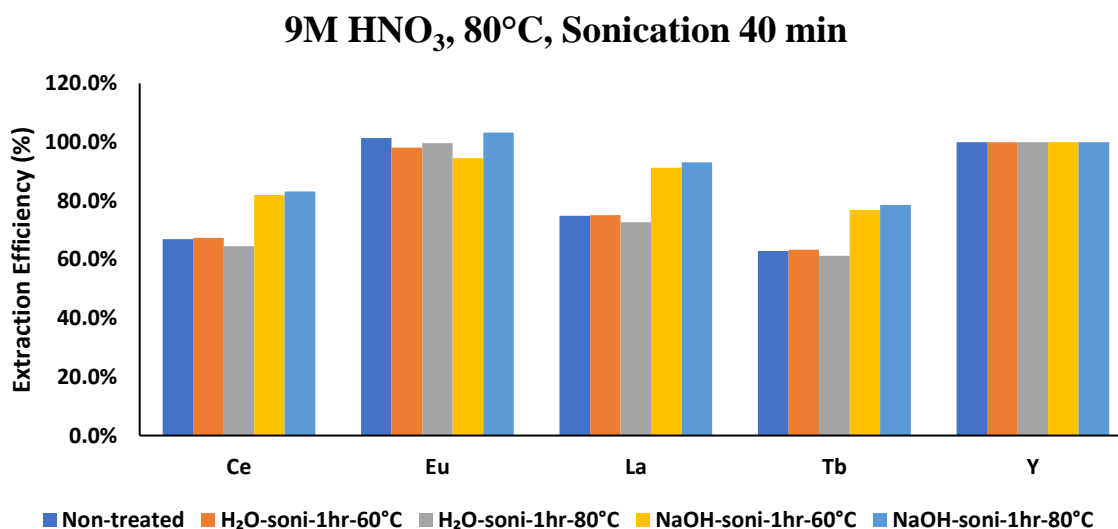


Figure 4-15. Acid leaching of non-treated, H₂O and NaOH treated phosphors with 9M HNO₃ under sonication at 80°C for 40 minutes.

H_2O_2 is one of the most powerful oxidizing agents. If the small quantity of H_2O_2 generated from H_2O under sonication could cause some change to extraction efficiencies, whether phosphors sonicated with H_2O_2 could bring on a greater improvement became a question. Consequently, samples of fluorescent phosphors were sonicated with hydrogen peroxide at room temperature for 1 hour and 2 hours. For comparison purposes, fluorescent phosphors were sonicated with H_2O at room temperature for 1 hour and 2 hours as the control experiments. All the pretreatments were followed by 1M HNO_3 sonication at 60°C . The results are shown in Figure 4-16.

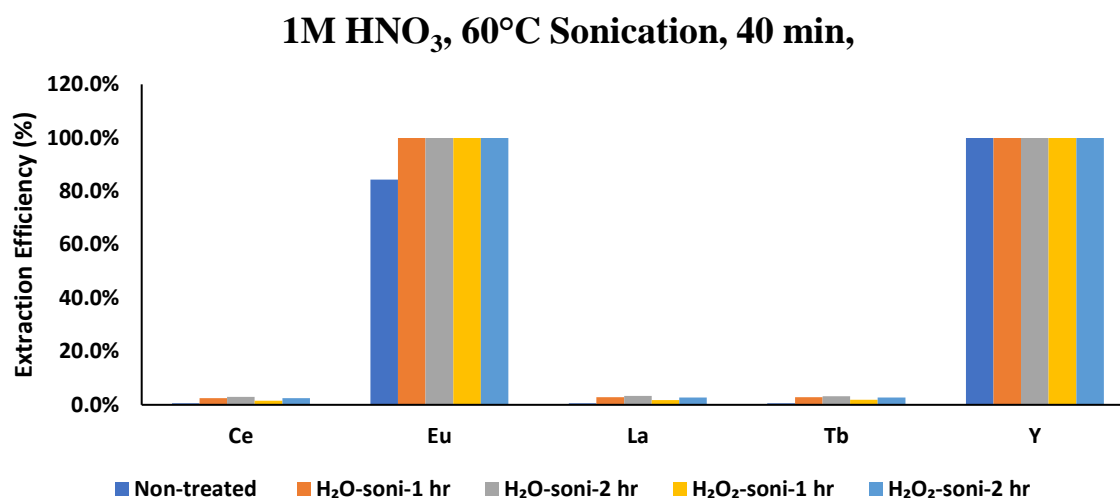


Figure 4-16. Acid leaching of non-treated, H_2O and H_2O_2 treated phosphors with 1M HNO_3 under sonication at 60°C for 40 minutes.

Compared to the non-treated phosphor, although the efficiencies for cerium, lanthanum and terbium of all the treated phosphors were slightly improved, approximately ranging from 2% to 3%, the difference of improvement between H_2O -treated and H_2O_2 -treated phosphors is very limited. Based on our observation, the possible explanation might be because 1) sonication for an extended time could cause temperature increase. When

temperature increases, hydrogen peroxide will start to decompose and generate oxygen and H₂O. Eventually it loses its reactivity; b) when oxygen evolves, the evolving bubbles of oxygen produce a foam and bring phosphor particles to the surface of solution, which makes the phosphor powder lose contact with the hydrogen peroxide solution.

Figure 4-17 (a)-(c) shows the appearances of the phosphors before and after the pretreatment. After sonication with H₂O and 12 M NaOH at 80°C for 1 hour, the phosphor became greyish and yellowish. The scanning electron microscope (SEM) was also employed to evaluate the morphologies and the particle sizes of the phosphor materials before and after ultrasonic treatment. The SEM micrographs for the non-treated phosphor, the phosphor sonicated with H₂O at 80°C for 1 hour, the phosphor sonicated with 12M NaOH at 80°C for 1 hour, and the phosphor ultrasonically extracted with 11M HNO₃ 80°C for 1 hour are shown in Figure 4-18, 4-19, 4-20 and 4-21, respectively. In Figure 4-19, we can see that sonication with H₂O seemed to have changed the particle size of the phosphor. There are more fine particles in the sonicated sample than in the non-treated sample. In Figure 4-20 and 4-21, compared to the non-treated phosphor, apparent dimensional and morphological changes can be observed on the treated phosphors. Obviously, sonication with the strong acid and base solutions have led to chemical and structural changes of the phosphors. In addition, based on the information of particle size and the extraction efficiencies of the water-sonicated phosphors in Figure 4-14 and Figure 4-16, the slight improvement of extraction efficiencies, if not resulted from analytical errors, could have also been attributed to the particle disintegration due to the effect of sonication. After all, the smaller the particle sizes, the larger the surface area and the better mass transfer rate.



Figure 4-17. (a) non-treated phosphor (b) phosphor sonicated with H₂O at 80°C for 1 hour (c) phosphor sonicated with NaOH at 80°C for 1 hour

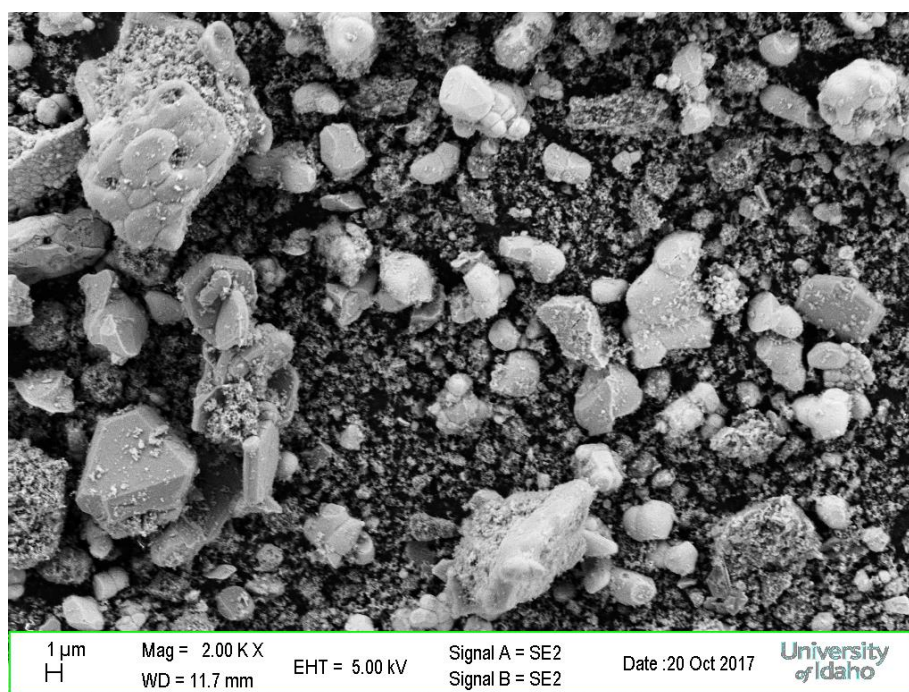


Figure 4-18. SEM micrograph of non-treated Sylvania phosphorus.

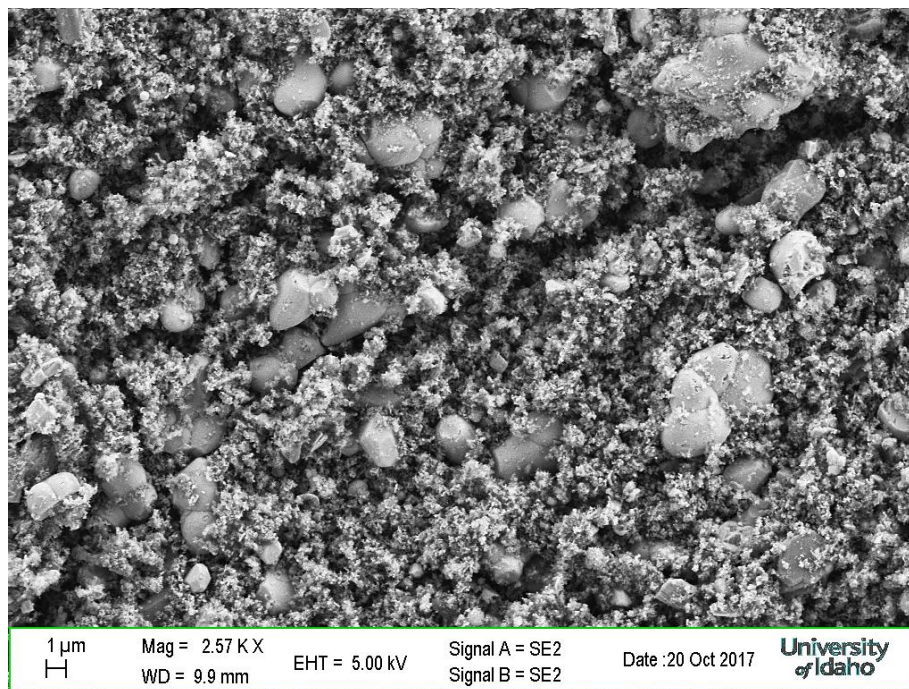


Figure 4-19. SEM micrograph of the phosphor sonicated with H₂O at 80°C for 1 hour.

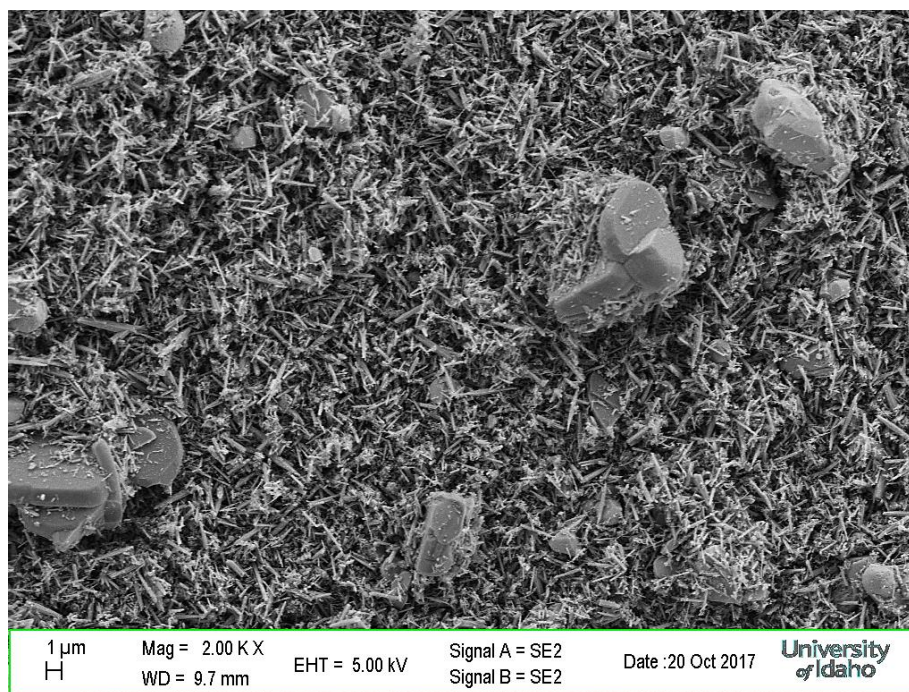


Figure 4-20. SEM micrograph of the phosphor sonicated with NaOH at 80°C for 1 hour.

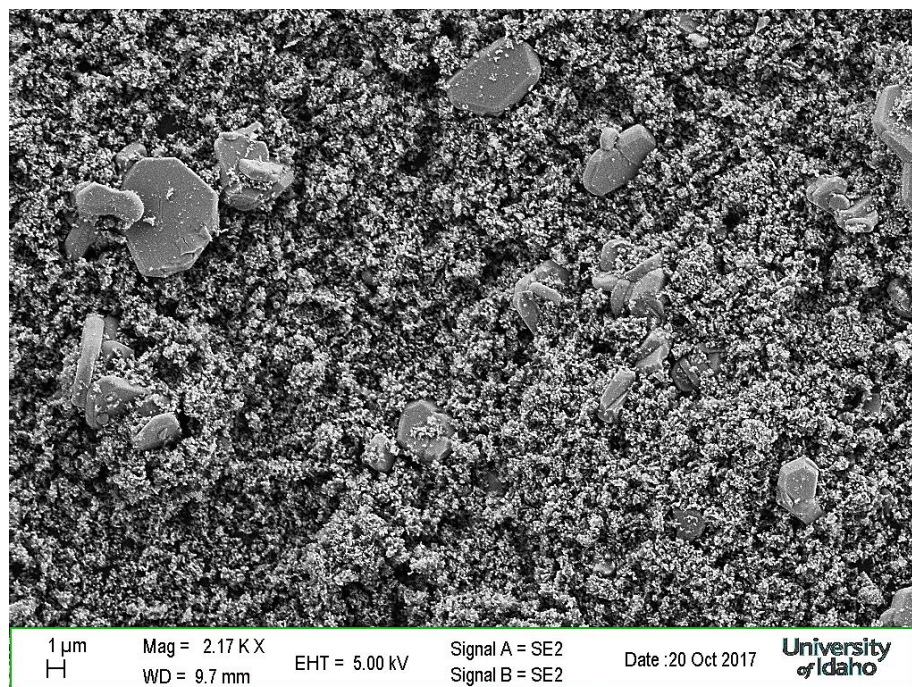


Figure 4-21. SEM micrograph of the phosphor ultrasonically extracted with 11M HNO₃ 80°C for 1 hour.

Fluorescence spectroscopy was employed to examine the change of emission spectrum after the ultrasonic extraction with 11M HNO₃ 80°C and the ultrasonic treatment with H₂O and 12M NaOH. In a fluorescent lamp, when electricity passes through a fluorescent lamp, the mercury vapor in the lamp will generate ultraviolet radiation (254 nm), which in turn excites the white coating on the inner wall of the lamp tube to emit visible light. As a result, UV light of 254 nm was used to excite fluorescence emission when taking fluorescence spectra of fluorescent phosphors. The spectra are shown in Figure 4-22. The strongest peak around 508 nm is the peak of 2nd order Rayleigh scattering (a monochromator with a combination of optical cut off filters must be used to get rid of it). The spectrum for the phosphor sonicated with H₂O at 80°C for 1 hour is not significantly different from the non-treated phosphor. However, the spectra for phosphors sonicated with NaOH and HNO₃ are

much different from the non-treated one. It is reasonable and understandable since strong acids and bases can cause decomposition of fluorescent phosphors, not to mention that they were treated under ultrasonic radiation, which can produce cavitation phenomenon that generates high temperature, high pressure as well as various chemical and physical effects.

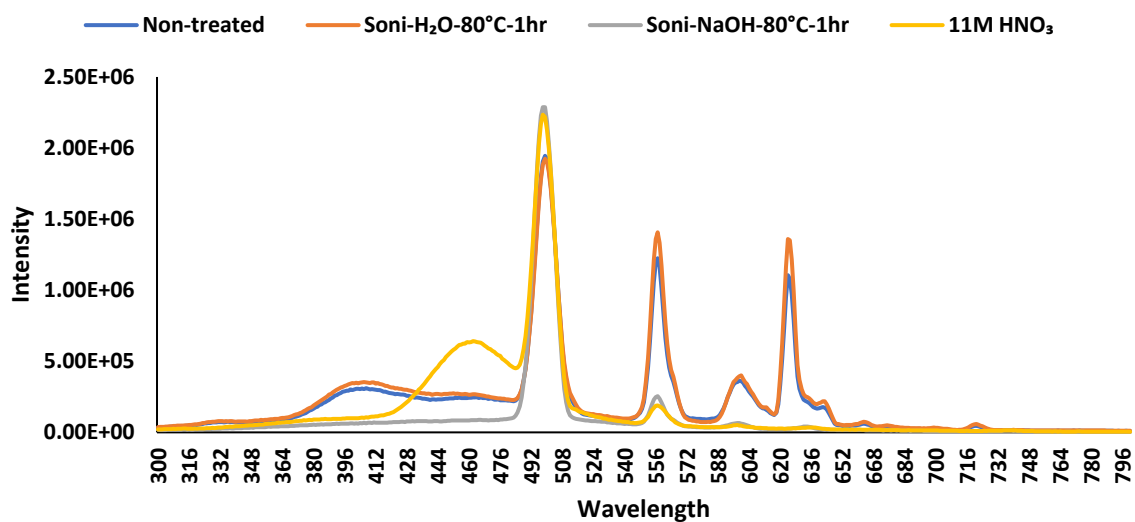


Figure 4-22. Fluoresce spectra of 1) non-treated phosphor; 2) phosphor sonicated with H₂O at 80°C for 1 hour; 3) phosphor sonicated with 12M NaOH at 80°C for 1 hour; 4) phosphor that has been ultrasonically extracted with 11M HNO₃ 80°C for 1 hour.

4.4. Conclusion

Based on the results of this investigation, the facilitation of ultrasonic irradiation for acid extraction of rare earth elements from fluorescent phosphor has been confirmed. A longer sonication time, higher sonication temperature, and higher solvent concentration will lead to higher extraction efficiencies of REEs. The kinetics analysis also suggests that the acid leaching process of REEs from fluorescent phosphors under sonication probably follows first order reaction, and the activation energies for acid leaching of Ce, La and Tb were calculated to be 56.9, 58.7, and 56.1 kJ·mol⁻¹, respectively. Ultrasound-assisted pretreatment of fluorescent phosphors was also proved to be able to improve extraction efficiencies of REEs from fluorescent phosphors. Spectroscopic spectra and SEM micrographic morphologies further confirmed the physical and chemical effects that ultrasound can cause on fluorescent phosphors.

Acknowledgement

We would like to express our appreciation to WSU GeoAnalytical Lab for ICP-MS analysis. Special thanks to ICP-MS technician Arron Steiner for running the samples for us, especially a few days before the deadline of dissertation submission. Without his assistance, this work would not have been completed. We also thank our colleague Horng-Bin Pan for his professional opinions about this work.

Reference

1. Mineral Commodity Summaries 2017. U.S. Geological Survey: 2017; pp 128-129.
2. https://www.wto.org/english/tratop_e/dispu_e/cases_e/ds431_e.htm. (accessed 10/2/2017).
3. Critical Materials Strategy (2011). U.S. Department of Energy: 2011; pp 1-190.
4. Critical Materials Strategy (2010). U.S. Department of Energy: 2010; pp 1-170.
5. Bremner, D., Chemical Ultrasonics. *Chemistry in Britain* **1986**, 22 (7), 633-638.
6. Suslick, K. S., Sonochemistry. *Science* **1990**, 247 (4949), 1439-1445.
7. Suslick, K. S.; Flannigan, D. J., Inside a Collapsing Bubble, Sonoluminescence and Conditions during Cavitation. *Annu. Rev. Phys. Chem.* **2008**, 59, 659-683.
8. Plesset, M. S.; Prosperetti, A., Bubble Dynamics and Cavitation. *Annual Review of Fluid Mechanics* **1977**, 9, 145-185.
9. Bang, J. H.; Suslick, K. S., Applications of Ultrasound to the Synthesis of Nanostructured Materials. *Advanced Materials* **2010**, 22 (10), 1039-1059.
10. Xu, H.; Zeiger, B. W.; Suslick, K. S., Sonochemical synthesis of nanomaterials. *Chemical Society Reviews* **2013**, 42 (7), 2555-2567.
11. Doktycz, S.; Suslick, K., Interparticle collisions driven by ultrasound. *Science* **1990**, 247 (4946), 1067-1069
12. Viculis, L. M.; Mack, J. J.; Kaner, R. B., A Chemical Route to Carbon Nanoscrolls. *Science* **2003**, 299 (5611), 1361.
13. Prozorov, T.; Prozorov, R.; Suslick, K. S., High Velocity Interparticle Collisions Driven by Ultrasound. *J. Am. Chem. Soc.* **2004**, 126 (43), 13890-13891.

14. Kass, M. D., Ultrasonically induced fragmentation and strain in alumina particles. *Materials Letters* **2000**, *42* (4), 246-250.
15. Shimizu, R.; Sawada, K.; Enokida, Y.; Yamamoto, I., Supercritical fluid extraction of rare earth elements from luminescent material in waste fluorescent lamps. *The Journal of Supercritical Fluids* **2005**, *33* (3), 235-241.
16. Jordens, J.; Appermont, T.; Gielen, B.; Van Gerven, T.; Braeken, L., Sonofragmentation: Effect of Ultrasound Frequency and Power on Particle Breakage. *Cryst. Growth Des* **2016**, *16*, 6167-6177.
17. Pokhrel, N.; Vabbina, P. K.; Pala, N., Sonochemistry: Science and Engineering. *Ultrasonics Sonochemistry* **2016**, *29* (Supplement C), 104-128.
18. Wahab, R.; Ansari, S. G.; Kim, Y.-S.; Seo, H.-K.; Shin, H.-S., Room temperature synthesis of needle-shaped ZnO nanorods via sonochemical method. *Applied Surface Science* **2007**, *253* (18), 7622-7626.
19. Romdhane, M.; Gourdon, C., Investigation in solid-liquid extraction: influence of ultrasound. *Chemical Engineering Journal* **2002**, *87*, 11-19.
20. Joyce, E.; Phull, S. S.; Lorimer, J. P.; Mason, T. J., The development and evaluation of ultrasound for the treatment of bacterial suspensions. A study of frequency, power and sonication time on cultured Bacillus species. *Ultrasonics Sonochemistry* **2003**, *10* (6), 315-318.
21. Brito, R. O.; Marques, E. F., Neat DODAB vesicles: Effect of sonication time on the phase transition thermodynamic parameters and its relation with incomplete chain freezing. *Chemistry and Physics of Lipids* **2005**, *137* (1-2), 18-28.

22. Morel, M.-H.; Dehlon, P.; Autran, J. C.; Leygue, J. P.; Bar-L'Helgouac'h, C., Effects of Temperature, Sonication Time, and Power Settings on Size Distribution and Extractability of Total Wheat Flour Proteins as Determined by Size-Exclusion High-Performance Liquid Chromatography. *Cereal Chemistry* **2000**, 77 (5), 685-691.
23. Mattila, H.-P.; Grigaliūnaitė, I.; Zevenhoven, R., Chemical kinetics modeling and process parameter sensitivity for precipitated calcium carbonate production from steelmaking slags. *Chemical Engineering Journal* **2012**, 192 (Supplement C), 77-89.
24. Eloneva, S.; Teir, S.; Salminen, J.; Fogelholm, C.-J.; Zevenhoven, R., Steel Converter Slag as a Raw Material for Precipitation of Pure Calcium Carbonate. *Ind. Eng. Chem. Res.* **2008**, 47 (18), 7104–7111.
25. Mincher, B. J.; Wai, C. M. W.; Fox, R. V.; Baek, D. L.; Yen, C.; Case, M. E., The separation of lanthanides and actinides in supercritical fluid carbon dioxide. *J Radioanal Nucl Chem* **2016**, 2543-2547.
26. Li, R. Q.; Wu, Y. F.; Zhang, Q. J.; Wang, W. In *Extraction of rare earth from waste three primary colors fluorescent powder in high temperature alkali fusion method*, Proceedings of CCATM' 2012 international conference & exhibition on analysis & testing of metallurgical process & materials, 2012; pp 795-799.
27. Porob, D. G.; Srivastava, A. M.; Nammalwar, P. K.; Ramachandran, G. C.; Comanzo, H. A. Rare earth recovery from fluorescent material and associated method. US8137645 B2, 2012.
28. Zhang, S.-G.; Yang, M.; Liu, H.; Pan, D.-A.; Tian, J.-J., Recovery of waste rare earth fluorescent powders by two steps acid leaching. *Rare Metals* **2013**, 32 (6), 609-615.

29. Wu, Y.; Wang, B.; Zhang, Q.; Li, R.; Yu, J., A novel process for high efficiency recovery of rare earth metals from waste phosphors using a sodium peroxide system. *RSC Advances* **2014**, *4* (16), 7927-7932.
30. Petrier, C.; Jeunet, A.; Luche, J. L.; Reverdy, G., Unexpected Frequency Effects on the Rate of Oxidative Processes Induced by Ultrasound. *J. Am. Chem. Soc.* **1992**, *114*, 3148–3150.
31. Mark, G.; Tauber, A.; Laupert, R.; Schuchmann, H.-P.; Schulz, D.; Mues, A.; von Sonntag, C., OH-Radical Formation by Ultrasound in Aqueous Solution – Part II: Terephthalate and Fricke Dosimetry and the Influence of Various Conditions on the Sonolytic Yield *Ultrason. Sonochem.* **1998**, *5*, 41-52.
32. Adewuyi, Y. G., Sonochemistry: Environmental Science and Engineering Applications. *Ind. Eng. Chem. Res.* **2001**, *40* (22), 4681–4715.
33. Makino, K.; Mossoba, M. M.; Riesz, P., Chemical Effects of Ultrasound on Aqueous Solutions. Formation of Hydroxyl Radicals and Hydrogen Atoms. *J. Phys. Chem.* **1983**, *87*, 1369–1377.